The Hong Kong Polytechnic University

Department of Applied Biology and Chemical Technology

Studies of protein-drug interactions by mass spectrometry

So Pui Kin

A thesis submitted in partial fulfillment of

the requirements for the degree of

Doctor of Philosophy

September 2008

CERTIFICATE OF ORIGINALITY

I declare that this thesis is my own work performed during the period 6.2004 – 8.2008 in the Department of Applied Biology and Chemical Technology, the Hong Kong Polytechnic University. All mass spectrometric results reported in this thesis were obtained by the author, who also prepared some of the proteins used in the study. Complementary molecular modeling, X-ray crystallography and some biophysical studies were conducted by other members of our research group, and these are explicitly acknowledged, where appropriate, in relevant parts of this thesis. The data reported in this thesis have not been included in any thesis, dissertation or report submitted to this University or to any other institution for a degree, diploma or other qualifications, or published by other research groups previously.

Pui-Kin So

September 2008

Abstract

β-Lactamase, a bacterial enzyme that hydrolyzes β-lactam antibiotics, has been recently modified and labeled with different fluorophores to act as fluorescence biosensors for detecting residual β-lactam antibiotics in food. E166Cf was constructed by replacing the glutamate residue on the Ω-loop of Class A β-lactamases at position 166 with cysteine to produce the E166C mutant, to which a fluorophore, fluorescein-5-maleimide, is attached. A second biosensor E166Cb was constructed by labeling with the fluorophore badan. These two biosensors were found to be able to emit enhanced and intense fluorescent signals upon specific binding to β-lactam antibiotics, enabling them to detect antibiotics like penicillin G, cefuroxime and cefotaxime down to the nanomolar level (10^{-9} M). To understand the biosensing mechanism of the β-lactamase-based biosensors, the kinetics and structural basis of the binding reactions between the biosensors and β-lactam antibiotics were investigated by electrospray ionization mass spectrometry (ESI-MS).

The identities of E166C and its fluorophore-labeled mutants were confirmed by ESI-MS. Complementary time-dependent mass spectrometric and fluorometric studies show that, in general, the time-resolved fluorescence profile correlate well with the concentration-time profile of the covalently bound enzyme-substrate complex (ES*, where E is E166Cf or E166Cb, and S is the substrate β-lactam antibiotic) monitored by ESI-MS. This observation demonstrates unambiguously that the fluorescence emission enhancement is due to specific substrate binding of a β-lactam type antibiotic.

Compared to the wild-type β-lactamases, detailed kinetics studies revealed that the hydrolytic (deacylation) dissociation rate (k_3 values) of the E166C, E166Cf and E166Cb mutants are much reduced to the order of 10^{-4} s^{-1}, and are ~ 5 orders of magnitude smaller than the rate of formation of ES* (k_2 values in the order of 10^1 s^{-1}). These kinetic properties ensure that ES* are formed at high concentrations at steady state, but dissociate very slowly thereafter. Consequently, a steady and intense fluorescent signal can be easily monitored over a reasonable analysis time period (say 1,000 seconds) in practical applications.

On the other hand, the specific binding efficiencies towards β-lactam antibiotics were found to have maintained and even enhanced for the E166C, E166Cf and E166Cb mutants. The overall binding efficiency, as indicated by the ratio of kinetic parameters k_2/K_d, is not significantly impaired by the introduction of fluorescein-5-maleimide at the C166 position of the Ω-loop of the β-lactamases, which is located near the active binding site. This is attributed to that the flexible nature of the Ω-loop and fluorophore-induced increase in flexibility of the active site binding pocket, thereby relieving the steric crowding effect exerted by the fluorophore. The effect of using a bulky fluorescein-5-maleimide versus a smaller but hydrophobic badan fluorophore in the biosensor were investigated. The fluorescence characteristics of E166Cf and E166Cb were found to be different. Specifically, the incorporation of badan was found to enhance the overall binding efficiency more significantly by ~10-folds. This surprising result might be due to the highly hydrophobic nature of badan, which tends to repel/displace the surrounding dense water clusters which serve to stabilize the structural integrity of the active site binding pocket. With the loss/lowering of the stabilizing effects offered by these water molecules, the

flexibility of the active site would be further enhanced, and therefore the steric blocking effect imposed by the fluorophore could be alleviated to a greater extent.

Mass spectrometric hydrogen-deuterium (H/D) exchange studies showed that for E166Cf and E166Cb, the H/D exchange levels of two peptide segments near the active site are higher than those of free E166C, indicating that the fluorophore may have induced local dynamic changes to the active site region. However, upon substrate binding, the H/D exchange levels of these two segments of E166Cf and E166Cb decrease and become similar to that of E166C, indicating that the dynamic changes mediated by the fluorophore are nullified. Based on these observations, a "spatial displacement" mechanism was proposed. The fluorophore (both fluorescein-5-maleimide and badan) may initially be oriented towards and close to the active binding site, and induce destabilizing effect to this confined region by displacing the "structural glue" water molecules and disrupting some noncovalent interactions involved in maintaining the structural integrity of the active binding pocket. Upon substrate binding, the fluorophore is displaced away from the active site in order to avoid the spatial clash with the incoming substrate, thus the destabilizing effects initially exerted by the fluorophore to this region are also withdrawn. This spatial displacement event is the major cause for changes in local environment surrounding the fluorophore, i.e. solvent polarity and accessibility, thereby changing the fluorescence emission properties of the fluorophore. This proposed mechanism is found to be consistent with the results of molecular modeling and preliminary X-ray crystallographic studies.

Due to discrepancies in reported results obtained by ESI-MS under acidic, denaturating conditions and other physical techniques such as X-ray crystallography and UV spectroscopy, the inhibition mechanism of tazobactam (MW=300 Da) towards β-lactamases was re-investigated by ESI-MS but under near physiological (pH 7) conditions. Unlike previous ESI-MS studies, a covalently bound enzyme-inhibitor complex (E-I complex) with a relative molar mass of [M + 300] Da was observed (M is the average molecular mass of the enzyme protein), which is consistent with the formation of a trans-enamine species as suggested by X-ray crystallography and UV spectroscopic methods. In addition, our results show that, for the first time, the E-I complex formed from the *Staphylococcus aureus* PC-1 β-lactamase and tazobactam dissociates further to form an inactive dehydrated enzyme. Based on the results obtained by protease digestion and tandem mass spectrometry, this dehydrated enzyme is proposed to be an alkene-like species formed from dissociation of the trans-enamine species. For this inhibition mechanism, the role of the inhibitor is initial binding to the active site of the enzyme, followed by triggering of a chemical reaction (or reactions) that result in the formation of an inactivated form of β-lactamase.

Research Publications

Journal Papers

1. Chan, P.H., So, P.K., Ma, D.L. Zhao, Y., Lai, T.S., Chung, W.H., Chan, K.C., Yiu, K.F., Chan, H.W., Siu, F.M., Tsang, C.W., Leung, Y.C. and Wong, K.Y. "Fluorophore-Labeled β-Lactamase as a Biosensor for β-Lactam Antibiotics: A Study of the Biosensing Process". *Journal of the American Chemical Society*, Vol 130, pp. 6351-6361 (2008)

Conference Papers

2. So, P.K., Chan, F.Y., Tsang, M.S., Tsang, M.W., Wong, K.Y., Leung, Y.C. and Tsang, C.W. "Study of tazobactam inhibition of β-lactamases by electrospray ionization mass spectrometry (ESI-MS) under near physiological conditions" *Proceedings of the 56th ASMS Conference on Mass Spectrometry and Allied Topics*, June 1 - June 5, 2008, Denver, U.S.A

3. So, P.K., Chung, W.H., Ringo Lai, T.S., Leung, Y.C., Wong, K.Y. and Tsang, C.W. "Study of β-lactamase-based biosensor – β-lactam antibiotic interactions by electrospray ionization mass spectrometry" *The Twelfth Symposium on Chemistry Postgraduate Research in Hong Kong*, City University of Hong Kong, Hong Kong (2005)

Manuscript soon to be submitted

4. So, P.K., Chan, F.Y., Tsang, M.S., Tsang, M.W., Wong, K.Y., Leung, Y.C. and Tsang, C.W. "Study of tazobactam inhibition of β-lactamases by electrospray ionization mass spectrometry (ESI-MS) under near physiological conditions". To be submitted to Rapid Communication in Mass Spectrometry (2008)

Acknowledgment

I would like to express my deepest gratitude to my chief supervisor, Prof. C. W. Tsang, for his guidance and supervision of my Ph. D. program of study by research. I also wish to express special thanks to my co-supervisors, Dr. Thomas Y.C. Leung and Prof. K.Y. Wong, who have offered valuable guidance and help throughout the conduct of this research project.

The award of the Hong Kong Polytechnic University graduate studentship to me, and the funding support of the Research Grant Council of Hong Kong (CERG Project No. PolyU 5463/05M and AOE Project No. P-10/01) for this project are gratefully acknowledged.

I would also like to thank all of my research group members, Dr. Ringo T. S. Lai, Dr. D. L. Ma, Dr. Y. X. Zhao, Dr. P. H. Chan, Dr. Emily M. W. Tsang, Dr. K. C. Chan, Dr. Annie F. M. Siu, Dr. Jackie M. K. Cheng, Miss. W. T. Wong, Miss. F. Y. Chan, Miss. M. S. Tsang, Miss P. Y. Lau, Mr. Angus C. L. Chan, Mr. W. H. Chung and Miss Toby P. Y. Lau, who have helped me in various ways during the years of my study. I also wish to express my gratitude to all academic and technical staffs, in particular Mr Y. K. Au, from the Department of Applied Biology and Chemical Technology for their technical support.

Table of Contents

List of Figures

List of Tables

List of Schemes

List of abbreviations

General abbreviations

Full Form	Abbreviation
Capillary high performance liquid chromatography	CapLC
Circular dichroism	CD
Collision-induced dissociation	CID
Charge state distribution	CSD
Daltons	Da
Glu166 --> Cys mutant of β-lactamase	E166C
Badan labeled biosensor	E166Cb
Fluorescein-5-maleimide labeled biosensor	E166Cf
Enzyme-inhibitor complex	E-I complex
Non-covalent enzyme-substrate complex	ES
Covalently bound enzyme-substrate complexes	ES*
Electrospray ionization	ESI
Hydrogen-deuterium exchange	H/D exchange
Proton	H^+
High performance liquid chromatography	HPLC
Mass to charge ratio	m/z
Maxtrix assisted laser desorption/ionization	MALDI
Mass spectrometry	MS

Penicillin-binding protein	PBP
6-aminopenicillanic acid	6APA
Tandem mass spectrometry	MS/MS
Quadrupole–(Time-of-flight)	Q-TOF
Nuclear magnetic resonance	NMR
Relative molar mass	M_α

Abbreviation and symbol of 20 essential α-amino acids

Full form	Abbreviation	Symbol
Alanine	Ala	A
Arginine	Arg	R
Asparagine	Asn	N
Aspartic acid	Asp	D
Cysteine	Cys	C
Glutamic acid	Glu	E
Glutamine	Gln	Q
Glycine	Gly	G
Histidine	His	H
Isoleucine	Ile	I
Leucine	Leu	L
Lysine	Lys	K
Methionine	Met	M
Phenylalanine	Phe	F
Proline	Pro	P
Serine	Ser	S
Threonine	Thr	T
Tryptophan	Trp	W
Tyrosine	Tyr	Y
Valine	Val	V

Chapter 1 Introduction

1.1 Application of electrospray ionization mass spectrometry (ESI-MS) in studies of biomolecules

Prior to the 1990s, mass spectrometry (MS) was only strictly applicable to the analysis of small and thermally stable compounds because of the lack of effective ionization techniques to (i) softly ionize non-volatile analyte molecules without significant fragmentation, and (ii) transfer the ionized analytes from the solution phase into the gas phase.[Domon and Aebersold, 2006] Since the early 1990s, the development of two soft ionization techniques, namely electrospray ionization (ESI) and matrix assisted laser desorption/ionization (MALDI), dramatically changed this situation and led to a revolution in the application of MS to the analysis and characterization of non-volatile, high molecular mass biomolecules, e.g. proteins. Nowadays, MS has become an essential analytical technique in protein research, such as the studies of protein-ligand (substrate) interactions, post-translational modifications, and protein folding.[Daniel et al., 2002; Domon and Aebersold, 2006; Loo., 1997]

The prevalence of MS is attributed to its several distinct advantages over other conventional biophysical techniques, including optical spectroscopy (e.g. UV-absorption, circular dichroism (CD), and fluorescence), nuclear magnetic resonance (NMR) and X-ray crystallography. The three major advantages of MS have often been described as the three "S" by mass spectrometrists: specificity, sensitivity and speed.[Daniel et al., 2002; Loo, 1997]

Specificity

Specificity is a critical advantage of MS in the study of protein-ligand binding interactions. The binding specificity between a protein and its ligand could be proved by a number of mass spectrometric approaches, and the two most common methodologies are the chemical and experimental strategies.

Chemical strategies usually involve modifying the amino acid residues that actively participate in the binding. One approach is to covalently modify the active site residues to disrupt or mediate the binding interactions. Examples of covalent modification include conversion of lysine to homo-arginine, trimethylamino-ethylation of cysteine thiol to thialamine, and some general methods of derivatizing amino acids such as methylation and acetylation. Another commonly used approach is carrying out site-directed mutagensis on the active site amino acid residues, from which the binding specificity and efficiency of the protein will be significantly impaired, or at least altered. Upon these modifications, the signal of peaks corresponding to the protein-ligand complexes in the mass spectrum would significantly decrease/disappear for the specific binding reactions.[Daniel et al., 2002]

Experimental strategies include varying the experimental conditions of analysis (e.g. temperature, pH and varying the buffer system) in order to induce conformation changes of proteins, which will directly affect the formation of specific protein-ligand complexes. Therefore, the effects of external conditions on the MS signal corresponding to the protein-ligand complexes could provide

direct experimental evidences and insight into the specificity of the binding reactions.[Daniel et al., 2002]

Speed and sensitivity

Speed and sensitivity are the two other distinct advantages of MS when compared with other biophysical techniques. Unlike NMR and X-ray crystallography that are highly sample consuming (milligram level of sample is required), MS only consumes very small quantities of samples, often in the low picomole to femtomole range. The speed of MS is also favourable since the signals are usually available for monitoring immediately after introduction of sample. This advantage is particularly obvious when compared with X-ray crystallography, which involves time-consuming and tedious sample crystallization steps.[Ashcroft., 2005; Daniel et al., 2002; Loo., 1997]

1.1.1 Characterization of covalently modified proteins by ESI-MS

ESI-MS has been a useful technique for characterization of protein-ligand (e.g. drug, substrate, and inhibitor) complexes.[Deterding et al., 2000; Shen et al., 2000; Domon and Aebersold, 2006] The stiochiometry of the binding reactions between proteins and their binding partners can be determined directly by molecular mass measurement, and the binding specificity can be confirmed.[Loo et al., 1997; Tullio et al., 2005; Daniel et al., 2002] In addition, the analytical capability of the conventional mass spectrometric method can be further extended by protease digestion followed by tandem mass spectrometry (MS/MS), in which the proteolytic peptide segments produced from protease digestion are

further subjected to fragmentation (dissociation) through collision-induced dissociation (CID) inside the mass spectrometer. From the analysis of the masses of the resulting MS/MS fragments, the specific site of modification can be definitively located.[Domon and Aebersold, 2006]

In recent years, several research groups have demonstrated that ESI-MS can also be adopted to study the mechanism of inhibitors, which often inhibit the biochemical activity of their protein targets through the formation of stable, covalently bound protein-inhibitor complexes.[Pratt., 1992; Knight et al., 1993; Yang et al., 2000; Rodriguez et al., 2004] In some cases, the inhibitor molecule undergoes further dissociation after binding to the protein target, leading to only parts (moieties) of the inhibitor molecule are bonded or conjugated with the protein. These events are often accompanied by changes in molecular mass of the protein-inhibitor complex, and thus can be directly monitored by MS. Furthermore, by protease digestion followed by MS/MS, the site of inhibitor attachment to the protein, and in some cases, the covalent crosslinking mediated by the inhibitor molecule can be determined.[Yang et al., 2000]

1.1.2 Study of enzyme kinetics by ESI-MS

The study of enzyme kinetics is important to the understanding of the behavior of enzymes towards their ligand targets. Conventionally, enzyme kinetic parameters, such as Michealis-Menten constant (K_m) and maximum velocity (V_{max}), are determined by spectroscopic methods in which the product released in the enzymatic reaction exhibits strong UV absorption or fluorescence emission at

a pa rticular w avelength t hat i s di fferent from t he r eactants. However, m any natural s ubstrates ar e i ntrinsically not chromophores, a nd require chemical modifications to r ender t hem a c hromogenic pr operty. These chemical modification pr ocesses often i nvolve tedious a nd t ime-consuming m ulti-step synthesis, a nd, more importantly, the ki netic be haviors of t he s ubstrate may be altered upon chemical modification.[Ge et al., 2001; Bothner et al., 2000]

In recent years, ESI-MS ha s become an i ncreasing i mportant t echnique in t he study of e nzyme ki netics. The m ost obvi ous a dvantage of E SI-MS ov er the conventional s pectroscopic m ethods is t hat c hromophore s ubstrates a re not required, since t he pr oducts and reactants can be detected and obs erved directly in the m ass s pectrum. With t he us e of i nternal s tandards, t he time-dependent abundances of these species involved in the enzymatic reaction can be accurately determined.[Ge e t a l., 2001] Recently, several groups have extended the application of t he mass s pectrometric approach by demonstrating that t he microscopic ki netics p arameters of indi vidual s teps in the e nzymatic r eaction could be di rectly m easured by monitoring t he f ormation of enzyme-substrate complex as a function of reaction time.[Lu et al., 2001; Houston et al., 2000]

1.1.3 Detection of conformational and dynamic changes of proteins by mass spectrometric hydrogen – deuterium exchange (H/D MS)

Background

Hydrogen-deuterium (H/D) exchange was first introduced in the mid-1950s by Linderstrom-Lang, who discovered that the kinetics of H/D exchange reaction could reflect the protein structure (3-D conformations) and dynamics.[Hvidt and Linderstronm-Lang, 1955] In the early 1980s, the H/D exchange method was further advanced by combining with the techniques of protease digestion and high performance liquid chromatography (HPLC), opening the possibility to study local structure and dynamics of proteins. In 1993, Zhang and Smith were the first to use mass spectrometry to monitor H/D exchange reactions on proteins, and since the mid-1990s, a range of significant advancements on H/D exchange mass spectrometry (H/D MS) have been made. Nowadays, H/D MS has become an important technique to investigate the local and global changes in protein structure and dynamics resulted from various processes, such as protein-protein interactions, modifications of protein (e.g. amino acid residue mutation), and ligand binding.[Busenlehner and Armstrong, 2005]

Kinetics of H/D Exchange

Among various types of exchangeable proton present in a protein, only amide protons are used for H/D exchange studies, since the exchange reactions of the protons on the side chain functional groups and the N- and C- terminus are too fast to be measured by most physio-chemical techniques. Studies on unstructured peptides (e.g. polyalanine) showed that the H/D exchange reaction of amide

proton is both acid- and base-catalyzed, and thus the overall intrinsic exchange rate constant (k_i) is dependent on solution pH as described in Eqn [1.1],

$$k_{ex} = k_D[D^+] + k_{OD}[OD^-] + kw \qquad [1.1]$$

where k_{OD}, k_D, and k_w correspond to the base-catalyzed, acid-catalyzed, and water-catalyzed rate constant, respectively (for polyalanine, $k_{OD} = 1.12 \times 10^{10}$ M^{-1} min^{-1}, $k_D = 41.7$ M^{-1} min^{-1}, $kw = 3.16 \times 10^{-2}$ M^{-1} min^{-1}, and $k_i = \sim 10^{-1}$ s^{-1}). [Mandell et al., 1998; Kaltashov and Eyles, 2005] At pH 7, the physiological condition for most proteins, the exchange reaction is mainly catalyzed by base (OD^-) since base-catalysis is ~10^4 - 10^8 times faster than acid-catalysis.[Mandell et al., 1998] As shown in Fig. 1.1, the relationship between the rate of H/D exchange and pH follows a V shape trend.[Konermann and Simmons, 2003; Kaltashov and Eyles, 2005] Typically, the H/D exchange rate is measured by incubating the protein with a deuterated buffer (i.e., D_2O added to the buffer solution) at physiological pH 7, and then quenching into a buffer at 0 ^oC with pH 2 - 3 at which the rate of exchange is very slow (Fig. 1.1). Under these quenched conditions (at 0^o C and pH = 2 - 3), the rate of exchange is reduced by ~ three orders of magnitude, allowing time for mass spectrometric analysis.[Mandell et al., 1998; Busenlehner and Armstrong., 2005; Hoofnagle et al., 2003]

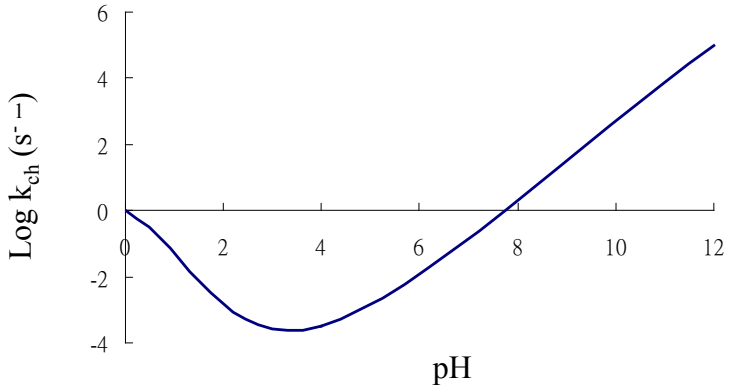

Figure 1.1 Plot of chemical H/D exchange rates (k_{ch}) as a function of pH.

Although the intrinsic rate of H/D exchange at pH 7 is rather fast ($10^1 - 10^3$ s^{-1}), the observed rate of exchange of amide protons on proteins usually occurs much slower, with half lives ranging from milliseconds to years. For a given exchangeable proton, the rate of exchange depends mainly on two factors: (i) degree of solvent (i.e., water) protection (or accessibility), and (ii) the hydrogen bonding configuration within the protein. Generally, the rate of H/D exchange is significantly slower when the solvent exposure of the amide proton decreases and when a network stable of hydrogen bonds are linked up with surrounding amino acid residues in the secondary and tertiary protein structure.[Hoofnagle et al., 2003]

In a compactly folded protein, a large fraction of amide protons are highly shielded from the solvent, hindering the access of the OD^- catalyst. These buried protons can be exchanged through fluctuations of the protein molecule that transiently break the intramolecular interactions, e.g. hydrogen bonds, and result in the formation of a solvent-exposed "open" state that is exchange-competent. So far, two models have been proposed to describe the formation of the "opened

state" from which exchange reactions are allowed: the "*solvent penetration*" model and the *"local unfolding*" model. The "*solvent penetration*" model suggests that the structural fluctuations of the protein allow access of the OD^- catalyst through transiently formed channels and cavities, while the "*local unfolding*" model postulates that small regions of a protein unfold cooperatively, thus exposing the amide protons to the bulk solvent.[Mandell et al., 1998; Busenlehner and Armstrong, 2005; Hoofnagle et al., 2003; Konermann and Simmons, 2003] Theoretical studies reveal that H/D exchange can be associated with both scenarios, and that it may also involve transient formation of conformations that are very different from the native state.[Konermann and Simmons, 2003]

A reaction scheme commonly used to describe the H/D exchange through structural fluctuations is depicted in Scheme 1.1. [Mandell et al., 1998; Busenlehner and Armstrong, 2005; Hoofnagle et al., 2003; Konermann and Simmons, 2003] Local unfolding and dynamic motions are described by equilibria between the "opened" state (exchange-competent) and the "closed" state (exchange-incompetent).

$$NH_{closed} \underset{k_c}{\overset{k_o}{\rightleftharpoons}} NH_{opened} \xrightarrow{k_i} ND_{opened} \underset{k_o}{\overset{k_c}{\rightleftharpoons}} ND_{closed}$$

Scheme 1.1 Mechanism of amide hydrogen exchange through structural fluctuations. k_o, k_c, and k_i are the rate constants for structural opening, structural closing, and H/D exchange in the fully unfolded form (the intrinsic rate of H/D exchange), respectively.

The apparent rate constant of the exchange reaction (k_{ex}) is given by Eqn [1.2], where k_i is the intrinsic rate constant for exchange (the rate of exchange in the fully unfolded form) and k_o and k_c are the rate constants for the formation of the "opened" and "closed" states, respectively.

For a native (folded) protein at physiological pH (pH 7), the rate of closing (folding) is highly favorable and often proceeds much faster than that of opening (unfolding) ($k_c >> k_o$). This situation is referred to as the EX2 regime in which the refolding of the locally unfolded regions is highly efficient, and takes place much faster than the intrinsic rate of hydrogen exchange ($k_c >> k_i$). The apparent exchange rate can therefore be simplified as in Eqn [1.3]. In this expression, the apparent rate of exchange is dependent on the intrinsic rate of exchange and the equilibrium constant between the opened and closed states ($K_{eq} = k_o/k_c$), which is an reflection on the molecular dynamics of protein occurring in a range of microsecond to millisecond time scale. Under the EX2 condition ($k_c >> k_i$), since only a small faction of amide protons can be exchanged upon one single opening event, the mass spectrum often shows a single mass peak that gradually shifts to a higher mass peak with increasing H/D exchange time.[Mandell et al., 1998; Busenlehner and Armstrong, 2005; Hoofnagle et al., 2003; Konermann and Simmons, 2003]

$$k_{ex} = k_o k_i / (k_o + k_c + k_i) \qquad [1.2]$$

EX2 regime: $k_c >> k_i$, $\qquad k_{ex} = (k_o / k_c)\, k_i \qquad [1.3]$

EX1 regime: $k_i >> k_c$, $\qquad k_{ex} = k_o \qquad [1.4]$

Another extreme is applicable to unstable proteins, whether native or induced by denaturant. For these proteins, the closing (folding) process is hindered and the rate of this process becomes significantly slower than the intrinsic rate of exchange ($k_c << k_i$). This situation is referred to as the EX1 regime in which the apparent exchange rate is dependent only on the rate of opening (Eqn [1.4]). Under EX1 condition ($k_c << k_i$), the mass spectrum usually displays two distinct mass peaks (or a bimodal distribution of peaks in the case of isotopic cluster of peaks), one corresponding to the protonated species and the other one corresponding to the highly deuterated species, since the opened state exists long enough (small k_c) to allow all amide protons to be exchanged during a single opening event.[Mandell et al., 1998; Busenlehner and Armstrong, 2005; Hoofnagle et al., 2003; Konermann and Simmons, 2003]

1.2 β–lactam antibiotics, β-lactamase and β-lactamase-based fluorescence biosensor

β–lactam antibiotics

β–lactam antibiotics are an important class of antibiotic used in the treatment of infections caused by Gram-negative and Gram-positive bacteria.[Poole, 2004; Sandanayako and Prashad, 2002] β–lactam antibiotics are characterized by a four-member β–lactam ring, and divided into two major classes: penicillin (e.g. penicillin G and ampicillin) and cephalosporins (e.g. cefoxitin, cefuroxime and cefotaxime) (Fig. 1. 2). These antibiotics target a bacterial enzyme called penicillin-binding protein (PBP), a component responsible for the peptidoglycan synthesis in the production of bacterial cell wall. β–lactam antibiotics bind to the PBPs and retard the cell wall synthesis, which leads to cell death.[Sandanayako and Prashad, 2002] It is generally accepted that the interaction between PBP (the enzyme protein labeled as E here) and β–lactam antibiotics (labeled as S here) follows a three-steps mechanism as depicted in **Scheme 1.2**. The first step is the formation of the non-covalent Michealis complex (ES), and the binding affinity between the two binding species is represented by the dissociation equilibrium constant K_d ($K_d = k_{-1}/k_1$, where k_1 is the forward rate constant for the formation of non-covalent ES, and k_{-1} is the backward rate constant for the dissociation of ES). A larger value of K_d would therefore indicate a lower binding affinity between E and S.

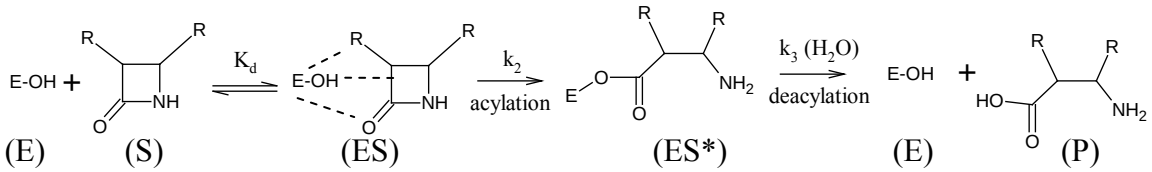

Scheme 1.2 Catalytic pathway of PBP / β-lactamase (E is the free enzyme, S is the β-lactam antibiotic substrate, ES is the non-covalent enzyme-substrate complex, ES* is the covalently bound enzyme-substrate complex, P is the product (hydrolyzed antibiotic), and $K_d = k_{-1}/k_1$.

The second step is acylation in which a covalently bound enzyme-substrate complex (ES*) is formed. The final step is deacylation which involves hydrolysis of the ester bond of the covalently bound complex, and regeneration of the active enzyme. The rate of acylation and deacylation are represented by k_2 and k_3, respectively.[Sandanayako and Prashad, 2002; Bonomo and Rice, 1999; Lu et al., 1999] As the reported values of k_3 for PBP-β–lactam reactions are generally very small ($< 10^{-4}$ s^{-1}), and are ~100-1000 folds smaller than k_2, the β–lactam antibiotics are generally considered as "inhibitors" for PBP.[Lu et al., 1999]

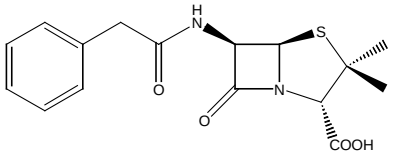

Penicillin G

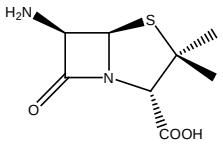

6-Aminopenicillanic acid (6APA)

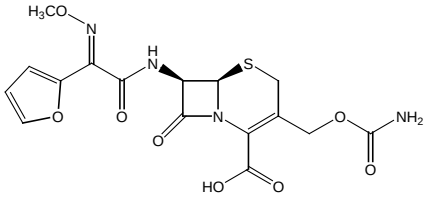

Cefuroxime

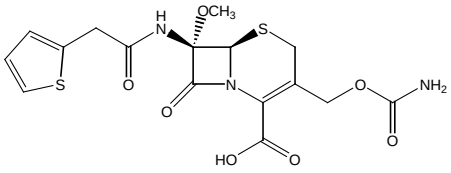

Cefoxitin

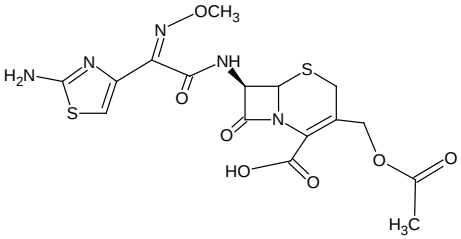

Cefotaxime

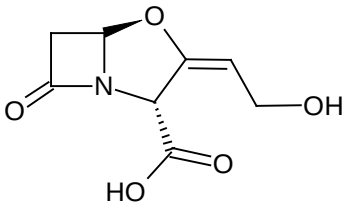

Clavulanic acid

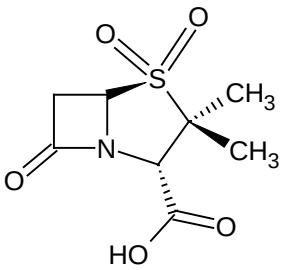

Sulbactam

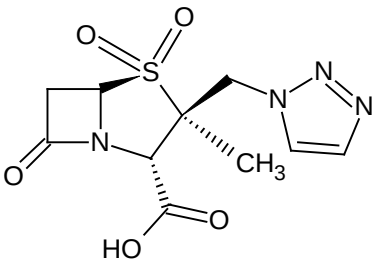

Tazobactam

Figure 1.2 Chemical structures of β-lactam antibiotics and inhibitors

β–lactamase

Unfortunately, due to the widespread use of β–lactam antibiotics, bacteria have developed a number of resistance mechanisms against these drugs. One significant mechanism is the bacterial production of β–lactamases, which are hydrolytic enzymes that efficiently destroy the β–lactam antibiotics before they reach their target, the PBP.[Poole, 2004; Sandanayako and Prashad, 2002] Based on similarities in the amino acid sequences, β–lactamase enzymes can be divided into four major classes, class A, B, C, and D. Class A, C, and D are serine-based enzymes in which the catalytic reaction leading to the disruption of the β–lactam ring is initiated by an active serine residue. Class B β–lactamases are metallo-enzymes, and the catalytic reaction involves the participation of a Zn atom. [Sandanayako and Prashad, 2002]

The hydrolytic reaction between β–lactamases and β–lactam antibiotics is mechanistically similar to, but kinetically very different from that of PBP (**Scheme 1.3**). The substrate recognition step (K_d), acylation (k_2), and particularly deacylation (k_3) are much more efficient than PBP, and therefore the antibiotics are mostly hydrolyzed and destroyed before they could gain access to the PBP. [Bonomo and Rice, 1999]

To tackle the problem of antibiotic resistance mediated by β–lactamases, β-lactamase inhibitors have been developed in last two decades. The three most commonly used β–lactamase inhibitors are clavulanic acid, sulbactam, and tazobactam (Fig. 1.1). These inhibitors inhibit the β–lactamases through the formation of covalently bound stable enzyme-inhibitor complexes (E-I complex).

[Malcolm, 2000] Practically, t hese i nhibitors a re us ed i n c ombination w ith susceptible antibiotics, from which the activity (effectiveness) of the antibiotics towards (β–lactamases)-producing bacteria can be restored.[Malcolm, 2000; Sandanayako a nd P rashad, 2002] Unfortunately, i n recent years, these inhibitors ha ve be en f ound t o be l ess e fficient because of t he re sistance developed by bacteria mutation.[Bonomo and Rice, 1999] For example, naturally occurring, inhibitor r esistant mut ants (e.g. M 69L, R 244C. R275L) of c lass A Tem-1 a nd S HV-1 β–lactamases have b een discovered i n *E col i*.[Bonomo a nd Rice, 1999] Therefore, di scovery of n ew β–lactamase inhibitors remains an important research problem nowadays in drug discovery.

β–lactamase-based fluorescence biosensor

One effective way to reduce the proliferation of antibiotic resistance in bacteria is to pr event the improper (and w idespread) use o f β–lactam a ntibiotics. In t his regard, the abuse of β–lactam antibiotics in raising domestic animals (e.g. cows) for t he food i ndustry is r ecognized to be a s ignificant route c ontributing t o t he problem of a ntibiotic r esistance. To tackle this pr oblem, de tection of t race antibiotic contaminants i n f oods (e.g. m ilk) i s of gr eat importance. So far, a wide range of screening tests have been developed to serve this purpose, and yet many have their own limitations. For example, the Charm test, the Penzym test, and the BetaScreen test are largely semi-quantitative. HPLC analysis of antibiotic residues us ually re quires t ime-consuming s ample p reparation s teps. T he f iber opt ic and electrochemical β–lactam sensors t hat de tect t he pH ch anges d uring hydrolysis o f t he β–lactam ring b y β–lactamases ar e hi ghly s usceptible t o interference from ch anges in e nvironmental pH . Thus, i t i s hi ghly de sirable t o

develop a simple, quantitative, and sensitive analytical method that can detect β–lactam type antibiotics at trace levels.[Chan et al., 2004]

Our research group has recently constructed a "switch-on" biosensor (E166Cf) for β–lactam antibiotics from the class A PenPC β–lactamase. Since β–lactamases is a nonallosteric enzyme (no significant conformational change is induced upon ligand binding), detecting the substrate binding requires the placement of an environment-sensitive fluorophore near the active binding site. The E166Cf is constructed by replacing the Glu166 residue with cysteine (refer to List of Abbreviations, p. xx, for letter symbol representation of α-amino acids), to which the fluorescence-5-maleimide, an environment-sensitive fluorophore, is attached (Fig. 1.3). The design of this biosensor was based on the rationale that the Glu166 position is a catalytically important residue, and thus mutation of this site will significantly impair the hydrolytic activity (further dissociation) of the enzyme, and the resulting enzyme-substrate complex is stable enough to function as a biosensor. In addition, X-ray structures show that the Glu166 side chain is pointing towards the active site. Therefore, if the fluorophore is placed at this position, there is a distinct possibility that substrate binding may induce changes in local environments around the fluorophore and hence the fluorescence properties of the fluorophore may be changed and monitored. Our previous results showed that the E166Cf could exhibit a fluorescence enhancement upon incubation with β–lactam antibiotics (e.g. Penicillin G and cefuroxime) (Fig. 1.4).[Chan et al., 2004]

Recently, we have developed a new biosensor, the E166Cb, in which a badan molecule is incorporated into the Cys166 residue (Fig. 1.3). Badan is an aromatic dye that is known to give a blue shift (to lower wavelength) in emission wavelength with a concomitant increase in fluorescence intensity when it experiences less polar solvent environment.[Hammarstrom et al., 2001; Owenius et al., 1999] With this photophysical property, the badan label at the active site of the E166C mutant is expected to exhibit changes in both emission wavelength and fluorescence intensity upon binding to β–lactam antibiotics. The characteristic change in emission wavelength exhibited by E166Cb is an advantageous in that this fluorescence respond is less susceptible to changes / fluctuations in instrumental conditions such as intensity fluctuations of the light source. Our preliminary results showed that a blue shift and increase in fluorescence intensity could be observed upon incubation with penicillin and cephalosporin antibiotics (Fig. 1. 4). In some cases, E166Cb can detect antibiotics down to the 10 nM level.

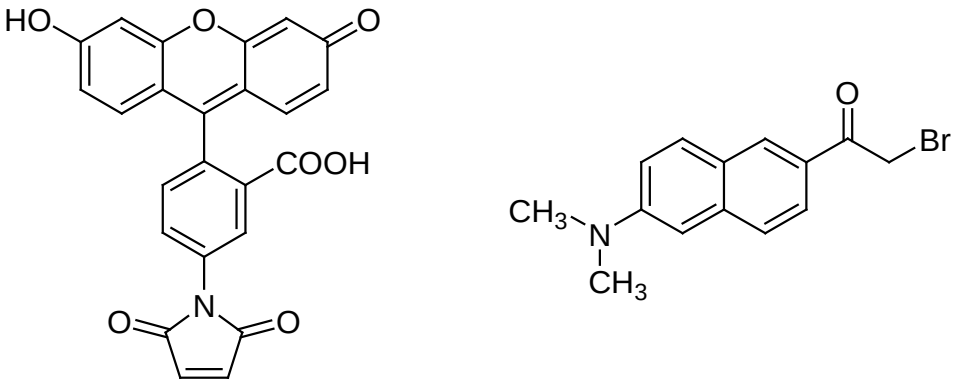

Fluorescein-5-maleimide Badan

Figure 1.3 Chemical structures of fluorophores used in this work

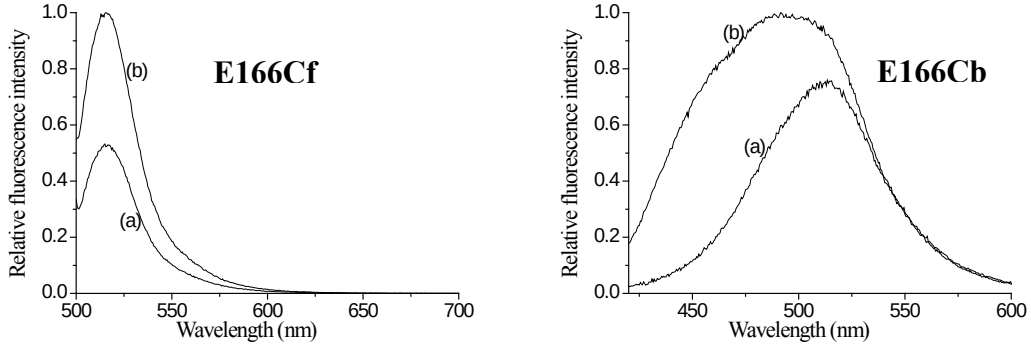

Figure 1.4 Fluorescence spectra of E166Cf and E166Cb (a) in the absence of 10^{-4} M penicillin G, and (b) in the presence of 10^{-4} M penicillin G.

1.3 Objectives of the present study

The present project is divided into two major parts. In the first part, the binding interactions between the β-lactamase based fluorescence biosensors, E166Cf and E166Cb, and β-lactam antibiotics were investigated. Issues related to the kinetics and structural basis of the biosensing mechanism of the biosensors were addressed in this part of study. In the second part, the inhibition mechanism of a β-lactam inhibitor, tazobactam, towards β-lactamases was investigated.

Part A: Studies on the biosensing mechanism of β-lactamase-based biosensor towards β-lactam antibiotics

Understanding the biosensing mechanism and properties of the biosensors is of paramount importance as this can provide an insight into the way to construct better biosensor analogs. The specific objectives of this part of investigation are:

1. to investigate the effects of the fluorophore label on the overall binding efficiency of the β–lactamase-based biosensor by mass spectrometric kinetics studies;

2. to evaluate the stability of the covalently bound enzyme-substrate complex (ES*) based on the kinetics parameters obtained in (1);

3. to determine the origin of the fluorescence changes of the β–lactamase-based biosensors upon binding with β-lactam antibiotics by complimentary time-resolved mass spectrometric and fluorometric studies; and

4. to study the structural mechanism leading to the changes in fluorescence properties of the biosensors upon binding to β-lactam antibiotics by hydrogen deuterium exchange mass spectrometry (H/D MS).

Part B: Mechanistic studies of tazobactam inhibition of β-lactamases

Understanding the inhibition mechanism of tazobactam towards β-lactamases is important for the further development of new inhibitor analogs. However, due to discrepancies in results obtained by ESI-MS under de-naturating acidic conditions and other techniques such as x-ray crystallography and UV spectroscopy, the identity of the covalently bound enzyme-inhibitor complex (E-I), and the inhibition mechanism is still controversial. In addition, the dissociation behaviour of the E-I complex, an important factor determining the inhibition efficiency of the inhibitor, remains unexplored. In present study, the specific objectives of investigation are:

1. to reinvestigate the inhibitor mechanism of tazobactam towards β-lactamases by ESI-MS under near physiological (pH 7) conditions, and

2. to study the mechanism of dissociation of the E-I complex formed between class A PC1 β-lactamase and tazobactam.

Chapter 2 Instrumentation

The mass spectrometer and other major equipments used in the present study are described in the following sections.

2.1 Waters-Micromass quadrupole – time-of-flight tandem mass spectrometer (Q-TOF 2) equipped with an ESI source

The Q-TOF 2 mass spectrometer (Manchester, UK) consists of four major components: the electrospray ionization (ESI) source, the quadrupole mass analyzer (MS1), the hexapole collision cell and the orthogonal reflectron time-of-flight (TOF) mass analyzer (MS2) (Fig. 2.1) Ions generated from the electrospray ionization (ESI) source are directed to pass through MS1, the collision cell, and eventually to a deflector electrode at which a high electric potential (980 V) is applied in pulses. This "pushing voltage" pushes the ion beam onto the TOF analyzer, in which the ions are reflected by the reflectron and finally detected by multichannel plate (MCP) detector held at 2.2 - 2.4 kV. The vacuum at the ion source, quadrupole analyzer and TOF region are ~2 mbar, 9 x 10^{-6} mbar (before introduction of extra argon gas for collision induced dissocation (CID)) and 2 x 10^{-7} mbar, respectively, and are maintained by three turbo-molecular pumps and backed by an Edwards rotary pump (Model: E1M18, North Aurora, USA). Instrumental operation is computer controlled via the Micromass MassLynx software (version 4.1).

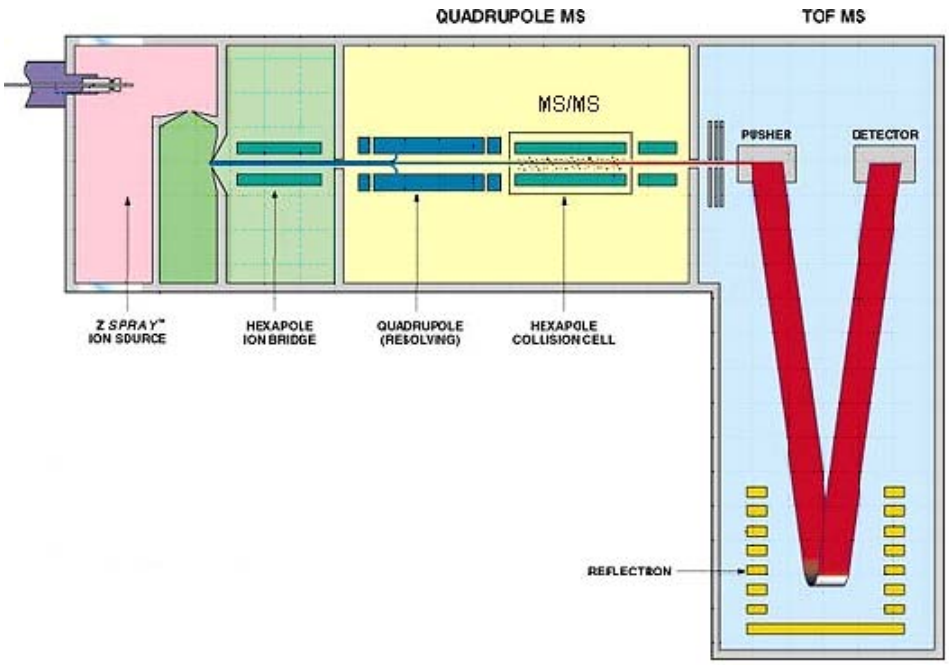

Figure 2.1 Schematic diagram of the Micromass Q-TOF 2 quadrupole time-of-flight mass spectrometer with Z-spray ESI source (taken from the Micromass Q-TOF 2 Operation Manual)

2.1.1 Electrospray ionization (ESI)

The ESI process

Solution samples are introduced into the Q-TOF 2 system via an ESI source (Fig. 2.1). Electrospray ionization is an ideal ionization method suited to biochemical analysis because it allows large and non-volatile molecules to be analyzed directly from the solution phase. In addition, the ESI source can be coupled to chromatographic interfaces such as high performance liquid chromatography

(HPLC), allowing simultaneous analysis of complex protein/peptide mixtures. ESI-MS is significantly faster, more sensitive, and more accurate than other conventional methods for molecular mass measurement of biomolecules, such as gel electrophoresis.

A schematic diagram of the ESI process is shown in **Scheme 2.1**. During ESI, the analyte sample solution is introduced through a capillary at a flow rate of (0.1 – 10 μL/min). A high voltage, which can be negative or positive depending on the type of analytes, is applied to the capillary. This applied voltage results in accumulation of charges in the liquid droplet at capillary tip. Due to Coulombic repulsion, the liquid protrudes from the tip of the capillary, which is known as the "Taylor cone". When the charges accumulate to a point at which the Coulombic repulsion exceeds the surface tension of the solution, droplets will detach from the capillary tip. With the aid of a potential difference applied between the capillary tip and the sample cone (i.e. the cone voltage), the charged droplets travel towards the sample cone (i.e. the entrance of the mass spectrometer) during which ions of the analytes are generated through several proposed mechanisms. The two most commonly applied models are the charge residue model and ion evaporation model. For the charge residue model, the increase in charge density due to solvent evaporation, which is assisted by applying a dry desolvation gas (i.e., N_2) and high temperature (100 – 200 ^{o}C), causes large charged droplets to divide into smaller and smaller droplets, and eventually into a single gaseous ion. Another mechanism, the ion evaporation model, suggests that the increase in charge density resulted from solvent

evaporation causes coulombic repulsion to overcome the surface tension of the droplets, resulting in the release of charged ions. By either mechanism, the charged ions generated by the ESI process are directed to the mass analyzer for detection in terms of their mass-to-charge ratios (m/z).[Yamashita and Fenn, 1984; Kebarle and Tang, 1993]

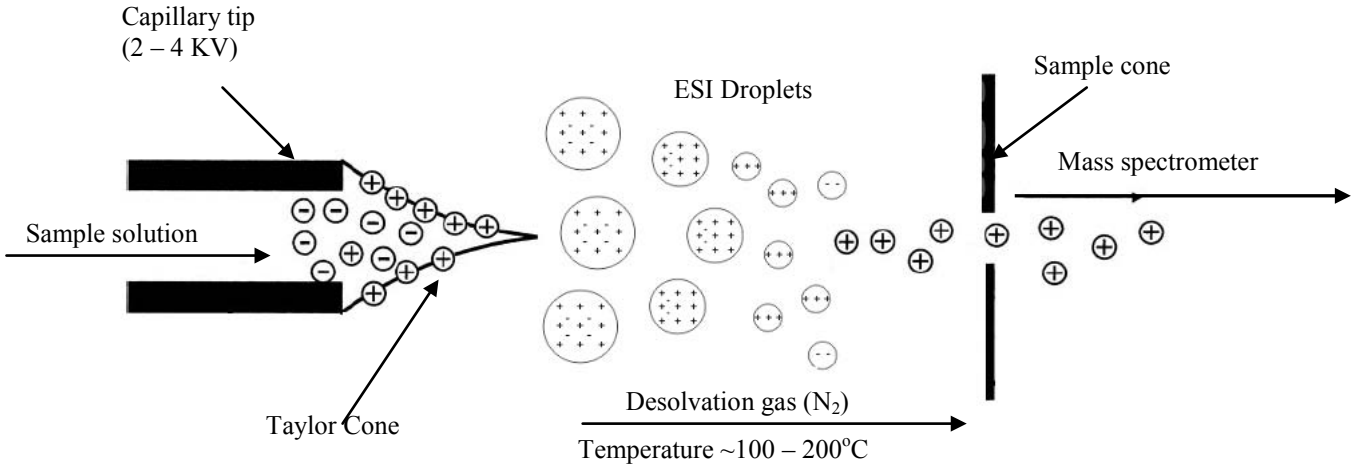

Scheme 2.1 Schematic diagram of electrospray interface

Multiply-charged mass spectra of proteins

Proteins have a wide range of ionizable sites, such as the basic amino functional group (e.g. $–NH_2$) for positive ion production (via protonation) and the acidic group (e.g. –COOH) for negative ion production (via deprotonation). Thus ESI of protein molecules often produces multiply charged ions (n= number of charge on the ion is greater than 1, and usually lies in the range of 2 – 30). It is indeed a great advantage since it extends the dynamic mass range of a mass spectrometer by n folds, allowing the analysis of large biomolecules. The raw ESI mass

spectra of proteins normally display a distribution of consecutive multiply charged ion peaks resulted from protonation $(M + nH)^{n+}$ or deprotonation $(M - nH)^{n-}$ (Fig. 2.2). The average molecular mass of the protein can be obtained by transformation (deconvolution) of the multiply charged spectra. The transformation process is based on the following equations:

$$(M + n_1 m_H) / n_1 = m_1 \qquad [2.1]$$

$$[M + (n_1 - 1)\, m_H] / (n_1 - 1) = m_2 \qquad [2.2]$$

These two equations lead to:

$$n_1 = (m_2 - m_H) / (m_2 - m_1) \quad \text{and} \quad M = n_1 (m_1 - m_H) \qquad [2.3]$$

where M is average molecular mass of the protein, m_H is the molecular mass of proton (i.e. $m_H = 1$), and m_1 and m_2 are the mass to charge ratio (m/z) of the multiply charged ions with charged state n_1 and $n_1 - 1$, respectively.

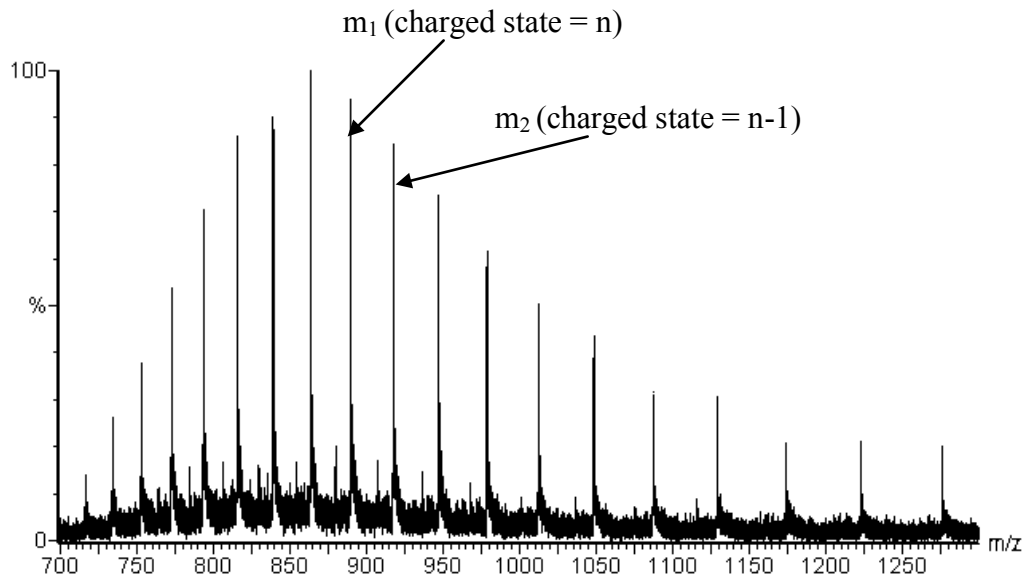

Figure 2.2 A typical multiply charged mass spectrum of a protein

2.1.2 Quadrupole mass analyzer (MS1)

In a quadrupole mass analyzer, a constant d.c. voltage (U) and R.F. voltage (Vcos(ωt), where $\omega = 2\pi f$, f = R.F. frequency (Hz), and t = time) are applied between opposite pairs of four parallel, equi-distant rods of circular cross section arranged symmetrically in the x-y plane (Fig. 2.3). The second-order Mathieu differential equation (Eqn [2.4]) is commonly used to describe the ion motions in the quadrupole mass analyzer. The motions of ions, expressed in terms of the Mathieu parameters a_u and q_u (u = x or y, and r_0 = radial distance between the centre and the rods), are given by Eqn [2.5] and [2.6].

$$\frac{d^2u}{d(\omega t)^2} + (a_u - 2q_u \cos\omega t)u = 0 \qquad \text{where u = x or y} \qquad [2.4]$$

$$a_u = 8zU / mr_0^2\omega^2 \qquad [2.5]$$

$$q_u = 4zV / mr_0^2\omega^2 \qquad [2.6]$$

Ions of a particular m/z value traveling along the *z*-direction will be stable only when its oscillatory trajectory remains within the bounds of the rods, i.e., both *x* and *y* remain less than r_0. By varying the U, V, and ω, ions of different m/z values can pass through the quadrupole filter, and thus be detected by MS2 at the downstream.

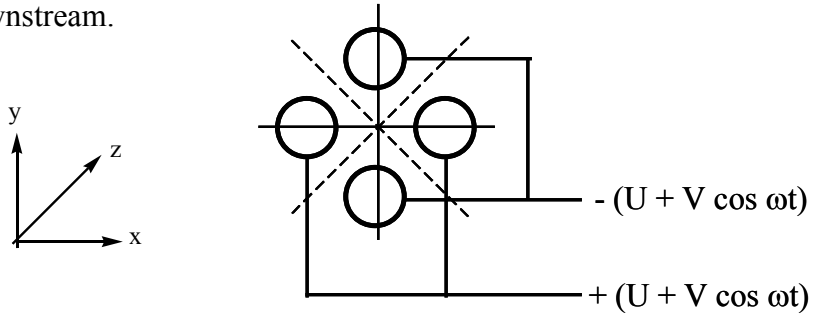

Figure 2.3 End view of a quadrupole assembly showing the applied potential and the planes of zero electric field

For simple molecular mass measurement by the TOF mass analyzer, only RF voltage is applied to the quadrupole rods, allowing all ions to pass through MS1 onto MS2. In the MS/MS scan mode (tandem mass spectrometry), the parent ion is first mass selected by the first quadrupole (MS1), accelerated to a collision energy of 0 - 200 eV, and enters the RF-only hexapole collision cell in which collision-induced dissociation (CID) of the parent ion in the presence of argon collision gas takes place. The fragment ions produced from collision-induced dissociation of the selected parent ion are directed to the second mass analyzer (MS2), the time-of-flight (TOF) mass analyzer, for m/z measurement.

2.1.3 Time-of-Flight (TOF) Analyzer

Time-of-flight (TOF) is an extensively used mass analyzer in the analysis of large biomolecules, mainly due to its high sensitivity and wide dynamic range of mass measurement (m/z range up to 100,000 – 300,000). The TOF analyzer differentiates ions of different mass-to-charge ratios (m/z) based on the difference in their kinetic energies, or simply, the time an ion takes to move through a particular distance of the flight tube. For an ion with mass ***m*** and charge ***q*** (***q*** = ze) traveling at a velocity ***v*** and processing kinetic energy (E_k):

$$E_k = \frac{mv^2}{2} = qV_s = zeV_s \qquad [2.7]$$

where V_s is the accelerating potential. The time ***t*** needed for the ion to travel the flight path with length ***d*** is given by ***t = d/v***. Thus, Eqn [2.7] becomes:

$$t^2 = \left(\frac{m}{z}\right)\left(\frac{d^2}{2V_s e}\right) \qquad [2.8]$$

Since ***d*** and V_s are fixed, *m/z* can be calculated from a measurement of t^2. That is, the lower the m/z of an ion, the faster it reaches the detector, and vice versa.

Even for ions with the same m/z, there is a thermal distribution of kinetic energy, which leads to poor resolution of mass measurement. To overcome the kinetic energy spread, an electrostatic reflector is applied. It creates a retarding field that acts as a mirror by deflecting the ions and sending them back through the flight tube (**Scheme 2.2**). The reflectron makes corrections on the energy dispersion of the ions with the same m/z value by allowing ions with more kinetic energy to penetrate into the reflectron deeper and thus spend more time in it. As a result, they can reach the detector at the same time as the slower ions.

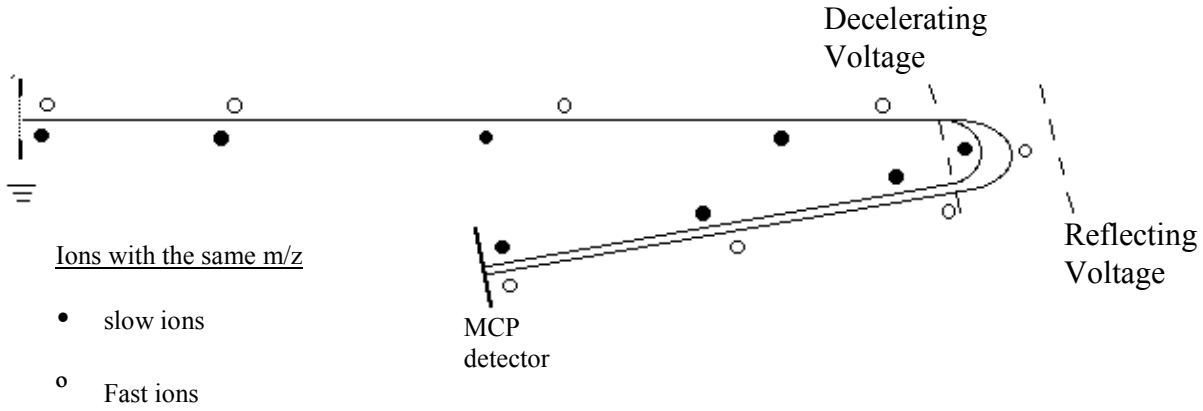

Scheme 2.2 Schematic diagram showing the ion pathways in the reflectron-TOF analyzer

2.3 Waters capillary high performance liquid chromatography (CapLC)

In the present study, a CapLC is coupled to the ESI source of the Q-TOF 2 mass spectrometer. Similar to a typical modern HPLC system, the CapLC contains a series of solvent pumps, auto-sampler, and a sample injection valve. The CapLC contains three individual solvent pumps (pump A, B, and C), and each pump delivers an eluent (solvent). Pump A, and B are mostly used for binary gradient generation, and pump C can be configured for auxiliary flow for use in column trapping or post-column delivery applications (pump C was not used in this study). A characteristic of the solvent pumping system of the CapLC is that it only delivers solvent at a very small flow rate range of 0.5 – 40 μL/min, which is compatible with the ESI process, enabling direct HPLC/MS analysis without splitting of the HPLC eluent.

The sample injection valve is a 8-ports valve with a 10 μL sample loop. Using a 96 wells auto-sampler, the sample injection process is entirely automatic, and controlled by the MassLynx 4.1 system.

In the present study, HPLC separation of peptides produced by protease digestion was achieved by the use of a Zorbax Poroshell C18 reversed phase column (Poroshell 300SB-C18, 1 x 75mm, 5 μ, Agilent Technology, USA). A distinct advantage of the poroshell column is that the stationary phase is based on superficially porous silica, rending the column capability of ultra-fast separation. This advantage is of particular significance in hydrogen-deuterium (H/D) exchange experiment since fast separation can reduce the time and hence the extent of back-exchange during the HPLC process.

2.3 Biologic SFM-400/Q quench-flow system

A schematic diagram of the SFM-400/Q quench-flow system is shown in Fig. 2.4. The SFM-400/Q instrument consists of four syringes (S1, S2, S3, and S4). In the present study, S1 was not used; S2 and S3 were used for injection of reagents, and S4 was used for injection the quench acid solution. These syringes are actuated by four independently programmable stepping motors controlled by the Bio-Kine software (version 4). The enzymatic reaction is initiated by injecting the enzyme and substration solutions via S2 and S3, respectively, into a mixer (M_1) and introduced into the delay line (DL). The reaction times are computer-controlled by varying the flow rates of the reactants in the delay line, which are in turn governed by the firing speed of the step motors. After passing through the delay line, the reaction mixture reaches the second mixer (M2), and mixes with the quench solution fired from S4. The final quenched reaction mixture is collected from the exit line (EL), and then analyzed by ESI-MS.

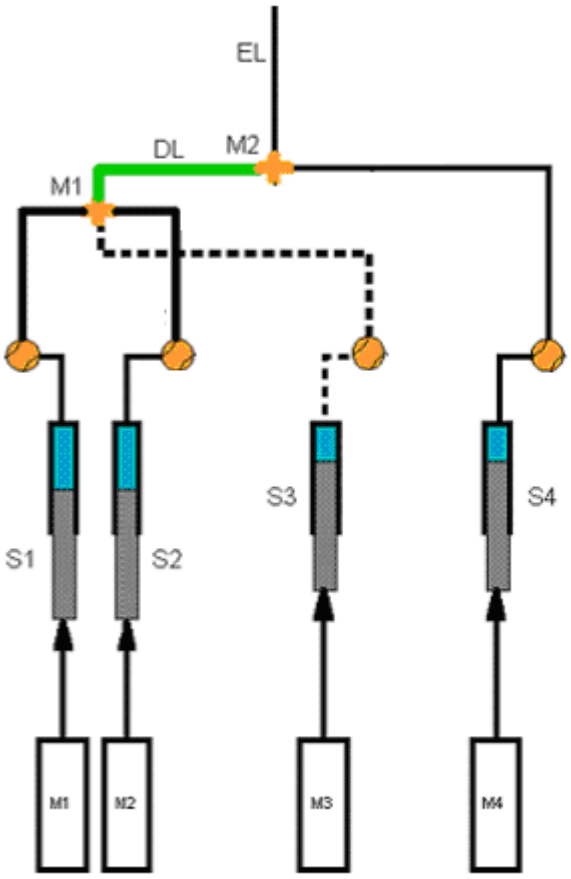

Figure 2.4 Schematic diagram of the SFM-400/Q quench-flow system (taken from the SFM-400/Q electronic manual)

2.4 Applied Photophysics SX.18MV-R Stopped-flow fluorescence spectrophotometer

Stopped-flow is one of a number of techniques used to study the kinetics of fast reactions in solution. In the simplest form of the technique, two reactant solutions from two independent syringes (S1 and S2) are rapidly mixed and introduced

into a mixing chamber, and then into an optical observation cell while the previous contents in the cell are flushed out and replaced with the fleshly mixed reacting solution. A stopping syringe abruptly stops the liquid flow while at the same time the fluorescence spectrophotometer is triggered to start data acquisition (Fig. 2.5).

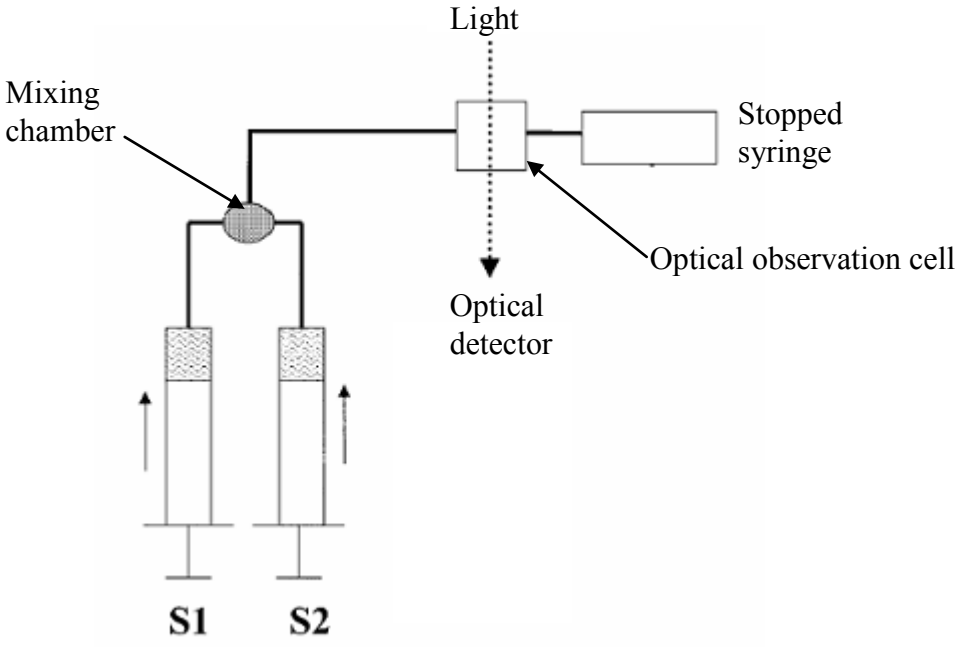

Figure 2.5 Schematic diagram of the SX.18 MV-R stopped-flow fluorescence spectrophotometer

Chapter 3 Materials

3.1 Chemicals

The chemicals used in the present study were purchased either from Panreac (Barcelona, Spain), Tedia (Fairfield, USA), and Sigma-Aldrich (St. Louis, USA). All solvents and chemicals were used as received.

Chemicals	Suppliers
Ammonium acetate (analytical grade, ≥ 99% purity)	Panreac
Acetonitrile (HPLC grade, ≥ 99.9% purity)	Tedia
Sodium iodide (analytical grade, ≥ 99% purity)	Panreac
Formic acid (~98% purity)	Sigma-Aldrich
Horse heart myoglobin (≥ 90% purity)	Sigma-Aldrich
Pepsin (from porcine gastric mucosa, (3,200-4,500 units / mg protein)	Sigma-Aldrich
Type XVIII protease (Fungal from Rhizopus species, 0.51 units / mg solid)	Sigma-Aldrich
Trypsin (from bovine pancreas, ≥6,000 units / mg protein)	Sigma-Aldrich
Deuterium oxide (D_2O) (≥ 99.9 atom % D purity)	Sigma-Aldrich
Leucine Enkephalin (≥95% purity)	Sigma-Aldrich
Penicillin G (> 99.5% purity)	Sigma-Aldrich
Ceufuroxime (> 99.5% purity)	Sigma-Aldrich
Cefotaxime (> 95% purity)	Sigma-Aldrich
Cefoxitin (>99% purity)	Sigma-Aldrich

3.2. Proteins

In this project, we have prepared the following β-lactamases / β-lactamases mutants:

(a) Class A PenPC β-lactamase E166C mutant (glutamic acid-166 mutated (replaced) with cysteine)

(b) Fluorescein-5-maleimide labeled E166C biosensor (fluorescein-5-maleimide attached to cysteine-166 of E166C, named E166Cf in this project)

(c) Badan labeled E166C biosensor (badan attached to cysteine-166 of E166C, named E166Cb in this project)

(d) Wild type class A PC1 β-lactamase

(e) Wild type class A TEM-1 β-lactamase

(f) Wild type class C P99 β-lactamase

The bacterial strains required for production of the various β-lactamases/ β-lactamase mutants were prepared/provided by Dr. Thomas C.Y. Leung's research laboratory (*Bacillics. subtilis* strain 1A304 (ϕ105MU331) for expression of E166C and P99; *BL21 (DE3)* for expression of PC1 and TEM-1). The

experimental procedures for production of these proteins are described below. The purities of the prepared proteins were all confirmed by subsequent ESI-MS analysis.

Preparation of Class A PenPC E166C β-lactamase

The E166C mutant was expressed in the *B. subtilis* strain 1A304 (ϕ105MU331). [Chan et al., 2008] The bacterial strain was streaked on an agar plate containing 5 μg/ml chloramphenicol, and the plate was incubated at 37 °C for 24 h. Afterwards, a few single bacterial colonies from the agar plate were transferred into a conical flask containing 100 ml of sterile BHY medium (37 g/l Oxoid brain heart infusion broth and 5 g /l Oxoid yeast extract) which was then incubated at 37 °C with shaking at 300 rpm overnight (about 11 -12 h) for inoculation. About 7 ml of the overnight inoculum was added to each of conical flasks containing 100 ml of sterile BHY medium, and the inoculated media were shaken at 300 rpm at 37 °C. When the OD_{600} reached 3.5-4.0, the bacterial cultures were shaken in a water bath at 50 °C for 5 min and then incubated at 37 °C with shaking at 300 rpm for another 6 h. The bacterial cultures were then centrifuged at 4 °C for 25 min at 9000 rpm. The supernatant was collected and adjusted to pH 7.0 with dropwise addition of HCl. The β-lactamase enzymes

were extracted by mixing the supernatant with 40 g of celite 545 for 20 min in an ice bath. After discarding the supernatant, the celite was washed with deionized water. The β-lactamase enzymes were eluted by mixing the celite with 300 ml of protein elution buffer (100 mM Tris-HCl, 2 M NaCl and 100 mM tri-sodium citrate, pH 7.0). The protein solution was then concentrated to 10 ml at 4 °C by means of an Amicon concentrator equipped with a piece of YM-1 membrane (Millipore MWCO = 1000).

Preparation of E166Cf and E166Cb: Labeling of fluorophore to E166C

The procedure for attachment (bonding) of the fluorophore to the E166C mutant is as follows. 4.5 ml of 5 mg/ml E166C mutant in 20 mM ammonium acetate (pH 7) was mixed with 0.5 ml of 50 mg/ml fluorophore (fluorescein-5-maleimide and badan) in dimethylformamide, and the mixture was stirred at room temperature for 1 h in dark, and then dialysed against 1 L of 20 mM ammonium acetate buffer (pH 7.0) at 4 °C for 1 day to remove excess dyes. After dialysis, the protein solution was concentrated and desalted with 20 mM ammonium acetate (pH 7.0) for at least five times using an Amicron® Ultra-15 (NMWL = 10000) centrifugal filter device.

Preparation of Class A PC1 and Class A Tem-1 β-lactamases

Histidine tagged TEM-1 and PC1 β-lactamases were prepared and provided by members of Dr. Thomas Leung's research group. Histidine tagged TEM-1 and PC1 β-lactamase were extracellularly expressed in BL21(DE3) cells transformed with plasmids pRSET K-TEM1 and pRSET K-PC1, respectively. The cultures were induced with 0.4 μM IPTG (USB) at an OD_{600} of about 0.8 and expressed at 25 °C for 20 hours. The medium collected was loaded on a nickel column, and then eluted with a linear gradient from 0 - 0.5 M imidazole. Purified proteins were buffer exchanged with 20 mM ammonium acetate (pH 7.0) at 4 °C using an Amicron® Ultra-15 (NMWL = 10000) centrifugal filter device.

Preparation of Class C P99 β-lactamase

Class C P99 β-lactamase was prepared and provided by members of Dr. Thomas Leung's research group. The *Bacillus subtilis* 1A304 (ϕ105MU331) was transformed with plasmid pSG1113/M (containing the *E. coloacae* P99 β-lactamase gene) and thermo-induced by incubating the late-log culture (O.D. ~ 3.0 – 3.5) at 50 ^{o}C for 5 min.[Tsang and Leung, 2007] The culture was harvested after 5 h at 37^{o}C. To purify P99 β-lactamase, the cells were allowed to lyse for 1 h at 30^{o}C in 20 mM sodium phosphate buffer (pH7.4) containing 0.5

M NaCl and 75 μg/ml lysozyme. The lysed cells were then sonicated with five 30 s -bursts us ing S oniprep 150 ul trasonic di sintegrator (MSE S cientific Instrument, England). Afterwards, the ba cterial l ysate w as cl eared of cel l debris by centrifugation a t 10, 000 r pm a nd 4 °C fo r 1 h. The s upernatant w as t hen loaded to a Ni^{2+} charged 5-mL HiTrap chelating column (Amersham-Pharmacia Biotech Inc.). T he ($His)_6$-tagged P99 β-lactamase w as el uted with a l inear gradient of i midazole f rom 0 – 0.2 M . T he pur ified enzyme was buf fer exchanged with 20 mM ammonium acetate (pH 7.0) at 4 °C using an Amicron® Ultra-15 (NMWL = 10000) centrifugal filter device.

Chapter 4 Experimental

4.1 Determination of average molecular mass of proteins and covalently bound protein-substrate complexes by ESI-MS

4.1.1 Analysis under typical ESI-MS conditions

Prior to mass spectrometric measurements, the proteins (i.e., the PC1, Tem-1, P99 and E166C β-lactamases and fluorophore labeled biosensors (E166Cf, E166Cb)) were concentrated, desalted, and buffer-exchanged with 20 mM ammonium acetate (pH 7.0) for at least five times by means of Amicron® Ultra-15 (NMWL = 10000) centrifugal filter devices (Millipore, Billerica, USA). The purified protein was mixed with equal volumes of acetonitrile (ACN) with 2% (v/v) formic acid, and the final sample solution was injected into the mass spectrometer via the ESI interface.

For detection of the covalently bound enzyme-substrate/enzyme-inhibitor (ES*/E-I) complexes, the binding reaction was initiated by mixing 60 μL of enzyme (E166C (1 μM), E166Cf (1 μM), E166Cb (1 μM), PC1 (20 μM), Tem-1 (20 μM), and P99 (20 μM)) in 20 mM ammonium acetate buffer at pH 7.0 with 60 μL of antibiotic/inhibitor at corresponding concentrations in the same buffer system. The reaction was allowed to take place at room temperature. At desired time intervals, the reaction was quenched by adding 120 μL of 2 % (v/v) formic acid in ACN to the enzyme solution (to unfold the protein), giving a reaction mixture in buffer/ACN (1:1 v/v) containing 1 % (v/v) formic acid (pH ~2). The final reaction mixtures were introduced into the mass spectrometer at a flow rate

of 5 μL/min with a syringe pump (Harvard Apparatus, model 22). For data acquisition, the mass spectrometer was scanned over a m/z range of 700–1600, within which the multiply-charged protein ion peaks were detected. The capillary voltage and cone voltage were set to 3KV and 30V, respectively. Nitrogen was used as the desolvation gas, cone gas and nebulizing gas. The nebilizing gas was fully opened. The desolvation gas and cone gas were adjusted to 400 and 50 L/hr, respectively. The m/z axis was calibrated externally with 10 μM horse heart myoglobin (M_α = 16950.5 Da). The raw multiply charged spectra were deconvoluted by the MassLynx 4.1 Transform Program.

4.1.2 Analysis under near physiological conditions

For analysis under near physiological conditions, the ESI source was operated in the nanospray injection mode (nano-ESI). 10 μL portion of the crude reaction mixtures in 100% aqueous ammonium acetate buffer system was directly loaded into a nanospray emitters (Model: Econo 10, New Objectives, Woburn, USA), which was then mounted into the nanospray source for analysis. The capillary voltage was tuned in a range of 1-1.5 KV until optimum sensitivity was achieved. The cone voltage was set to 30V. The nitrogen cone gas was adjusted to 50 L/hr. The desolvation gas and neubulizing gas were not required, and thus turned off in the nano-ESI mode. The mass spectrometer was scanned over a m/z range of 2,000-4,000, and the raw multiply charged spectra were deconvoluted by the MassLynx 4.1 Transform Program. The mass spectrometer was calibrated externally using sodium iodide as the mass reference compound.

4.2 Determination of specific site of modification of proteins

4.2.1 Protease digestion

Digestion with pepsin – type XVIII protease mixture

50 μL of 20 μM protein in 20 mM ammonium acetate buffer at pH 7.0 was acidified by mixing with equal volume of 20 mM ammonium acetate buffer with 2% formic acid (pH 2.2). The acidified protein solution was incubated with equal volume of protease solution, which was prepared by mixing 1mg/ml pepsin in 20 mM ammonium acetate buffer with 2% (v/v) formic acid with equal volume of 1mg/ml type XVIII protease in the same buffer system. The digestion was allowed to take place at room temperature (0^{o}C for H/D exchange experiments) for 5 minutes. The digestion product was mixed with equal volume of ACN with 2% (v/v) formic acid, and the final solution was introduced into the ESI source of the mass spectrometer at a flow rate of 5 μL/min with a syringe pump (Harvard Apparatus, model 22).

Digestion with trypsin

10 μL of 20 μM protein in 20 mM ammonium acetate buffer at pH 7.0 was incubated with trypsin in the same buffer at a mass ratio of protein:trypsin = 25:1 at 37 ^{o}C for 12 hours. The digest was introduced into the mass spectrometer via a nano-ESI needle.

ESI-MS analysis of protein digests

The mass spectrometer was scan over a m/z range of 200 – 2000, within which the singly to thirdly charged peptide ions were detected. The mass spectrometer was calibrated externally with sodium iodide. Protein fragments were identified by accurate mass measurement (<20 ppm) and tandem mass spectrometry (MS/MS). For accurate mass measurement, an internal standard, leucine enkephalin (MW = 555.2692), was used for internal lock mass calibration to achieve a mass accuracy of < 20 ppm. The mass peaks of the individual peptide fragments were assigned using the Findpept Program at http://us.expasy.org.tools/findpept.html.

4.2.2 Tandem mass spectrometry (MS/MS)

The mass spectrometer was operated in MS/MS acquisition mode. Individual peptide segment was first mass selected by the first quadrapole (MS1) and then directed into the hexapole collision cell in which collision induced dissociation (CID) took place. During the CID, depending on the size of peptides, the collision energy was set in a range of 20-70 eV until maximum number of fragment ions could be obtained. The argon pressure in the collision cell was adjusted to 4.0 $x10^{-5}$ mbar as indicated by the reading of the ionization gauge located near the collision cell.

4.3 Study of enzyme kinetics

Determination of concentration-time profiles of ES* by ESI-MS

The enzyme-substrate binding reaction was initiated by mixing 72.5 μL of 1 μM enzyme (E166C, E166Cb and E166Cb) in 20 mM ammonium acetate buffer (pH = 7.0) with 72.5 μL of desired concentrations of antibiotic in the same buffer system, and then quenched at various time intervals by addition of 145 μL of 8 % (v/v) formic acid. For short reaction times, the reaction was initiated and quenched by a quench-flow system (Biologic SFM-400/Q, Claix, France) in which the reaction times were computer-controlled by varying the flow rate of the reactants. The final pH of the quenched solution was ~2. The quenched reaction mixtures were injected into the ESI source of the Q-TOF 2 mass spectrometer (Waters-Micromass, Manchester, UK) with a flow rate of 5 μL/min. The mass spectrometer was scanned over a m/z range of 700–1600, and the raw multiply charged spectra were deconvoluted by the MassLynx 4.1 Transform Program (Waters, Manchester, UK). The resulting ESI spectrum was found to show two major peaks attributed to the free enzyme E and the enzyme-substrate complex ES^*, respectively (refer to Figure 5.3). The ratio of the concentration of the covalent enzyme-substrate complex to the total enzyme concentration ($[ES^*]/[E_{total}]$) at different time intervals was determined by measuring the peak areas of the [E] and [ES*] peaks in the mass spectrum, where $[E_{total}] = [E] + [ES^*]$.

Determination of K_d, k_2 and k_3

All kinetic equations were derived according to the reaction mechanism shown in **Scheme 1.2**. The kinetic equation for the formation of ES* is given by Eqn [4.1]:

$$[ES^*]/[E_{total}] = 1 - \exp -(k_a\, t) \qquad [4.1]$$

k_a, the apparent first order rate constant for the formation of ES*, was obtained by computer fitting the experimental values of $[ES^*]/[E_{total}]$ versus time (t) to Eqn [4.1]. A greater k_a would indicate that formation of ES* is kinetically favorable.

For the mechanism shown in **Scheme 1.2**, k_a is related to K_d and k_2 according to Eqn [4.2]:

$$k_a = k_2\, [S_0]/(K_d + [S_0]) \qquad [4.2]$$

where $[S_0]$ is the initial substrate concentration, and k_2 and K_d were obtained by computer fitting the experimental data of k_a versus $[S_0]$ to Eqn [4.2].

The first order deacylation rate constant k_3 was obtained by monitoring the degradation of ES* as a function of time.

$$[ES^*]/[E_{total}] = \exp -(k_3\, t) \qquad [4.3]$$

The k_3 values were obtained by fitting the experimental data of $[ES^*]/[E_{total}]$ versus time to Eqn [4.3].

All curve fittings were performed with Origin 6.1. A similar procedure was adopted previously by Lu et al to determine the kinetics parameters of penicillin binding proteins with β-lactam antibiotics. [Lu et al., 1999]

Fluorescence spectroscopy

50 μL of 1 μM E166Cf/E166Cb in 20 mM ammonium acetate (pH 7.0) was mixed with equal volume of 5 μM antibiotic (Penicillin G, Cefuroxime and Cefoxitin) in the same buffer system using a stopped-flow instrument equipped with a fluorescence readout device (Applied Photophysics SX.18MV-R, Leatherhead, UK). The sample was excited at 494 nm (E166Cf) / 385 nm (E166Cb) and the fluorescence signal was monitored at 515 nm (E166Cf) / 494 nm (E166Cb). Both excitation and emission slit widths were adjusted to 5 nm.

4.4 Mass spectrometric hydrogen–deuterium (H/D) exchange studies

H/D exchange reaction

The apo-enzyme and covalently bound enzyme-substrate complex (ES*) were subjected to H/D exchange. The ES* was prepared by incubating the enzyme (5mg/ml) with a 10 fold molar excess of substrates for 15 minutes. Separate experiments were performed to confirm that most enzymes were in the form of substrate-bound state within the time scale of the H-D exchange reaction. The H/D exchange reaction was initialed by mixing 20 μL of the protein solution (5mg/ml) with 180 μL of deuterium-based buffers (20 mM ammonium acetate in D_2O, pH 7). At desired time points, 20 μL portion of the reaction mixture was withdrawn and mixed with equal volume of quench buffer, which is composed of 20 mM ammonium acetate with 2% (v/v) formic acid (pH 2.2), to achieve a final pH 2.5. The quenched solutions were then frozen in liquid nitrogen and stored under –80 ^{o}C until subsequent protease digestion.

Protease digestion

The frozen sample solution was thawed in an ice bath (0^{o}C), then mixed with equal volume of protease solution (pepsin – type XVIII protease mixture) at a mass ratio of 1:1 (refer to Section 4.2.1 for details). To minimize the extra in- and out- H/D exchange, the digestion was allowed to take place for 5 minutes at 0 ^{o}C. The digest was then analyzed by HPLC-MS.

HPLC-MS Anslysis

30 μL of the digested sample was transferred into a pre-cooled auto-sampler compatible vial. 10 μL portion of the sample solution was used to rinse the sample injection needle and sample loop, and a 2 μL portion was injected into the C18 reversed phase HPLC column by an auto-sampler/injector. To minimize the extra in- and back-exchange, first, the HPLC column was immersed in an ice bath during HPLC separation, and second, the solvent gradient profile was designed to achieve fast elution in the expense of resolution. In the present experiment, all peptides were eluted within 12 minutes by a 25 minutes 8% solvent A (H_2O, 0.05%TFA) to 50% solvent B (90% ACN, 0.05%TFA) gradient at a flow rate of 40 μL/min. The mass spectrometer was scanned over a m/z range of 400 – 2000 m/z. The mass spectrometer was calibrated externally with sodium iodide.

Determination of deuterium incorporation

The percentage of deuteriums incorporation was calculated according to Eqn [4.4].

$$\% \text{ of deuteriums incorporation} = (M_t - M_o / M_{100\%} - M_o) \times 100\% \qquad [4.4]$$

where M_t, M_o, and $M_{100\%}$ are the average molecular mass of peptide after exchanging for a period of time t, non-deuterated peptide, and maximally deuterated peptide, respectively.

The deuterium contents of various peptides were determined from the centroid of the average molecular mass, which was obtained by smoothing followed by centroiding the entire isotopic envelop after the H/D exchange reaction. The back-exchange experiment was not performed since the extent of back-exchange experienced by a particular segment of apo- and substrate-bound enzyme (E166C, E166Cf, and E166Cb) were expected to be the same, and thus insignificant in the comparative analysis of data.

Chapter 5 Characterization of β-lactamase based fluorescence biosensors and their covalently bound complexes with β-lactam antibiotics

5.1 Background

Before performing various detailed studies on the biosensing mechanism of the β-lactamase based fluorescence biosensors, it is necessary to ensure that the proposed biosensors (fluorophore labeled β-lactamase mutants) were successfully constructed.

In this chapter, the identities of the fluorescein-5-maleimide labeled biosensor (E166Cf) and bandan labeled biosensors (E166Cb) were confirmed by mass spectrometric analysis, including (i) molecular mass measurement, and (ii) protease digestion followed by tandem mass spectrometry. Molecular mass measurement could confirm the successful synthesis of the fluorophore labeled proteins and estimations on the labeling efficiency (% yield) of the fluorophore labeling reaction. The specific site of fluorophore incorporation could be precisely located by tandem mass spectrometry of the peptide segments obtained after protease digestion.

An important objective of the present project is to investigate the kinetics of the binding reaction between the biosensors and β-lactam antibiotics by ESI-MS. The present mass spectrometric enzyme kinetics study is based on quantification of the enzyme–substrate complexes (ES and ES*) formed at different time

intervals throughout the course of the enzymatic reaction, and thus the capability in detecting the specific enzyme–substrate complex is a basic requirement for performing the kinetics study. In this study, we first attempted to detect and quantify by ESI-MS the covalently bound acyl-enzyme complexes (ES*) formed when the biosensors bind to β-lactam antibiotics.

5.2 Results and Discussion

5.2.1 Mass spectrometric characterization of the fluorophore labeled biosensors

The identity of the E166C mutant produced by site-directed mutagenesis was confirmed by molecular mass measurements. As shown in the transformed mass spectrum of the E166C mutant (Fig. 5.3 (a)), the measured molecular mass is 28787.2 Daltons (Da), which is in good agreement with the theoretical average molecular mass (28787.7) calculated based on the primary amino acid sequence. This result indicates that the glutamic acid at the 166 position of the wild type Pen-PC β-lactamase was successfully replaced by cysteine through site-directed mutagenesis.

After performing the mutation, the E166C mutant was subsequently labeled with fluorescein-5-maleimide and badan, producing E166Cf and E166cb, respectively. The identity of the resulting fluorophore labeled proteins was first confirmed by molecular mass measurement. The transformed mass spectrum of E166Cf shows

a single peak with a molecular mass value of 29232.5 Da, which is 445.3 Da higher than E166C. The mass increment of 445.3 Da is consistent with the sum of molecular masses of a fluorescein-5-maleimide (427.1 Da) and a water molecule (18.0 Da), suggesting that a fluorescein-5-maleimide molecule was successfully attached to E166C, and furthermore, an additional water molecule was attached to this fluorophore labeled protein. The addition of a water molecule was likely due to the formation of a protein–water adduct during electrospray ionization, since formation of adducts between protein and small solvent molecules (e.g. H_2O) derived from the solvent or the buffer during electrospray ionization is a commonly observed phenomenon.[Sun et al., 2006; Tolic et al., 1998] For E166Cb, a single peak at 28999.3 Da appears in the transformed mass spectrum. This observation is consistent with the incorporation of a badan molecule (M_α = 212.1 Da) onto the E166C mutant. The molecular masses measurements also showed that the fluorophore label was incorporated into the E166C mutant with a stiochiometry of 1:1.

Furthermore, the peaks of the fluorophore-labeled proteins for E166Cf and E166Cb account for > 95% of the total ions intensities of the mass spectra obtained, indicating that the labeling reactions were carried out with high synthetic % yield.

Table 5.1. Measured and calculated molecular masses of E166C, E166Cf and E166Cb and their covalently bound enzyme-substrate complexes formed with β-lactam antibiotics.

β-Lactamase	Calculated molecular mass (Da)	Measured molecular mass (Da)
E166C	28787.7	28787.2
E166Cf	29233.1	29232.3
E166Cb	28999.8	28999.3
E166C + PenicillinG	29121.8	29123.0
E166Cb + PenicillinG	29333.9	29334.7
E166Cf + PenicillinG	29567.2	29565.8
E166C + Cefuroxime	29151.7	29150.4
E166Cf + Cefuroxime	29597.1	29595.9
E166Cb + Cefuroxime	29363.8	29363.5
E166C + 6APA[a]	29003.8	29003.0
E166Cf + 6APA[a]	29449.2	29450.1

[a] 6APA is 6-aminopenicillanic acid (refer to Figure 1.2)

5.2.2 Determination of the location of the fluorophore label by protease digestion and tandem mass spectrometry

Although fluorescein-5-maleimide and badan are most commonly labeled on sulfhydryl group of cysteine, the specificity of the labeling reactions is highly sensitive to the external environment, such as pH. It has also been reported that the maleimide group in fluorescein-5-maleimide could also react with the primary amino groups.[Chen et al., 1985] For this reason, it is highly desirable to confirm experimentally that the fluorophore is indeed incorporated into the 166-cysteine sulfhydyl site. The site of fluorophore attachment can be determined by protease digestion of the fluorophore-labeled mutant, followed by MS/MS analysis of the peptide segments, a technique commonly used in locating the site of covalent modification of proteins.

Protease digestions

The E166C, E166Cf and E166Cb were first subjected to protease digestion. The protease solution used in the present study was a mixture of pepsin and type XVIII protease. The reasons for choosing this combination of proteases are twofold. First, these proteases are active under acidic conditions (pH 2), and thus the information obtained on the peptide segments could be usefully applied to the hydrogen-deuterium (H/D) exchange studies in the later part of the present project, which requires the protein to be digested under acidic conditions. Second, after several trials, we found that a maximum number of identifiable peptide segments could be obtained with this combination of two proteases.

The peptide segments produced by protease digestions of E166C, E166Cf and E166Cb are summarized in Table 5.2. Digestion of E166C produced 23 peptide segments, covering ~80% of the primary amino acid sequence, and including a partial segment of the Ω-loop, C166 – L169 (464.2 Da). Comparison between the peptide mass fingerprints of E166Cf and E166C shows that 22 out of the 23 peptide segments are the same, indicating that most of the peptide segments remain unchanged after the fluorophore labeling reaction. Interestingly, the peak of the free C166 – L169 segment (m/z 465.2) is found to vanish completely, and a new peak at m/z 910.2 appears in the peptide mass fingerprint of E166Cf (Fig. 5.1). The m/z value of 910.2 is consistent with the sum of molecular masses of the free C166 – L169 peptide segment, a fluorescein-5-maleimide, and a water molecule (465 + 427 + 18 = 910 Da), revealing that the fluorescein-5-maleimide is indeed incorporated onto the C166 – L169 peptide segment.

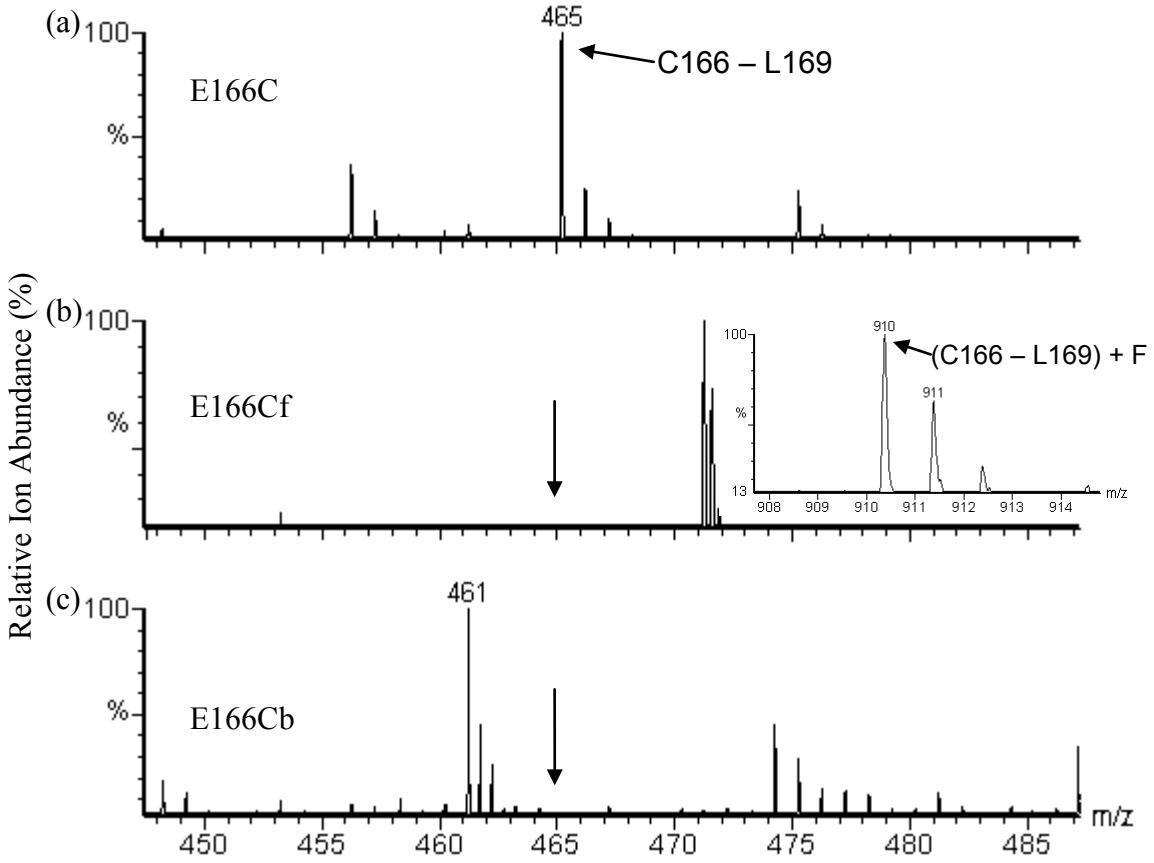

Figure 5.1. Peptide mass fingerprints of (a) E166C, (b) E166Cf, and (c) E166Cb produced from protease digestion. (F represents (fluorescein-5-maleimide + H_2O))

Table 5.2. Peptide segments produced by protease digestions of E166C, E166Cf and E166Cb. (F and B correspond to (fluorescein-5-maleimide + H_2O) and badan, respectively. √ = present and x = absent)

Measured molecular mass $[M + H]^+$	Theoretical molecular mass $[M + H]^+$	Error (ppm)	peptides	E166C	E166Cf	E166Cb
465.208	465.201	15.0	C 166 – L 169	√	x	x
910.282	910.285	-3.3	[C 166 – L 169] + F	x	√	x
-	677.309	-	[C 166 – L 169] + B	x	x	x
632.353	632.361	12.6	I 279 – K 284	√	√	√
643.307	643.309	2.4	F 66 – T 71	√	√	√
661.366	661.356	-15.8	I 206 – W 210	√	√	√
730.455	730.446	-12.6	I 186 – A 192	√	√	√
738.370	738.367	-4.3	N 92 – Y97	√	√	√
765.377	765.378	0.9	Y 274 – I 279	√	√	√
777.438	777.425	16.7	F40 – V 46	√	√	√
842.481	842.473	-9.4	I 221 – D 228	√	√	√
905.540	905.545	6	Y 72 – L 80	√	√	√
984.530	984.511	-19.4	N 170 – R 178	√	√	√
1017.524	1017.521	-2.8	L 81 – L 91	√	√	√
1028.557	1028.552	-4.5	I 221 – W 229	√	√	√
1098.746	1098.736	-9.3	A 282 – R 291	√	√	√
1205.658	1205.637	17	D 179 – L 190	√	√	√
1220.608	1220.609	0.9	W 210 – L 220	√	√	√
1374.826	1374.826	-0.3	V 249 – I 261	√	√	√
1388.714	1388.713	-0.8	A 125 – L 138	√	√	√
1445.865	1445.863	-1.6	V 249 – A 262	√	√	√
1567.801	1567.798	-2.2	H 24 – L 36	√	√	√
1768.826	1768.825	-0.6	W 229 – D 245	√	√	√

To further pin-point the site of fluorophore attachment down to the amino acid residue level, the free and fluorescein-5-maleimide attached C166 – L169 peptide segments were subjected to MS/MS analysis. Typically, interpretation of MS/MS spectrum for locating the site of covalent modification of protein is mainly based on b_i and y_i series of fragment ions, the sequence-specific fragment ions.[Paizs and Suhai, 2005] However, since the y_i series fragment ions were found to be absent in the MS/MS spectrum of the fluorescein-5-maleimide labeled peptide segment, and only the b_i series fragment ions are predominantly present in the MS/MS spectra of both the fluorophore free and fluorescein-5-maleimide labeled segments, our interpretation of the MS/MS spectrum was only based on b_i series of fragment ions only. As shown in Fig. 5.2, the MS/MS spectrum of the fluorophore free peptide segment displays distinct peaks of b_2 to b_4 ions. Interestingly, these ions were found to vanish completely in the MS/MS spectrum of the fluorescein-5-maleimide labeled peptide segment, and the corresponding ((b_2 + 445 Da) to (b_4 + 445 Da)) ions appear. The mass increment of 445 Da is consistent with the incorporation of a fluorescein-5-maleimide and a water molecule. Since the appearance of the fluoroscein-5-maleimide attached b_i (i = 2, 3, and 4) fragment ions begin at the T167 (b_2) position, the fluorophore is likely attached to the first two amino acids, the C166 or T167. As fluorescein-5-maleimide is known to most favorably bind to the sulfhydryl group of cysteine, the fluorescein-5-maleimide is most likely attached to the cystiene at the 166 position.

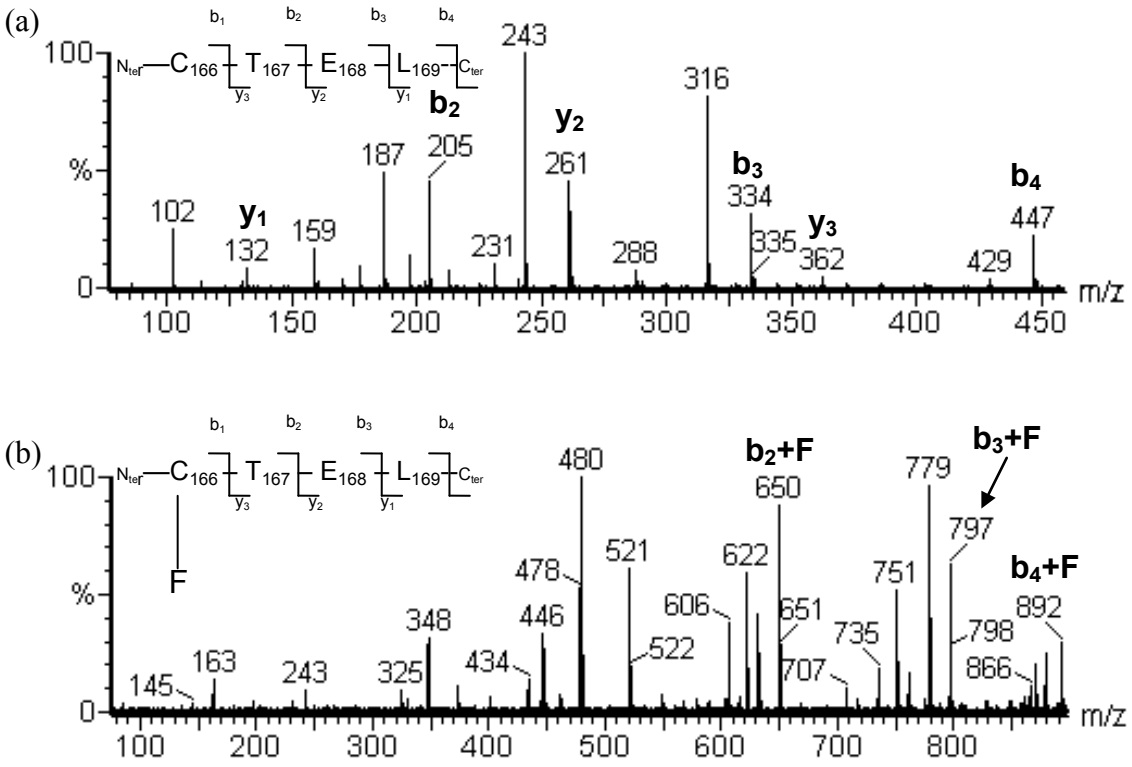

Figure 5. 2 MS/MS s pectra o f (a) f ree and (b) f luorescein-5-maleimide l abeled C166 – L169 peptide segments of E166Cf (F represents fluorescein-5-maleimide + H_2O).

For E166Cb, 22 out of 23 peptide segments are the same as E166C, and the peak of the free C166 – L169 peptide segment (465.2 Da) disappears completely in the peptide mass fingerprint. However, unlike the case of E166Cf, the corresponding badan attached C166 – L169 peptide segment peak (at 667.3 Da) could not be found, presumably the protease digestion process did not produce this peptide segment. In spite of this, the sole absence of the C166 – L169 peptide segment peak while other peptide segments do not bond to badan strongly suggests that the badan is most likely attached to the C166 – L169 segment at the C166 position.

5.2.3 Characterization of the covalently bound acyl enzyme complexes (ES*) formed between the biosensors and β-lactam antibiotics

The second part of the present study is to detect and characterize the covalently bound enzyme-substrate complexes (ES*) formed between the biosensors and β-lactam antibiotics by ESI-MS. Here we adopted the acid unfolding method (acidify to pH ~2), a commonly used technique for characterization of covalently bound protein-substrate complexes by ESI-MS.[Deterding et al., 2000; Shen et al., 2000] Under very acidic conditions, the protein is unfolded, and thus all non-covalent protein-substrate complexes, if present, are most likely to have dissociated to the free proteins. Covalently bound protein complex, however, is free from such protein-ligand dissociation since a much more stable chemical bond is formed between the protein and the substrate (ligand). Therefore, only

covalently bound protein-ligand complex is detected by this "acid unfolding" method.

The transformed mass spectra for the reaction mixtures between the biosensors and various β-lactam antibiotics are shown in Fig. 5.3, and the measured and theoretical average molecular masses of the protein-substrate complexes are summarized in Table. 5.1. Upon incubating with β-lactam antibiotics and followed by acid unfolding, a new peak at a higher molecular mass value corresponding to the covalent bound enzyme-substrate complex was generally found in the transformed mass spectrum. For penicillin G (M_α = 334.1 Da) and 6APA (M_α = 216.0 Da), the measured molecular masses of the observed complexes peaks are in good agreement with the theoretical value of adding of one molecule of the corresponding β-lactam antibiotic to the protein. For cefuroxime (M_α = 424.1 Da), a new peak at [M + 363.2] Da was detected, indicating that a -$OCONH_2$ moiety of cefuroxime (M_α = 60.5 Da) was lost upon binding to the enzyme. The loss of a moiety of -$OCONH_2$ was also observed in a previous ESI-MS study of the reaction between Tem-1 β-lactamase and cefotaxime, an analogous cephalosphorin type β-lactam antibiotic.[Saves et al., 1995] The ESI-MS results obtained also indicate that the stiochiometric 1:1 covalently bound enzyme – substrate complex was formed.

Although it appears that the covalently bound enzyme-substrate complexes (ES*) could be successfully detected, it should be pointed out that formation of non-specific complex between proteins and small molecules during electrospray ionization is also a commonly observed phenomenon.[Sun et al., 2006] To

ensure that the observed enzyme-substrate complexes were indeed formed from specific covalent binding reactions between the protein and substrates, we carried out negative control experiments in which the protein was denatured by addition of acid prior to incubation with β-lactam antibiotics. Analysis of the antibiotics under similar acidic conditions would show intense molecular ion peaks in the ESI-MS spectra, suggesting that the antibiotics were not significantly degraded under acidic conditions. As expected, only the apo-enzyme peak was present and no peak corresponding to the enzyme-substrate complex was observed when a de-naturated enzyme was incubated with the β-lactam substrate, indicating that non-specific protein-substrate complexes had not been formed to any observable or significant extent. These observations indicate that formation of the enzyme – substrate complex requires the protein to be present in its native conformation, and thus was due to specific binding of the substrate to the active site of the enzyme (protein).

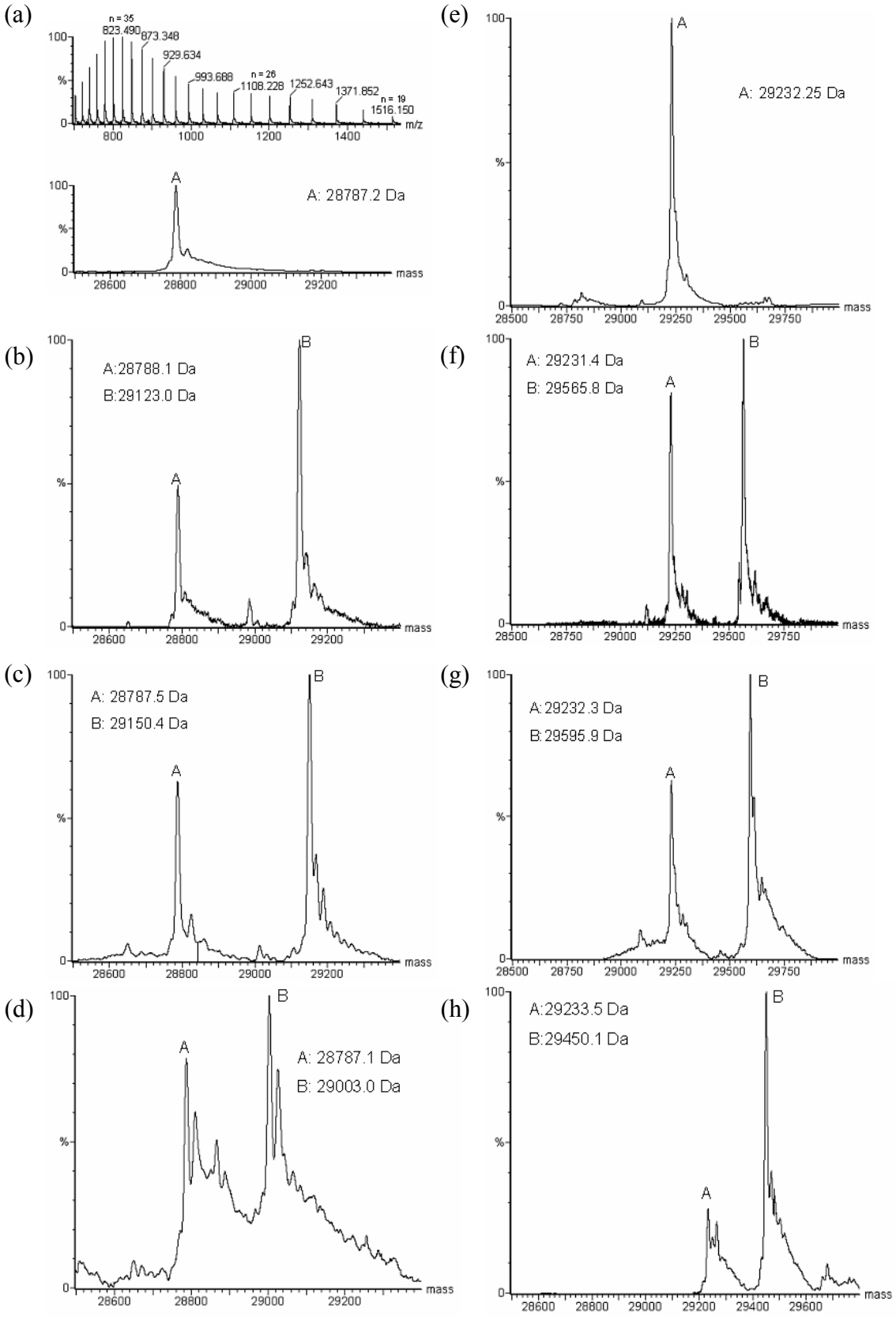
(a)
n = 35
823.490
873.348
929.634
993.688
n = 26
1108.228
1252.643
1371.852
n = 19
1516.150
m/z
A
A: 28787.2 Da
mass
(b)
A:28788.1 Da
B:29123.0 Da
(c)
A: 28787.5 Da
B: 29150.4 Da
(d)
A: 28787.1 Da
B: 29003.0 Da
(e)
A: 29232.25 Da
(f)
A: 29231.4 Da
B: 29565.8 Da
(g)
A:29232.3 Da
B:29595.9 Da
(h)
A:29233.5 Da
B:29450.1 Da

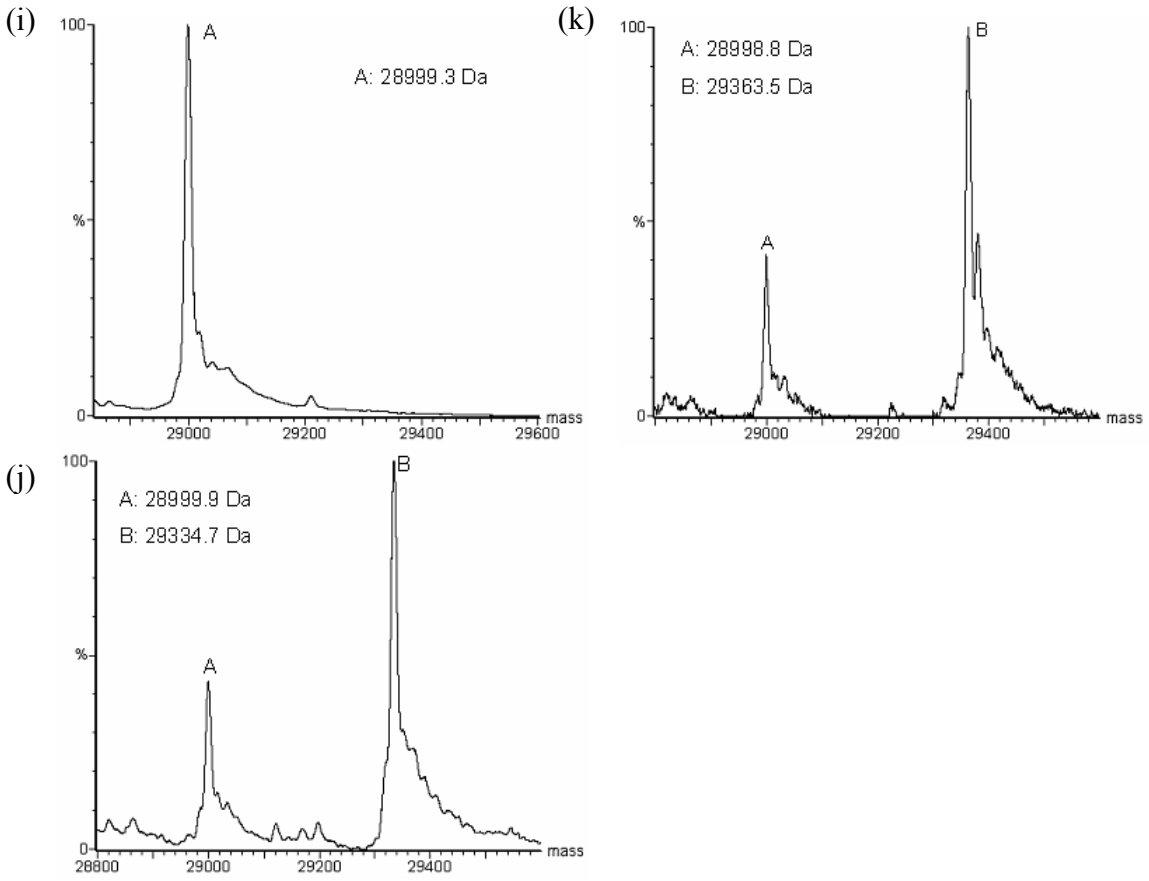

Figure 5.3. (a) Multiply-charged ESI mass spectrum (upper) and transformed mass spectrum (lower) of E166C. Transformed mass spectrum of the reaction mixtures of (b) E166C – PenG, (c) E166C – Cefuroxime, (d) E166C – 6APA, (e) E166Cf, (f) E166Cf – PenG, (g) E166Cf – Cefuroxime, (h) E166Cf – 6APA, (I) E166Cb, (j) E166Cb – PenG, and (k) E166Cb – Cefuroxime. (Peak A and B correspond to the free enzyme (β-lactamase mutant) E and the covalently acyl enzyme-substrate complex ES* **(Scheme 1.2)**, respectively.)

5.3 Conclusions

The identities of the β-lactamase based fluorescence biosensors, E166Cf and E166Cb, were confirmed by ESI-MS analysis. In general, the measured average molecular masses of the two biosensors are consistent with addition of one corresponding fluorophore molecule onto the E166C mutant, indicating that the fluorophores are successfully incorporated with a stiochiometry of 1:1. Protease digestion and tandem mass spectrometry experiments showed that the fluorophore is most likely attached to the C166 position. These experimental results confirm that the biosensors, E166Cf and E166Cb, were successfully constructed.

The covalently bound enzyme-substrate complexes (ES*) formed between the biosensors and β-lactam antibiotics were characterized. In general, the measured molecular mass of the observed enzyme – substrate complex mass peak is in excellent agreement with the theoretical molecular mass of the stiochiometric 1:1 complex. For the binding reaction with cefuroxime, the measured molecular mass suggests that a moiety of -$OCONH_2$ of the substrate was lost upon binding. The observed enzyme–substrate complexes were confirmed to be due to specific binding between the enzyme and substrate by negative control experiments. The successful detection and quantification of the ES* allowed us to proceed to the kinetics study on the binding reactions between the biosensors and β-lactam antibiotics as described in Chapter 6 of this thesis.

Chapter 6 Kinetics of binding between the β-lactamase based biosensors and β-lactam antibiotics: an ESI-MS study

6.1 Background

The previous chapter has shown that the biosensors based on E166C mutant of class A PenPC β-lactamase, E166Cf and E166Cb, have been successfully constructed. In this study, the kinetics of binding between the biosensors and β-lactam antibiotics were investigated in detail. To function as a successful fluorescence biosensor for specific molecular recognition, three criteria should be fulfilled. First, the binding affinity (efficiency) of the bionsenor towards its binding partner (i.e., β-lactam antibiotics) should be acceptably high to achieve a desired biosensing sensitivity. For this reason, it is of great importance that the artificial incorporation of the fluorophore should not significantly impair the binding affinity of the protein. Second, for enzyme-based biosensors like E166Cf and E166Cb, the substrate-bound state of the protein-substrate should be reasonably stable, so that the fluorescence emitted by this state of the complex, which is expected to be different (stronger/weaker) from that of the apo-state, is steady and measurable over a relative long period of time. Third, the biosensing process should be specific, i.e., the change in fluorescence intensity should result from the specific binding between the biosensor and a particular β-lactam antibiotic or class of the antibiotics. In this chapter, the extent of compliance of the β-lactamase-based biosensors with these three requirements was evaluated in terms of the kinetics parameters obtained from the mass spectrometric studies.

The current mass spectrometric method in studying enzyme kinetics is based on time dependent quantification of the covalently bound enzyme–substrate complex (ES*), which was described in Sections 4.3 and 5.3. For conventional spectroscopic kinetics study, Michaelis constant (K_m) and turnover number (k_{cat}) are determined to evaluate the overall binding affinity and the catalytic power of the enzyme towards its substrate. However, these two parameters are actually composed of groups of microscopic kinetic constants, and thus provide no direct information on the individual steps of the binding reaction. A distinct advantage of the present mass spectrometric method is that microscopic kinetic parameters (K_d, k_2 and k_3) of the individual steps of the binding reaction can be directly measured.[Houston et al., 2000]

In the present study, the dissociation rate constant for the formation of the reversible non-covalent ES complex (K_d), acylation rate constant (k_2), and deacylation rate constant (k_3) for the reactions between E166C, E166Cf and E166Cb towards cefuroxime, a cephalosphorin type β-lactam antibiotic, were determined. Based on the measured kinetic parameters, two parameters closely related to the biosensing properties of the biosensors were evaluated. First, the stabilities of ES* formed from each biosensor were evaluated by the relative values of k_3 and k_2. Second, the effects of different fluorophore labels on the substrate recognition step (K_d), acylation (k_2), and the overall binding efficiency (k_2/K_d) were investigated by comparing the related kinetic parameters of E166C with those of the fluorophore labeled proteins (E166Cf and E166Cb).

Another objective of this study is to confirm that the increases in fluorescence intensities of the biosensors upon incubation with β-lactam antibiotics were due to specific substrate bindings. To accomplish this task, complementary time-resolved mass spectrometric and fluorometric experiments were performed under the same reaction (binding) conditions.

Since the formation of the ES* throughout the time course of the binding reaction could be unambiguously monitored by the mass spectrometric method, the correlation (or non-correlation) between the fluorescence time profile and concentration-time profile of the ES* monitored by ESI-MS could provide an insight into whether the observed fluorescence enhancement is indeed due to formation of ES* arising from specific binding between the biosensors and β-lactam antibiotics.

6.2 Results and Discussion

6.2.1 Determination of kinetic parameters of the binding reaction between the E166Cf and E166Cb biosensors and β-lactam antibiotics:

The concentration of the covalently bound protien-substrate complex, ES*, was monitored by ESI-MS throughout the time course of the binding reaction, and the kinetics parameters (K_d, k_2 and k_3) were obtained by curve-fitting the experimental data into the kinetic equations [4.1], [4.2] and [4.3] (refer to Section 4.3) derived according to the reaction mechanism shown in **Scheme 1.2**. As shown in the time-dependent mass spectra depicted in Fig. 6.1 for cefuroxime

binding to E166Cf, the relative concentration of ES* increased as the binding reaction progressed. Plots of the relative concentrations of ES* against time (Fig. 6.2) show that the increase in concentration of the ES* with time follows an exponential rise trend as described by Eqn [4.1], and from these plots the apparent first order rate constants (k_a) (refer to Eqn. [4.1], Section 4.3) for the formation of ES* were obtained. The k_a values were found to increase with the initial substrate concentration [S_0], and the plots of k_a vs [S_0] show that the increases in k_a values with [S_0] fit well with the hyperbolic relationship as described by Eqn [4.2] (Fig. 6.2). These evidences strongly suggest that the binding reactions between our β-lactamase mutants and β-lactam antibiotics could be best explained by the binding mechanisms depicted in **Scheme 1.2**.

The kinetic parameters, K_d, k_2 and k_3, for the binding reactions of E166C, E166Cf and E166Cb with cefuroxime are summarized in Table 6.1.

Table 6.1 Kinetic parameters of E166C, E166Cf, and E166Cb binding with cefuroxime as determined by ESI-MS.

	K_d (mM)	k_2 (s^{-1})	k_2/K_d ($M^{-1}s^{-1}$)	k_3 (s^{-1})
E166C	2.9 ± 0.3	2.5 ± 0.2	$(0.9 \pm 0.1) \times 10^3$	$(7.0 \pm 0.3) \times 10^{-5}$
E166Cf	0.91 ± 0.09	1.9 ± 0.1	$(2.0 \pm 0.2) \times 10^3$	$(2.0 \pm 0.1) \times 10^{-4}$
E166Cb	0.20 ± 0.03	21.0 ± 2.7	$(105.2 \pm 21.0) \times 10^3$	$(7.6 \pm 0.6) \times 10^{-4}$

Similar to the kinetics studies by Lu et al. on penicillin binding protein (PBP), the present mass spectrometric kinetics studies were based on the 'rapid

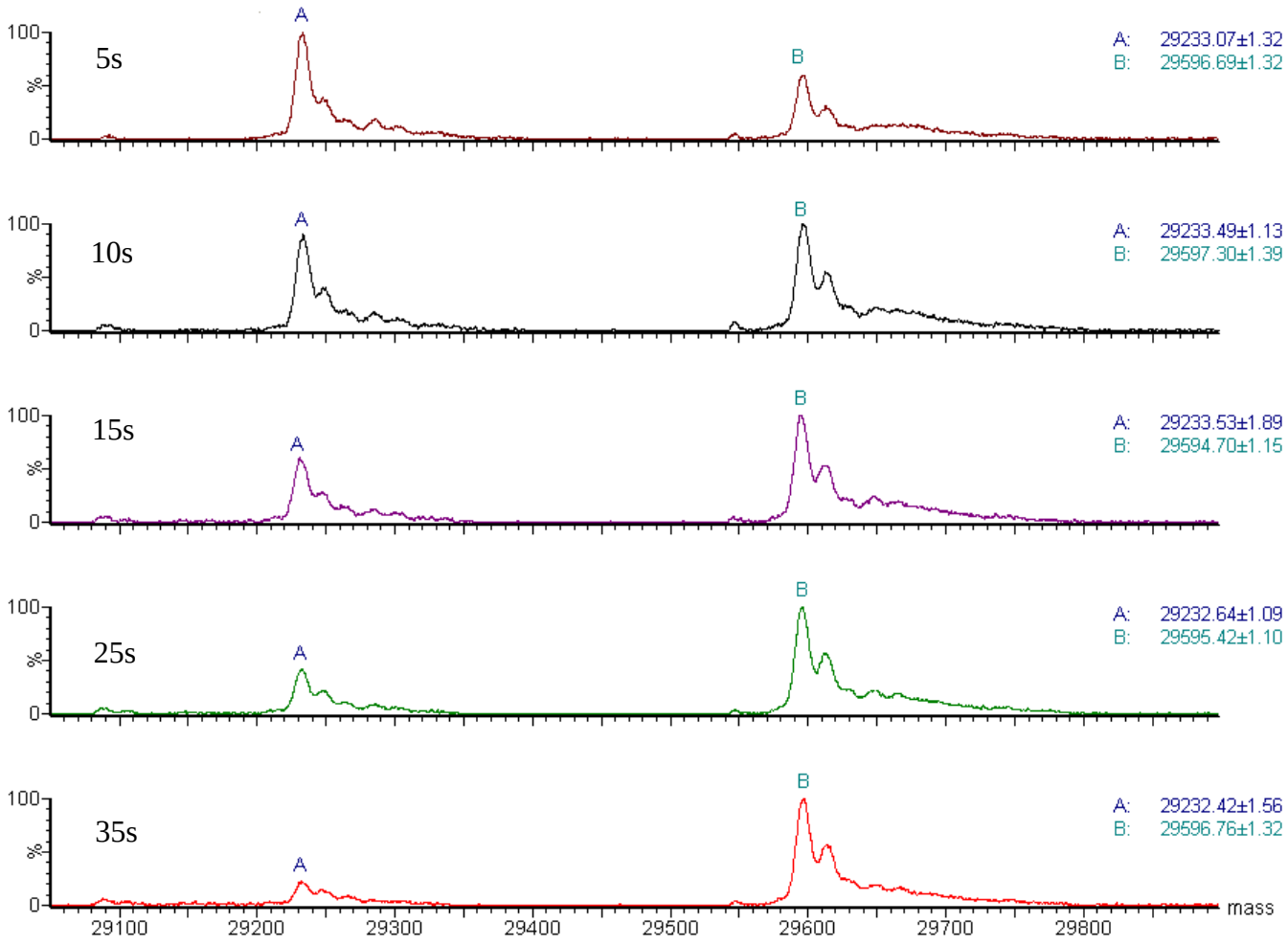

Figure. 6.1 Transformed mass spectra acquired after incubation of E166Cf (0.5 μM) with cefuroxime (25 μM) in 20 mM ammonium acetate (pH 7.0) at different time intervals. (Peaks A and B correspond to the free enzyme E and the covalent acyl enzyme-substrate complex ES*, respectively.)

equilibrium assumption' (i.e., $k_2 << k_{-1}$), so that K_d could be regarded as an equilibrium constant for the dissociation of the non-covalent enzyme-substrate complex, ES ($K_d = k_{-1}/k_1$, refer to Section 1.2). In our case, with the relatively large K_d (millimolar range) and small k_2 values (2-21 s^{-1}), and the fact that reported k_1 values for protein-ligand interactions in the literature are in the range of $10^5 - 10^8$ $M^{-1}s^{-1}$,[Lu et al.,1999] the estimated k_{-1} value is 100 – 100,000 folds larger than the k_2 value. This argues that the kinetic properties of our E166C mutant are consistent with the rapid equilibrium assumption, and the assumption could be equally applicable to the case of β-lactamase mutants (biosensors).[Lu et al.,1999; Lu et al.,2000]

The K_d values determined in our studies are generally in the millimolar range (0.2 – 3 mM), which are ~ three order of magnitudes larger than that previously determined for the reaction between the PenPC E166D mutant (glutamic acid-166 replaced by aspartic acid) and penicillin G (~ 10 μM).[Gibson et al.,1990] A larger K_d value would indicate that the first step of the binding reaction, i.e., formation of the non-covalent ES complex, is less favorable for cefuroxime than penicillin G. The kinetic results are consistent with the fact that class A β-lactamases bind rather poorer to cephalosphorin (e.g. cefuroxime used in the present study) than penicillin type β-lactam antibiotics.[Fisher et al., 2005]

The k_2 (10^1 s^{-1}) and k_3 (10^{-5} s^{-1}) obtained for our E166C mutants are in the same orders of magnitude with those predicted for E166 mutants of other class A β-lactamases.[Guillaume et al.,1997; Gibson et al.,1990] Moreover, the k_2 and k_3 values are about ~3 and ~9 orders of magnitude, respectively, smaller than those

of the *wild-type* β-lactamase–β-lactam antibiotics reaction systems.[Gibson et al.,1990] Thus, substituting Glu166 with cysteine dramatically lowers the rate of acylation (formation of ES*) and deacylation (hydrolytic dissociation of ES*) as depicted in **Scheme 1.2**. This observation is consistent with the crucial role of the Glu166 in the acylation and, in particular, the deacylation steps during the hydrolytic reaction of β-lactam antibiotics.[Meroueh et al., 2005;]

Comparison of the kinetics parameters between E166C and E166Cf shows that the K_d, k_2, and k_2/K_d of E166Cf are indeed comparable to those of E166C, suggesting that the efficiency of the initial substrate recognition step, acylation, as well as the overall binding efficiency were not impaired by the incorporation of the fluorescein-5-maleimide onto the Cys166. On the other hand, it is particularly surprising to find that the K_d and k_2 of E166Cb are ~ 10-folds smaller and larger, respectively, than that of E166C, respectively, resulting in a ~ 120-fold increase in the overall binding efficiency.

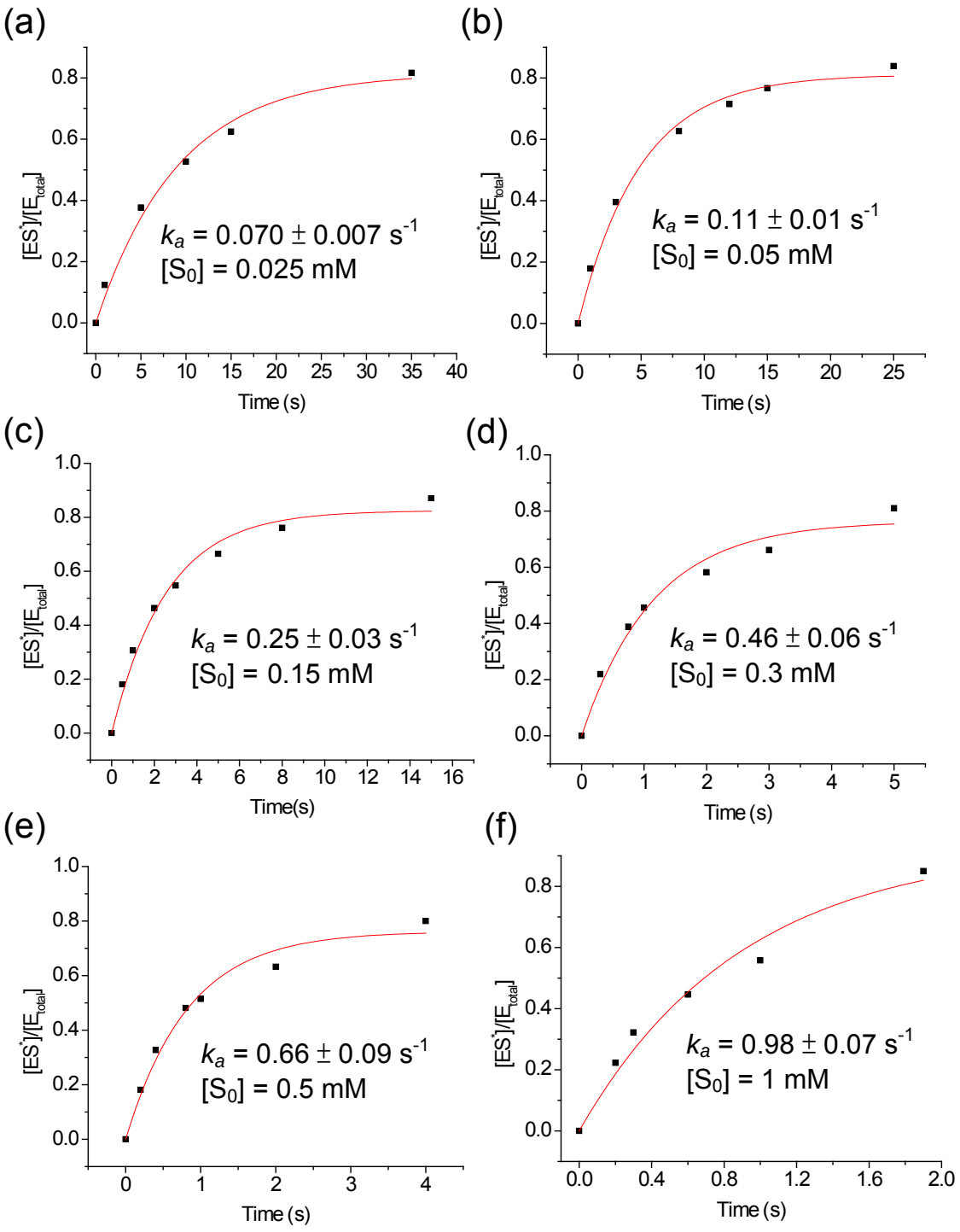
(a)
k_a = 0.070 ± 0.007 s^{-1}
[S$_0$] = 0.025 mM
(b)
k_a = 0.11 ± 0.01 s^{-1}
[S$_0$] = 0.05 mM
(c)
k_a = 0.25 ± 0.03 s^{-1}
[S$_0$] = 0.15 mM
(d)
k_a = 0.46 ± 0.06 s^{-1}
[S$_0$] = 0.3 mM
(e)
k_a = 0.66 ± 0.09 s^{-1}
[S$_0$] = 0.5 mM
(f)
k_a = 0.98 ± 0.07 s^{-1}
[S$_0$] = 1 mM
[ES*]/[E$_{total}$]
Time (s)

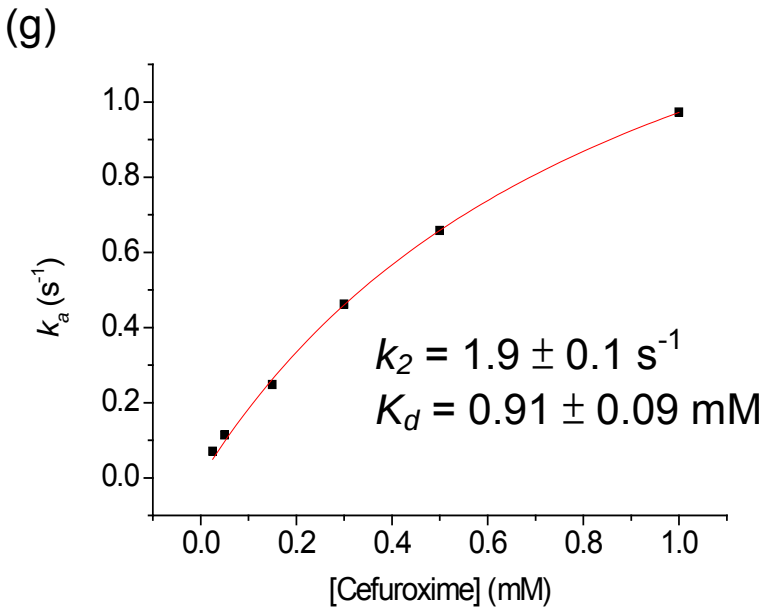

Figure 6.2 (a) Kinetic studies of E166Cf binding with cefuroxime monitored by ESI-MS. (a)–(f) Concentration-time profiles of the reaction of E166Cf with different initial concentrations of cefuroxime [S_0]. The red lines represent the best fit of the experimental data to Eqn 4.1, from which the k_a values were obtained. (g) Plot of the k_a values as a function of cefuroxime concentrations. The red line represents the fit of the experimental data to Eqn 4.2, from which the K_d and k_2 values were obtained.

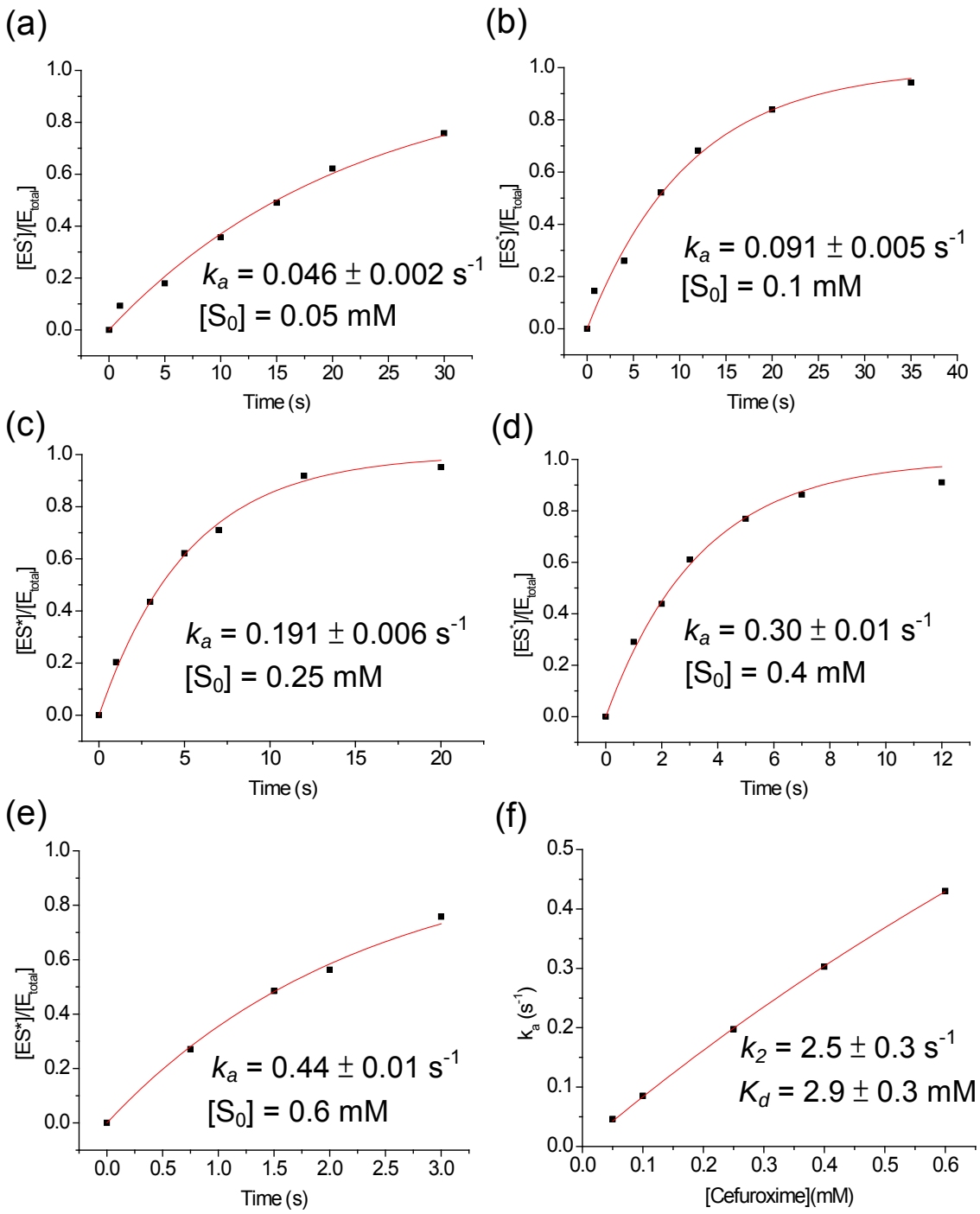

Figure 6.2 (b). Kinetic studies of E166C binding with cefuroxime monitored by ESI-MS. (a)–(e) Concentration-time profiles of the reaction of E166C with different initial concentrations of cefuroxime [S_0]. The red lines represent the best fit of the experimental data to Eqn 4.1, from which the k_a values were obtained. (f) Plot of the k_a values as a function of cefuroxime concentrations. The red line represents the fit of the experimental data to Eqn 4.2, from which the K_d and k_2 values were obtained.

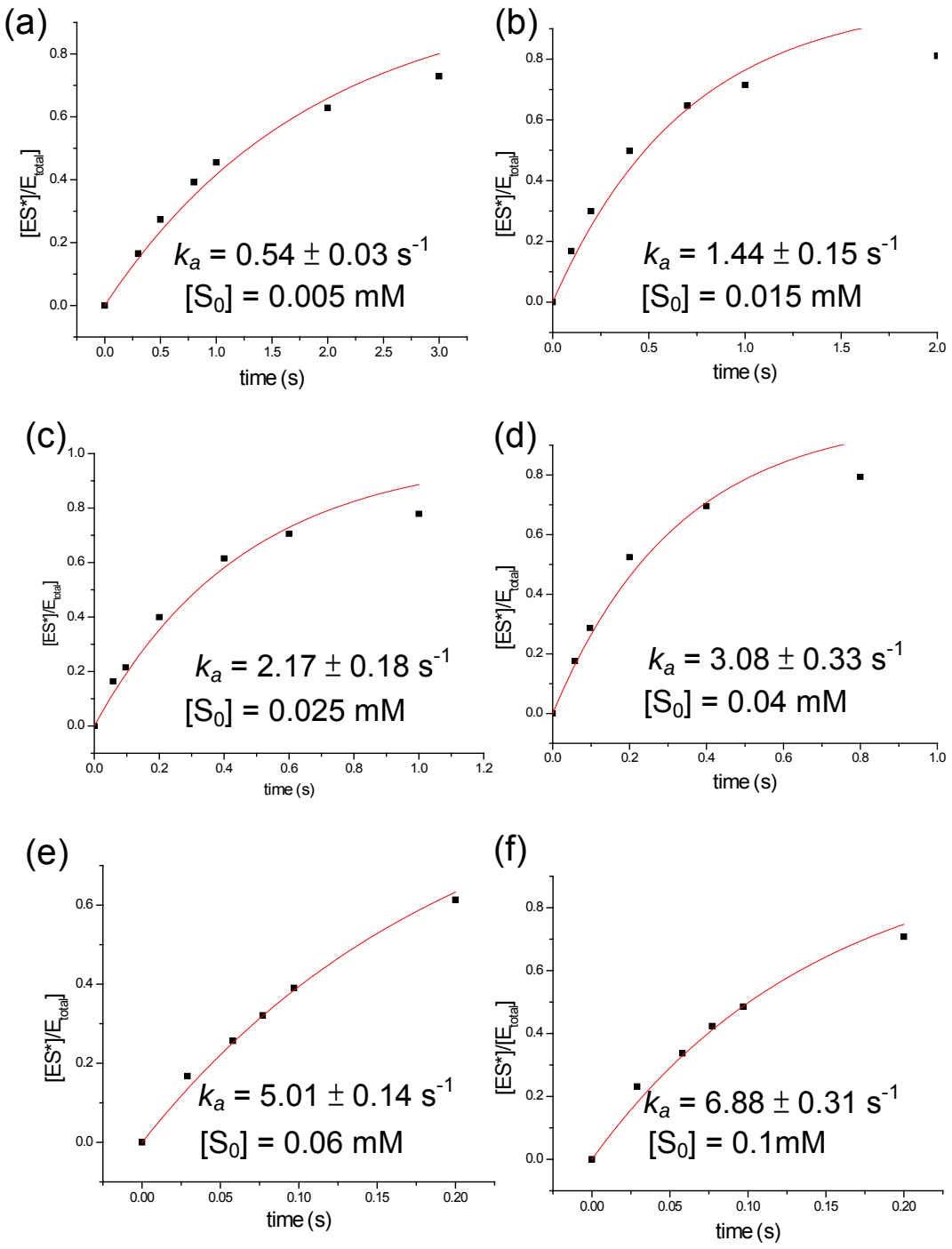
(a)
[ES*]/E_total
time (s)
k_a = 0.54 ± 0.03 s^-1
[S_0] = 0.005 mM
(b)
[ES*]/E_total
time (s)
k_a = 1.44 ± 0.15 s^-1
[S_0] = 0.015 mM
(c)
[ES*]/E_total
time (s)
k_a = 2.17 ± 0.18 s^-1
[S_0] = 0.025 mM
(d)
[ES*]/E_total
time (s)
k_a = 3.08 ± 0.33 s^-1
[S_0] = 0.04 mM
(e)
[ES*]/E_total
time (s)
k_a = 5.01 ± 0.14 s^-1
[S_0] = 0.06 mM
(f)
[ES*]/[E_total]
time (s)
k_a = 6.88 ± 0.31 s^-1
[S_0] = 0.1mM

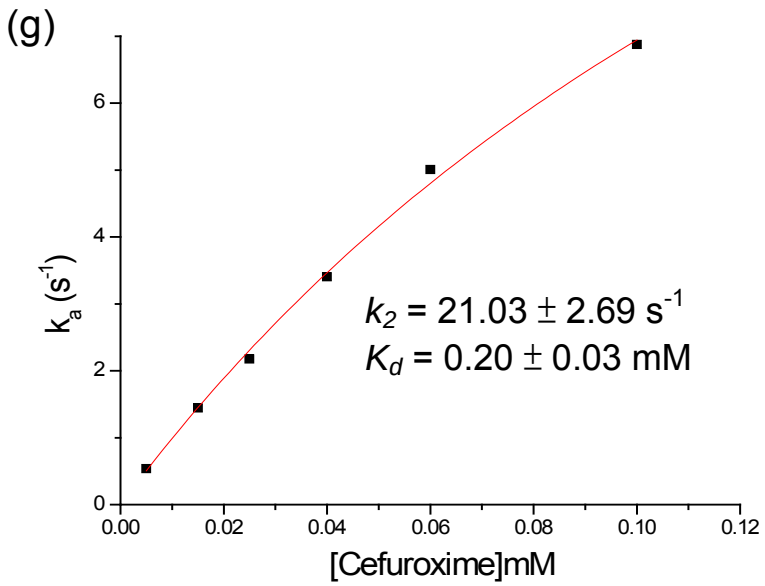

Figure 6.2 (c). Kinetic studies of E166Cb binding with cefuroxime monitored by ESI-MS. (a)–(f) Concentration-time profiles of the reaction of E166Cb with different initial concentrations of cefuroxime [S_0]. The red lines represent the best fit of the experimental data to Eqn 4.1, from which the k_a values were obtained. (g) Plot of the k_a values as a function of cefuroxime concentrations. The red line represents the fit of the experimental data to Eqn 4.2, from which the K_d and k_2 values were obtained.

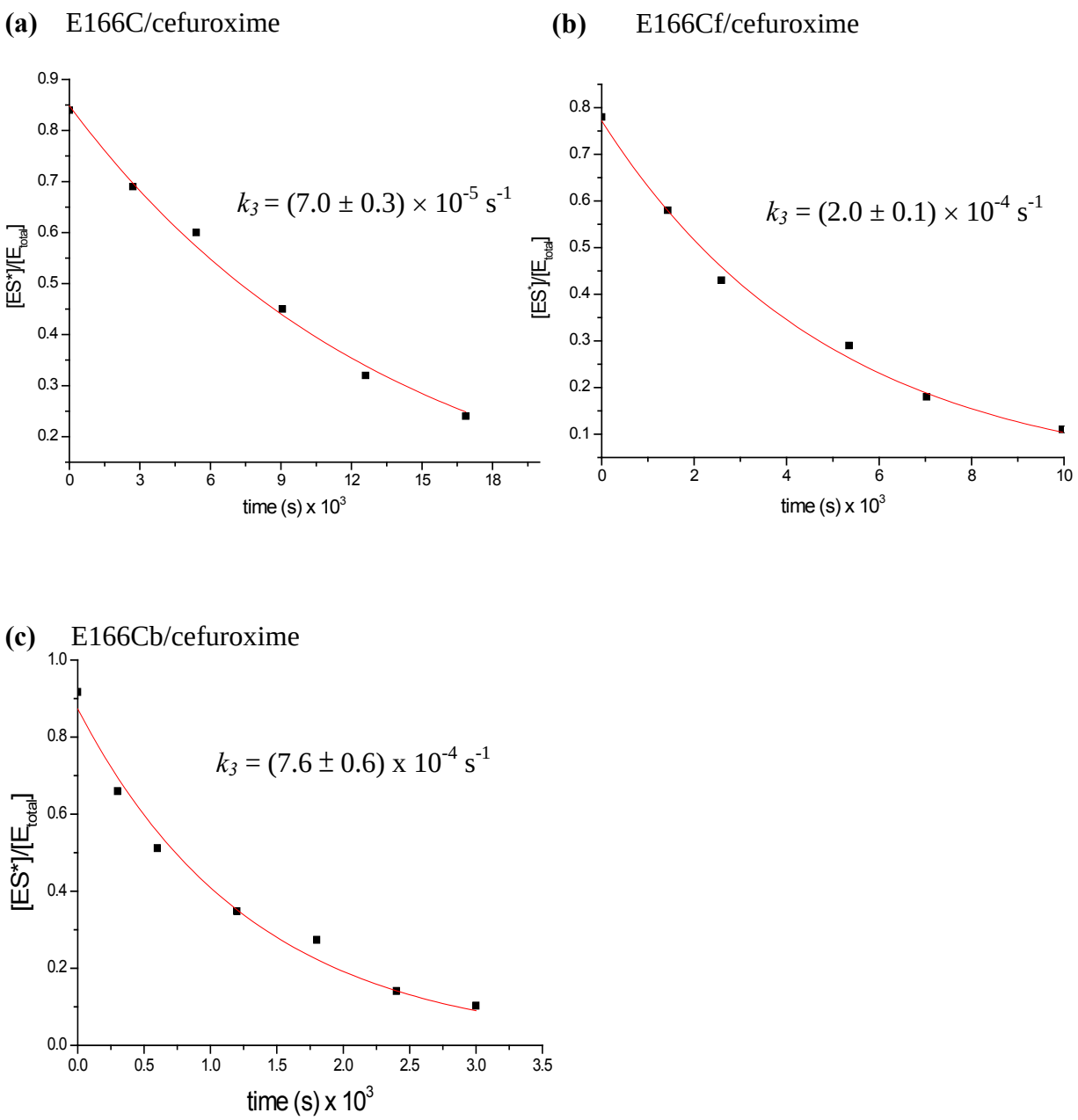

Figure 6.2 (d). Kinetic studies of the deacylation of the covalent E166C-, E166Cf-, and E166Cb-cefuroxime complexes monitored by ESI-MS. The experimental data for the deacylation of the E166C-cefuroxime, E166Cf-cefuroxime, and E166Cb-cefuroxime complexes are shown in (a), (b), and (c), respectively. The red lines represent the fit of the experimental data to Eqn 4.3, from which the k_3 values were obtained.

6.2.2 Evaluation of the stability of the covalently bound enzyme substrate complex (ES*)

The relative ease of dissociation of the covalently bound enzyme-substrate complex (ES*) is an important parameter determining the stability of the enhanced fluorescence signal produced upon substrate binding. Herein, the stability of the ES* was evaluated by comparing the values of k_3 and k_2. The k_3 values determined are generally as small as 10^{-4} s^{-1}, and are ~ 5 orders of magnitude smaller than the k_2 values (10^1 s^{-1}), reflecting that ES* is formed efficiently (relatively large k_2), and subsequently dissociates to regenerate the free enzyme with a much slower rate (small k_3). As the rate of formation is much greater than the rate of dissociation ($k_2 >> k_3$), ES* could accumulate to a relatively high concentration at steady state, allowing its fluorescence signal to remain stable over a sufficiently long period of time to be recorded. On the other hand, wild type class A β-lactamases are known to display fast k_3 deacylation rates (~10^3 s^{-1}) with cephalosphorins and penicillin type antibiotics.[Gibson et al., 1990] Thus, this kinetics property of our fluorophore-labeled mutants, E166Cf and E166Cb, is highly desirable and essential for them to function as biosensors.

6.2.3 Effects of fluorophore labeling on binding efficiency

To be a sensitive biosensor, the binding efficiency of the biosensor towards its binding target should be acceptably high. Unfortunately, in some cases, artificial incorporation of a fluorophore onto proteins has been shown to significantly

impair the binding affinities towards their binding partners, and probably due to steric hindrance mediated by the bulky fluorophore.[De Lorimier et al., 2002] In view of this, it is of paramount importance that the attachment of the fluorophore onto the residue Cys166 of our mutants, which is located near the active binding sites, should not significantly affect its binding efficiencies towards β-lactam antibiotics.

As shown in Table 6.1, the kinetic parameters related to the initial substrate binding step (K_d) and the acylation step (k_2), and therefore the overall binding efficiencies (as indicated by the k_2/K_d values, $M^{-1}S^{-1}$), show an increasing trend of 9×10^2, 2×10^3 and 1×10^5 for E166C, E166Cf and E166Cb, respectively. Clearly, the binding efficiencies were not impaired by the incorporation of the bulky fluorophores to the E166C. This could be attributed to the flexible nature of the Ω-loop and fluorophore-induced increase in flexibility of the active binding pocket, which might relieve the additional steric crowding effect exerted by the fluorophore, and thus E166Cf and E166Cb could still bind to cefuroxime efficiently.

The property of the Ω-loop of class A β-lactamases has been extensively studied. [Banerjee et al., 1998; Taibi-Tronche et al., 1996; Arpin et al., 2001; Bos et al., 2008] It is generally accepted that the Ω-loop is highly flexible, mainly because of the fact that the loop is not compactly packed with the rest of the protein molecule.[Banerjee et al., 1998; Taibi-Tronche et al., 1996; ; Bos et al., 2008; Guillaume et al., 1997] In wild-type class A β-lactamases, the residue Glu166 on the Ω-loop plays an important role in maintaining the loop's

structural integrity since it directly participates in several interactions in stabilizing the conformation of the loop. Specifically, Glu166 forms strong hydrogen bonds with the Asn170, Lys73, and Asn136 residues.[Strynadka et al., 1992; Banerjee et al., 1997] Therefore, replacement of Glu166 by cysteine in the E166C mutant might weaken these hydrogen binding interactions, and further enhance the flexibility of the Ω-loop. This argument is supported by results of an independent thermal denaturation experiment (The thermal denaturation experiments were performed by Dr. P.H. Chan of our research group), which showed that the mid-point of thermal denaturation (T_m) for the E166C mutant (50 °C) was lower than that of the wild-type enzyme (56 °C), indicating that the Glu166→Cys mutation has destabilizing effects on the protein structure and increases the flexibility of the Ω-loop.[Chan et al., 2008] Because the fluorophore is located on this loop, it is very likely that the highly flexible nature of the loop prevents the active sites from being "blocked" by the presence of a fluorophore, and therefore the overall binding efficiency of the E166Cf and E166Cb are not significantly impaired.

In addition, as indicated by results of hydrogen-deuterium exchange (H/D exchange) studies (Chapter 7), the flexibility of the active binding site region might also be enhanced by the incorporation of the fluorophore. Our H/D exchange data show that the extent of deuterium incorporations to several proteolytic segments of E166Cf and E166Cb containing the active sites were found to be higher than those of E166C, suggesting that the incorporation of the fluorophore has apparently destabilized and increased the flexibility of the binding pocket. This fluorophore-induced enhancement in the flexibility of the

active site binding pocket may also contribute to alleviating the crowded space at the active sites (Details on the effects of the fluorophore on the local dynamics at the active site region are discussed in Chapter 7).

A particularly surprising finding is that the overall binding efficiency of E166Cb towards cefuroxime is significantly higher by ~120 folds than that of E166C (Table 6.1). We hypothesize that this could be related to the significantly greater hydrophobicity of the badan molecule, and its tendency to displace/expel water molecules associated with the protein. Recently, it has been reported that a dense cluster of water molecules is packed between the Ω-loop and other regions of the binding pocket, acting as a "structural glue" to maintain the structural integrity of the binding pocket.[Bos et al., 2008] In E166Cb, the highly hydrophobic badan molecule, which is expected to be located near the binding pocket (the initial orientation of the badan molecule is discussed in Chapter 7), may compete for some of the common space with these water molecules, and displace or expel them away from the protein core. Consequently, the structural stabilization effects exerted by these water molecules are reduced/disrupted, and the flexibility of the binding pocket would be further enhanced. We propose that the ~ 10-fold increase in the efficiency of the initial substrate recognition step (as reflected by a 10-folds decrease in K_d) could be due to the further increase in flexibility of the active site binding pocket, which further relieves the steric blocking effect of the fluorophore. The increase in the rate of acylation could be attributed to the fact that as the active site becomes more accommodative and compatible with the substrate (as reflected by the decrease in K_d value), the substrate is better positioned to proceed with the

follow-up binding step. A similar scenario may also be applied to E166Cf. However, as fluorescein-5-maleimide (log D_{pH7} = 1.95) is less hydrophobic than badan (log D_{pH7} = 3.53), the effect exerted by fluorescein-5-maleimide on the cluster of water molecules may be less significant than that of the badan, and therefore the binding efficiency of E166Cf (increase by ~ 2 folds only) is not significantly increased as in the case of E166Cb. This argument is again supported by our H/D exchange results, which show that an active site segment (segment A) of E166Cf is indeed less flexible than that of E166Cb (Details are discussed in Chapter 7).

The enhancement in catalytic efficiency of β-lactamases towards β-lactam antibiotics arising from the increase in flexibility of the active site region has been previously noted by several groups.[Vakulenko et al., 1999; Taibi-Tronche et al., 1996; Banerjee et al., 1997] For example, Vakulenko's group has discussed the effects of increase in flexibility of the Ω-loop on the kinetics of the catalytic reaction with third generation cephalosphorin using the R164 and D179 mutants of class A TEM_{pUC19} β-lactamase.[Vakulenko et al., 1999] Class A β-lactamase was found to bind poorly to third generation cephalosphorin, mainly because of the severe steric hindrance between the bulky side chain of the substrate and the Ω-loop. In light of this, Vakulenko's group attempted to replace the R164 and D179 by other amino acids in order to disrupt the salt-bridge between these two residues to maintain the structural integrity of the Ω-loop. These point mutations were found to enhance the rate of acylation, deacylation, and the overall activity (reflected by k_{cat}/K_m) towards third generation cephalosphorin, most likely due to the fact that the increase in

flexibility of the Ω-loop alleviates the steric clash with the bulky side chain of the substrate. We believe that a similar scenario in relieving the steric hindrance between the enzyme and substrate may also be applicable to our biosensors.

6.2.4 Mechanism of enhanced fluorescence emission by the biosensors upon binding with β-lactam antibiotics

Complementary time-resolved mass spectrometric and fluorometric studies

It is well known that the fluorescence properties of the fluorescein-5-maleimide and badan used in this study are highly sensitive to external chemical environments, such as pH, temperature, ionic components and polarity of solvent. [Hammarstrom et al., 2001; Chen and Scott., 1985] To ensure the specificity of the biosensing process of the biosensors, it is imperative to confirm that the change in fluorescence signal is resulted from specific binding reaction upon addition of a β-lactam antibiotic, but not subtle changes in external chemical conditions. In this study, the biosensing specificity of the biosensors was confirmed by complementary time-dependent mass spectrometric and fluorometric studies. Time-dependent fluorescence spectra and concentration – time profiles of ES* monitored by ESI-MS are shown in Fig. 6.3. In general, the fluorescence signals of the biosensors increase as a function of time upon addition of β-lactam antibiotics. Interestingly, the fluorescence time profiles correlate remarkably well with the [ES*]-time profile monitored by ESI-MS, indicating unambiguously that the increases in fluorescence signals of the biosensors upon incubations with β-lactam antibiotics are most likely resulted

from specific substrate binding, i.e., mainly the formation of the covalent ES* complex (the non-covalent ES is expected to fluoresce stronger than E). In addition, these observations also reveal that the rate of change in fluorescence signal is mainly limited by the acylation binding reaction (i.e., the formation of ES*), and not other factors such as the motions of the fluorophore.

Mathematical simulation of concentration-time profiles

To validate that the increase in fluorescence signal of the biosensor is mainly due to the formation of ES*, we performed mathematical simulations of the concentration-time profiles of different species in the reaction between E166Cf and cefuroxime to estimate the relative contribution of the ES and ES* in the binding reaction (the simulations were carried out by Dr. Cedric Yiu and Miss. Kimmy Chan of our research group). More details of the mathematical simulation are described in Supporting information I. As shown in Fig. 6.4, the concentration of ES* increases with concomitant decreases in the concentrations of E and ES, and the concentration of ES* is 2 – 1,700 times higher than that of ES over the time course of the binding reaction (1 – 300 s), suggesting that the ES* is the major accumulated species in the binding reaction. This observation is consistent with the argument that the increase in fluorescence of the biosensor is mainly due to the formation of ES*.

.

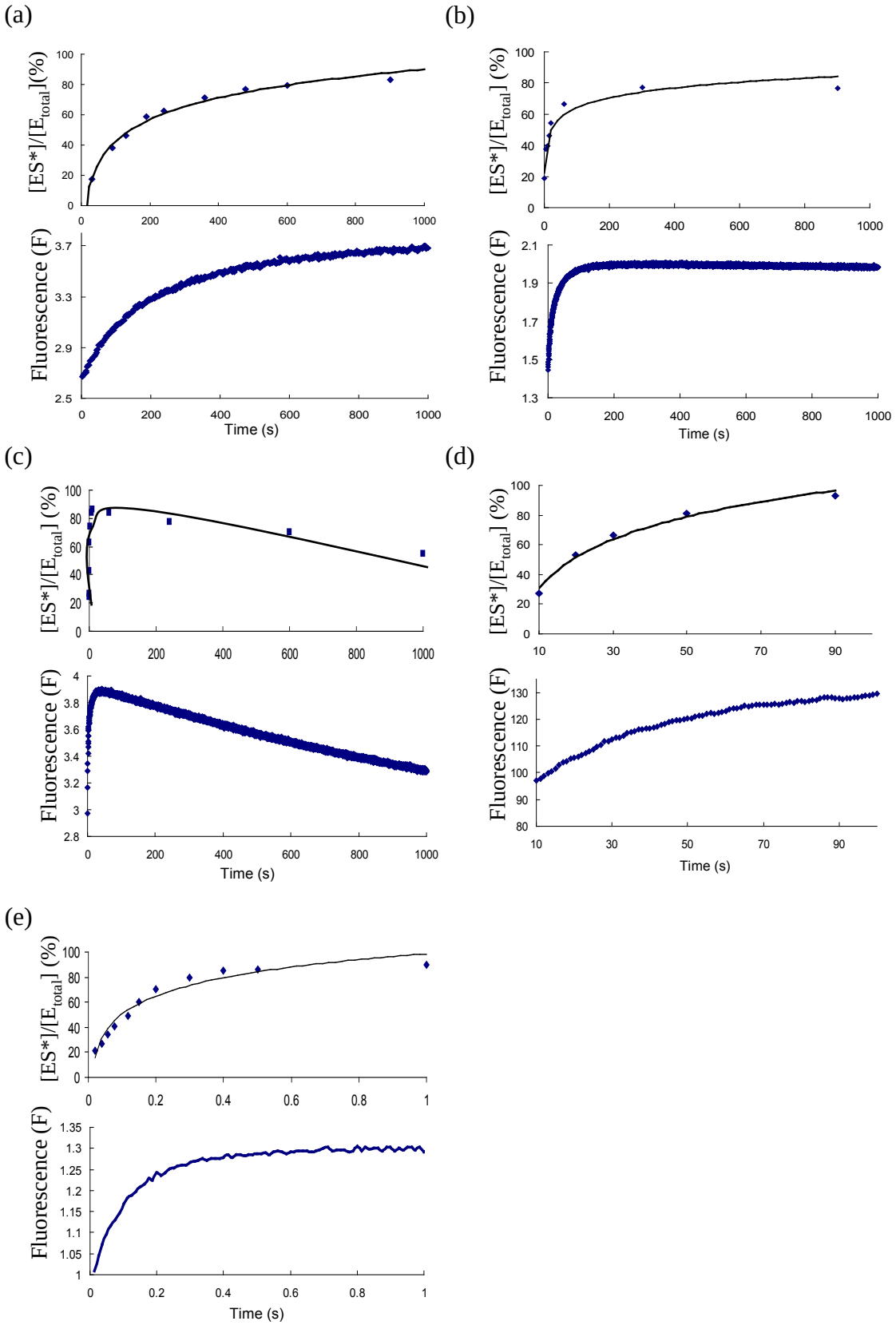

Figure 6.3. Concentration-time profiles of ES* monitored by ESI-MS (upper) and fluorescence time profiles (lower) for the binding reactions between (a) E166Cf - cefuroxime, (b) E166Cf - 6APA, (c) E166Cf - penicillin G, (d) E166Cb – cefoxitin, and (e) E166Cb – penicillin G. ([ES*] is equated to the area of Peak B, and $[E_{total}]$ is equated to the sum of Peak A and Peak B, Figure 6.1)

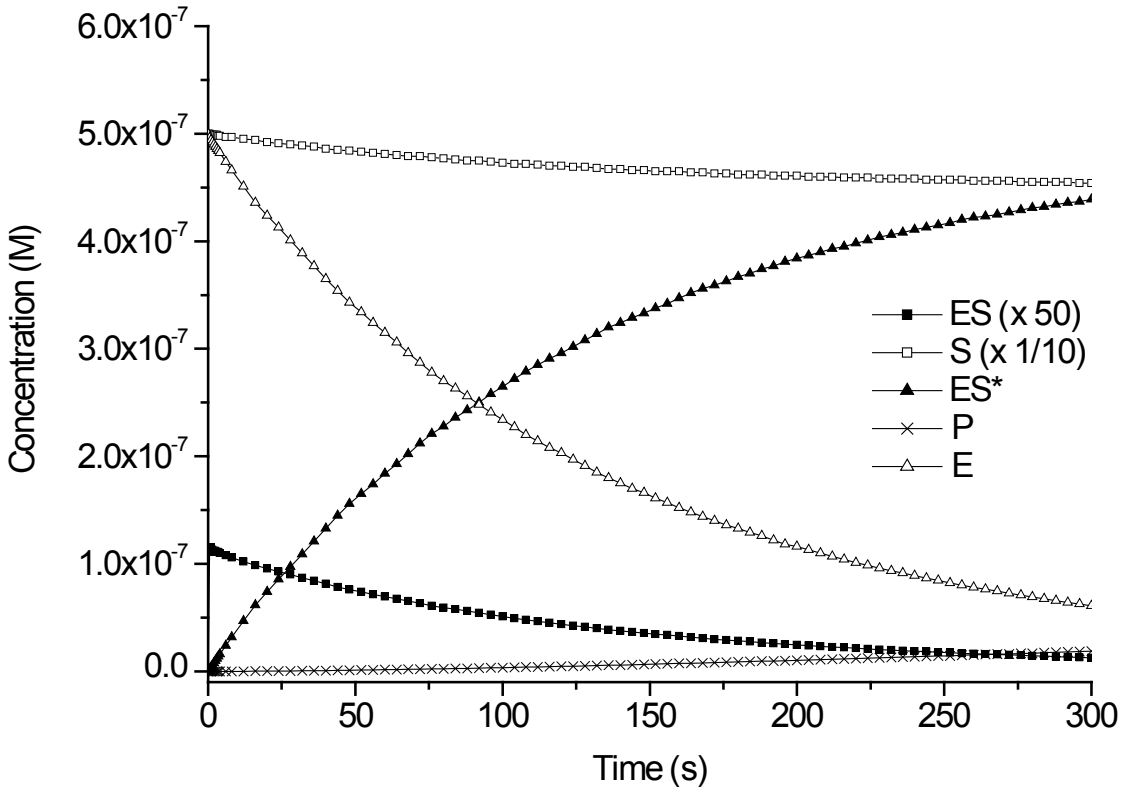

Figure 6.4. Concentration-time profiles of various states of E166Cf with cefuroxime obtained by mathematical simulation. E, ES, ES*, S and P represent free E166Cf, the non-covalent E166Cf-cefuroxime complex, the covalent E166Cf-cefuroxime complex, unhydrolyzed cefuroxime and hydrolyzed cefuroxime, respectively. To show the concentration profiles of ES and S on the same concentration scale, the concentration values for ES and S were multiplied by a factor of 50 and 1/10, respectively.

6.3 Conclusions

The kinetic properties of E166Cf and E166Cb were investigated in detail by mass spectrometric methods in this study. The microscopic kinetics parameters, K_d, k_2 and k_3 for the binding reactions between the biosensors and β-lactam antibiotics were unambiguously determined. Unlike the wild type class A β-lactamase, the E166C, E166Cf and E166Cb mutants show significantly reduced k_3 (deacylation dissociation rate) values in the order of 10^{-4} s^{-1}, and are ~5 orders of magnitudes smaller than k_2 (10^1 s^{-1}), so that the ES* could accumulate to a high concentration for its fluorescence signal to be easily monitored. This special kinetic property of the E166Cf and E166Cb enables them to function as specific and sensitive biosensors for β-lactam antibiotics.

Interestingly, our results show that the K_d, k_2 and k_2/K_d values of E166Cf are comparable to that of E166C, indicating that the substrate recognition (K_d), acylation (k_2), and therefore the overall binding efficiency (k_2/K_d) were not impaired by the incorporation of the bulky fluorescein-5-maleimide. We believe that these results are probably due to the flexible nature of the Ω-loop and the fluorophore-induced enhancement in the flexibility of the active binding pocket, relieving the steric blocking effects produced by the introduction of the fluorophore.

To our surprise, the overall binding efficiency was increased by ~120 folds by incorporation of the badan fluorophore. The extraordinary increase in overall binding efficiency in the case of E166Cb might be attributed to the highly

hydrophobic nature of the badan molecule, which tends to expel/displace the dense water cluster responsible for stabilizing the structural integrity of the active site binding pocket. Consequently, the flexibility of the active site binding pocket would be enhanced to an even greater extent, and therefore the steric hindrance imposed by the fluorophore could be further relieved.

Complementary time-dependent mass spectrometric and fluorometric studies show that, in general, the time-resolved fluorescence profiles correlated well with the concentration-time profiles of the covalently bound acyl enzyme-substrate complex (ES*) monitored by ESI-MS. This observation implies that the fluorescence emission enhancement observed for the biosensors is due to specific substrate binding, i.e., mainly the formation of ES*. This argument was further validated by mathematical simulations of concentration-time profiles of different reacting species in the binding and dissociative hydrolysis of cefuroxime, which show that the ES* is indeed the major accumulated species throughout the course of the binding reaction.

To conclude, our present kinetics data suggested that the biosensors are capable of forming a stable substrate-bound state (ES*) with reasonable binding efficiency and specificity. Hence, our biosensors are desirable candidates applicable to the specific detection of β-lactam antibiotics.

Chapter 7 Biosensing mechanism of β-lactamase based fluorescence biosensors: studies by mass spectrometric hydrogen-deuterium exchange

7.1. Background

In the previous chapter, it has been shown that the changes in fluorescence properties of the biosensors upon addition of β-lactam antibiotics were mainly due to specific substrate binding and formation of the covalent substrate-bound complex (ES*). Here we come to another question: "Why does the substrate-bound state of the biosensor fluoresce stronger than the apo-state (in the absence of the substrate)?". According to the intrinsic properties of the fluorophores, the changes in fluorescence properties are likely to have resulted from changes in solvent polarity of the local environment surrounding the fluorophores. For E166Cf, the increase in fluorescence signal upon substrate binding suggests that the fluorescein-5-maleimide fluorophore is exposed to a more polar environment (gaining a higher solvent accessibility) in the substrate-bound state.[Chan et al., 2004] In contrast, the observed fluorescence enhancement at lower wavelength upon substrate binding for E166Cb is probably due to exposure to a less polar solvent environment (and reduction in solvent accessibility) around the badan molecule.[Hammarstrom et al., 2001; Owenius et

al., 1999] In this part of our study, the mechanisms leading to the changes in local environments around the fluorophores were investigated by hydrogen-deuterium (H/D) exchange mass spectrometry, a technique extensively used to study changes in protein structure and dynamics (refers to Section 1.1.3 on the basic theory of H/D exchange reaction of amide protons in proteins).

We adopted a two step approach to this research problem. First, the initial orientation of the fluorophore was predicted based on the effect of the fluorophore on H/D exchange behavior, which may reflect the structure and dynamics of various regions (peptide segments) of the protein. Second, the "movement" (change in orientation) of the fluorophore that may lead to enhancement in fluorescence upon binding to β-lactam antibiotic was probed according to the differences in H/D exchange properties between the apo- and substrate-bound states of the biosensor. Taking these information together, a biosensing mechanism by which the biosensors change their fluorescence signals upon binding to a β-lactam antibiotic was proposed. This proposed mechanism was further validated by results from complementary X-ray crystallographic and molecular modeling studies.

7.2 Results and Discussion

7.2.1 Interpretation of H/D exchange results: evidence for a 'spatial displacement' mechanism between the binding substrate and the fluorophore

Interpretation of H/D exchange results

The H/D exchange reactions were initiated by incubating the proteins with 10-fold volume excess of buffer in D_2O, and then quenched at different time intervals by lowering the pH to ~ 2.2. To obtain local conformational and dynamic information of the protein, the quenched samples were digested with protease (sequence coverage is ~ 80 % as described in Section 5.2), and the proteolytic segments were subjected to HPLC-ESI-MS analysis. Examples of ESI-MS spectra for the proteolytic segment Tyr72 – Leu80 obtained at different time intervals are shown in Fig. 7.1. In general, the H/D isotopic distributions were shown to gradually shift to higher m/z values as the H/D exchange reaction proceeded, and no evidence for a bimodal distribution of isotopic masses could be found. These observations strongly suggest that the H/D exchange reactions

of our β-lactamase mutant biosensor most likely follow the EX2 regime (details of EX1 and EX2 kinetics are discussed in Section 1.1.3). The % of deuterium incorporation at different time intervals were quantified according to Eqn [4.4], from which plots of % deuterium incorporation versus time (H/D exchange time profile) were constructed (Fig. 7.2).

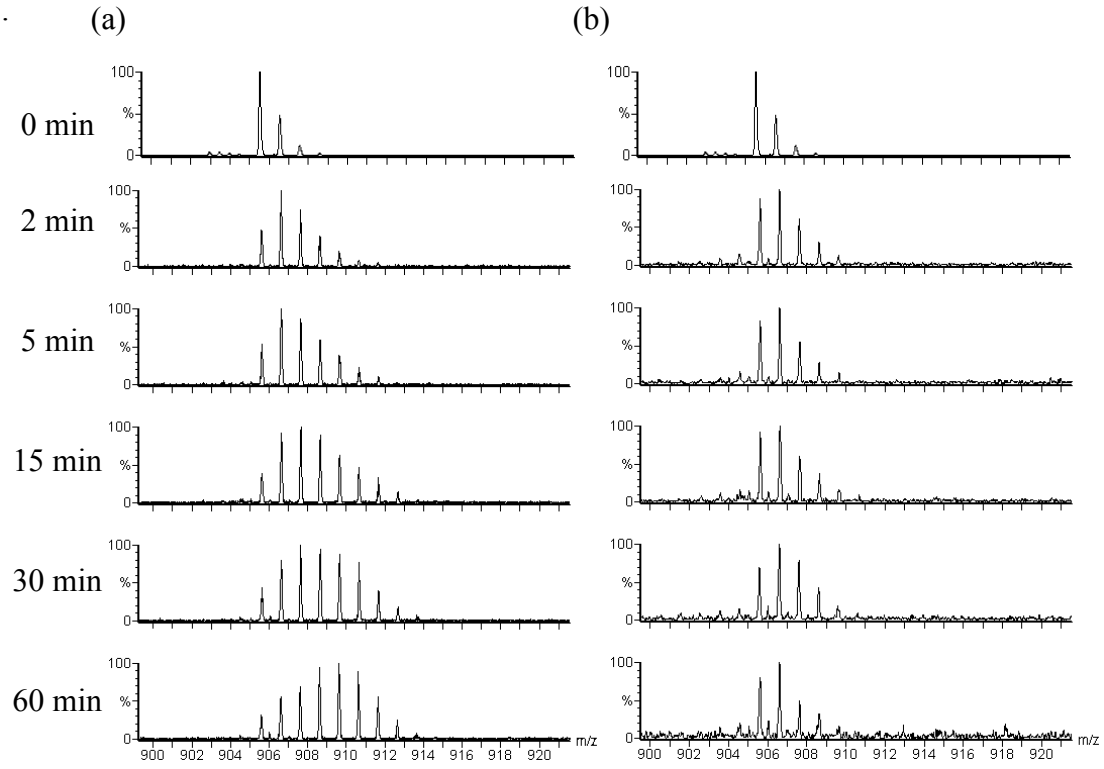

Figure 7.1 ESI-MS spectra of the proteolytic Tyr72 – Leu80 peptide segment (segment A) of (a) apo-state, and (b) substrate-bound state of E166Cb with cefotaxime acquired at different H/D exchange time intervals.

To investigate the effects of the fluorophore on the structure and dynamics of the protein, the H/D exchange results of E166C, E166Cf and E166Cb in the apo-form are compared. H/D exchange time profiles for proteolytic segments of the three protein species are shown in Fig. 7.2. Comparative analysis of these profiles shows that the extent of H/D exchange for 16 of the 19 proteolytic segments are similar for E166C, E166Cf and E166Cb, indicating that the incorporation of fluorescein-5-maleimide or badan does not induce significant global conformational and dynamic changes on the protein (Fig. 7.2). This observation is consistent with results of complementary circular dichroism (CD) and preliminary X-ray crystallographic studies (The CD and X-ray crystallographic studies were performed by Dr. P.H. Chan and Dr. Y. X. Zhao, respectively, of our research group, refer to Supporting information III). The CD spectra obtained for E166C, E166Cb and E166Cf exhibit no significant differences (data not shown), and the X-ray structures of these three proteins can be superimposed with each other. These results indicate that the incorporation of the fluorophore does not significantly perturb the overall protein structure (Fig. 7.3 (a)).

On the other hand, the extent of deuterium incorporation of several proteolytic segments of the fluorophore-labeled proteins (E166Cf and E166Cb) are different from that of E166C, revealing that the incorporation of fluorescein-5-maleimide or badan might induce local conformational and/or dynamic changes on specific peptide segments of the protein. For both E166Cf and E166Cb, three proteolytic segments, Tyr72 – Leu80 (segment A), Ala125 – Leu138 (segment B), and Ile221 – Trp229 (segment C), exhibit higher % of deuterium incorporation than those of E166C. For segment A, the increase in % of deuterium incorporation for E166Cb (~30 %) is more significant than that of E166Cf (~13 %). These changes are not overtly large (13 - 30 %), but reproducibly observed as indicated by results from independent multiple runs (n = 3). The standard derviaiton (represented by the displayed error bars in the H/D exchange time profiles shown in Fig. 7.2) obtained were found to be ≤ 3% for these three peptide segments.

To examine the changes in local conformation and dynamics induced upon substrate binding, the proteins were incubated with the substrate, cefotaxime, prior to initiating the H/D exchange reactions. Cefotaxime was used in this study because this antibiotic is highly resistant to the hydrolytic reaction of the

enzyme, and thus the resulting ES* formed is expected to be stable for observation of the H/D exchange reactions. In addition, both E166Cf and E166Cb exhibit distinct fluorescence changes upon binding to cefotaxime, making this antibiotic a good candidate for studying the mechanism leading to the observed changes in fluorescence behavior of the two biosensors. As shown in Fig. 7.2, no remarkable change in H/D exchange level could be observed for proteolytic segments of E166C upon binding to cefotaxime. This result is consistent with literature reports that no significant global conformational change was induced when class A Glu-166 mutants were bound to β-lactam antibiotics.[Strynadka et al., 1992; Maveyraud et al., 1998] Interestingly, for E166Cf and E166Cb, the H/D exchange levels of segments A and B appeared to decrease and returned to the levels similar to that of E166C upon substrate binding, suggesting that the local conformation / dynamics of these regions of substrate-bound E166Cf and E166Cb are similar to that of E166C.

Segment	E166Cb	E166Cf	E166C
(a) Y72 – L80 (Segment A)	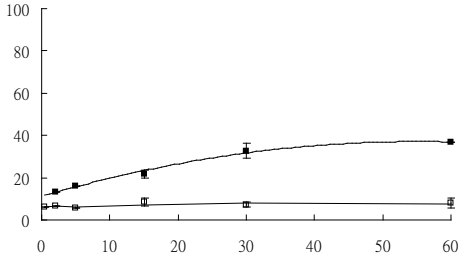	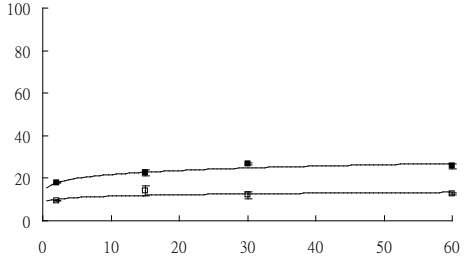	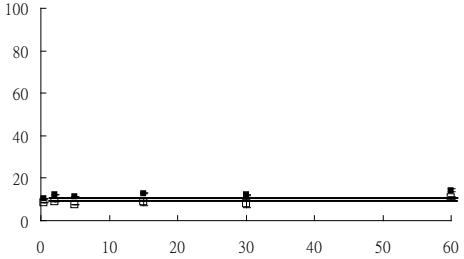
(b) A125 – L138 (Segment B)	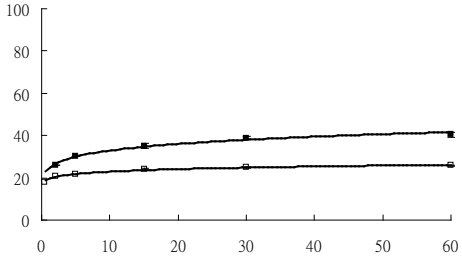	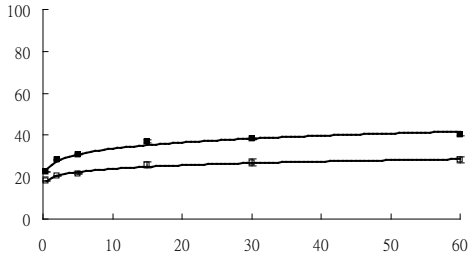	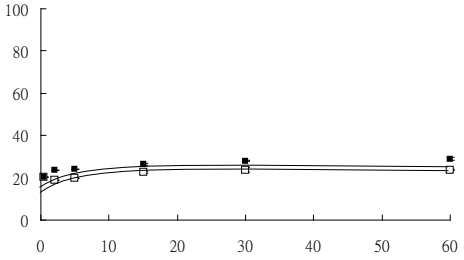
(c) I 221 – W229 (Segment C)	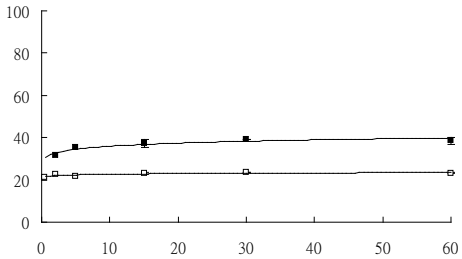	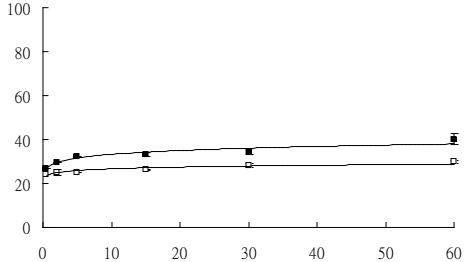	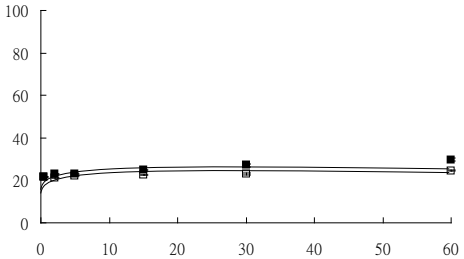

Segment	E166Cb	E166Cf	E166C
(d) E166 – L169 (Ω-loop)	N/A	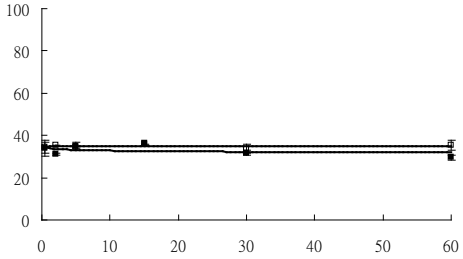	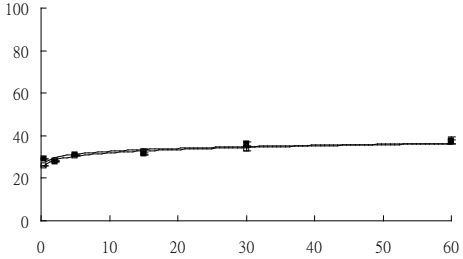
(e) W229 – D245	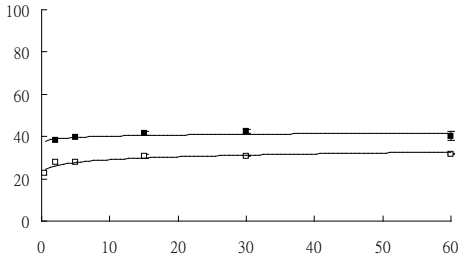	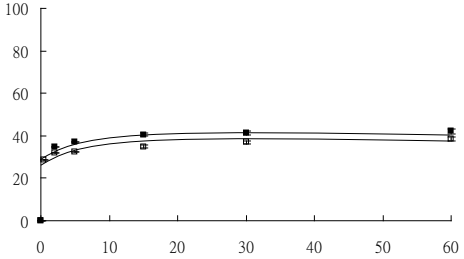	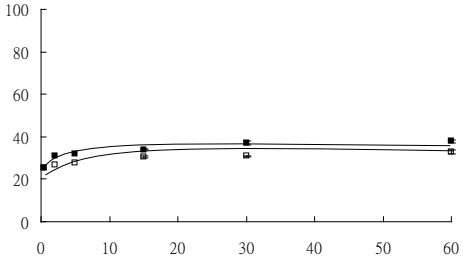
(f) I206 – W210	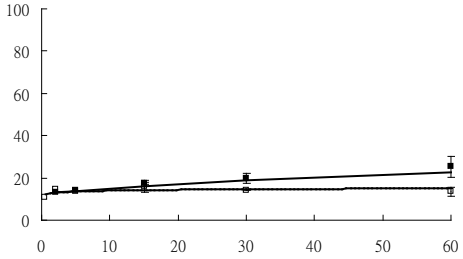	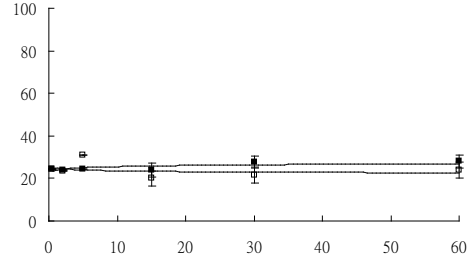	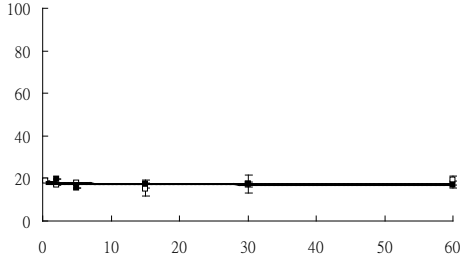

Segment	E166Cb	E166Cf	E166C
(g) I186 – A192	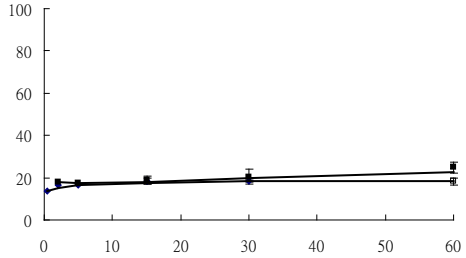	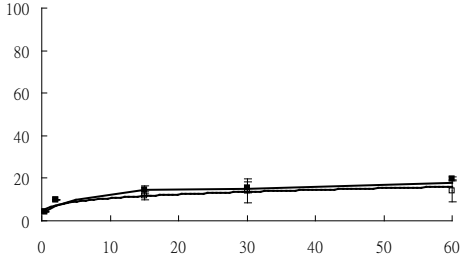	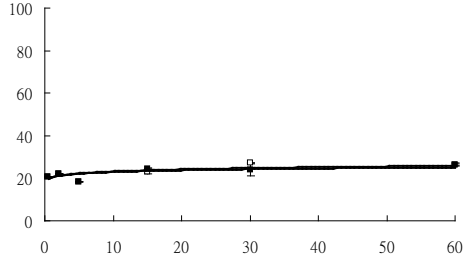
(h) N92 – Y97	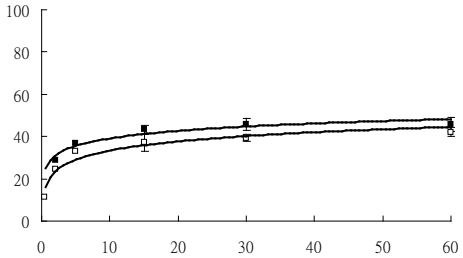	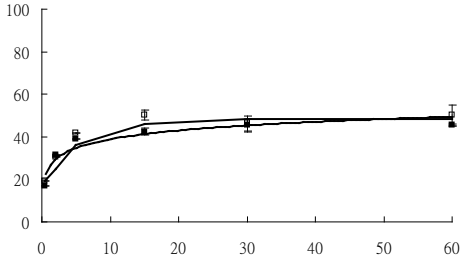	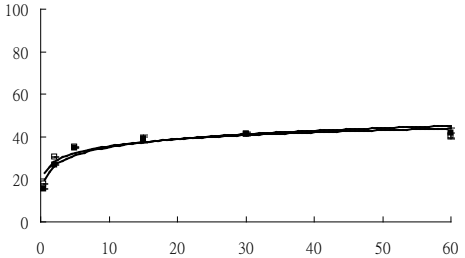
(i) Y274 – I 279	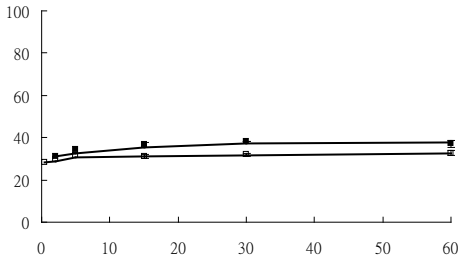	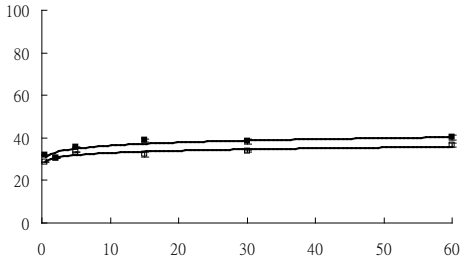	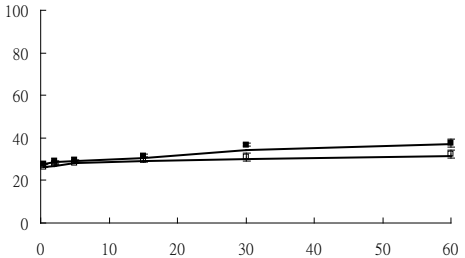

Segment	E166Cb	E166Cf	E166C
(j) F40 – V46	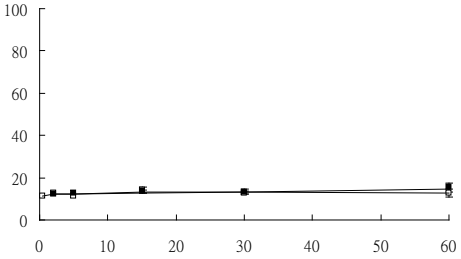	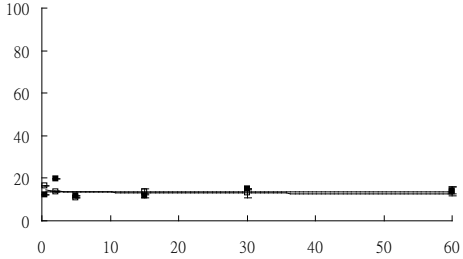	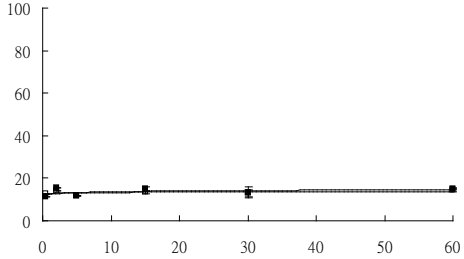
(k) N170 – R178 (Ω-loop)	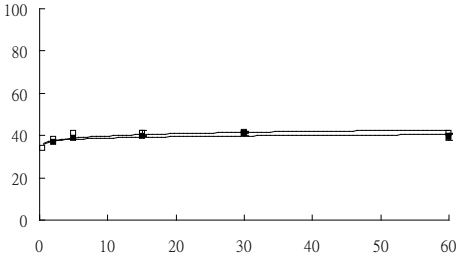	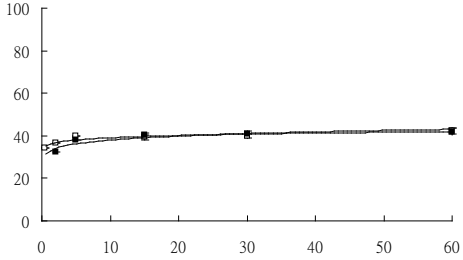	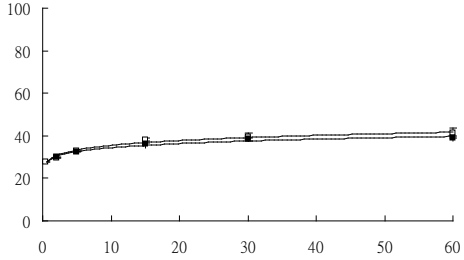
(l) L81 – L91	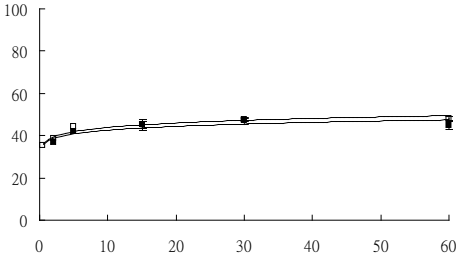	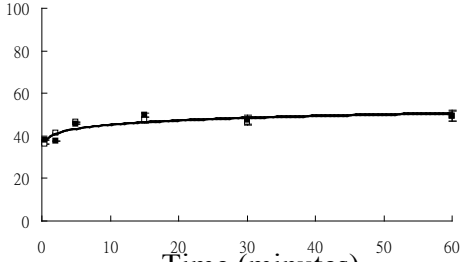	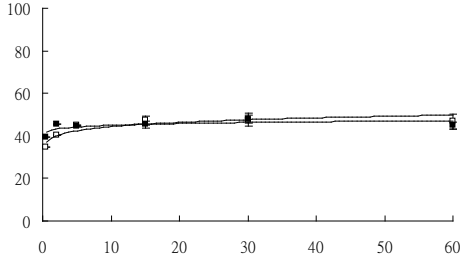

Segment	E166Cb	E166Cf	E166C
(m) D179 – L190	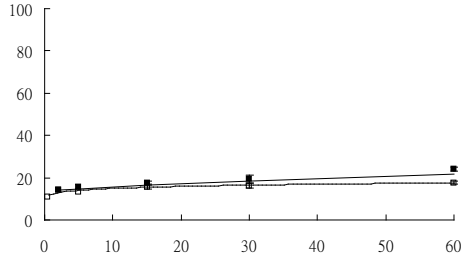	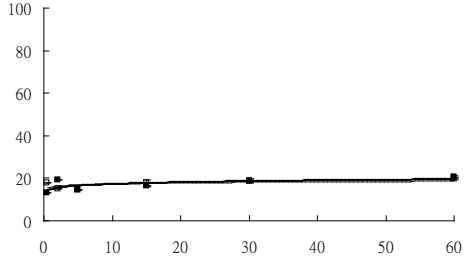	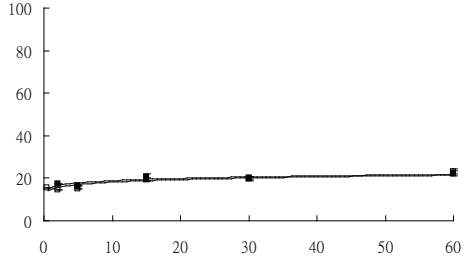
(n) W210 – L220	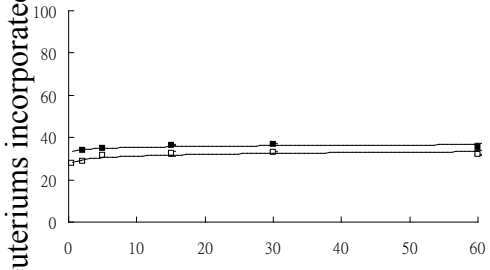	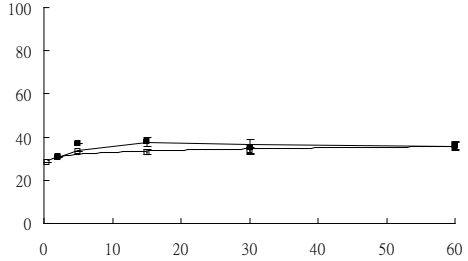	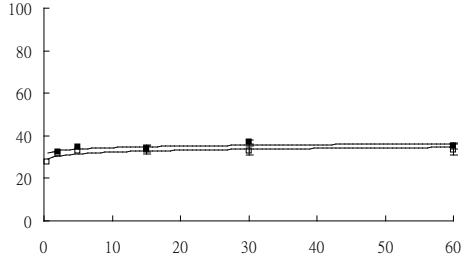
(o) V249 – I261	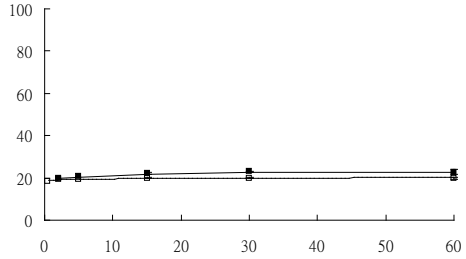	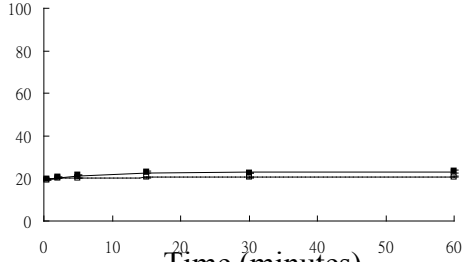	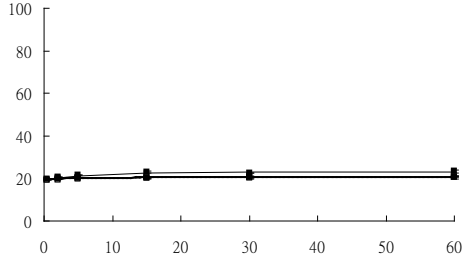

Segment	E166Cb	E166Cf	E166C
(p) V249 – A262	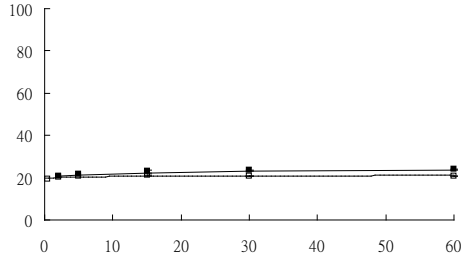	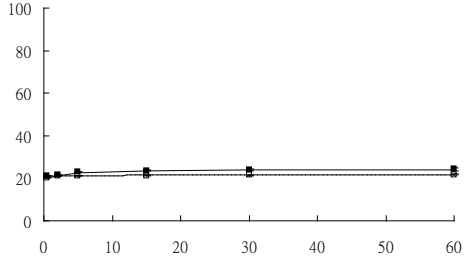	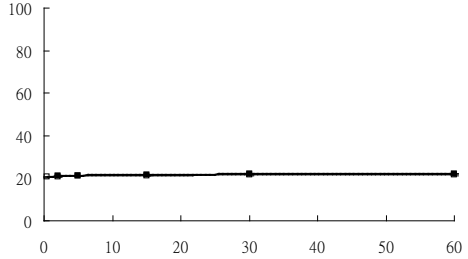
(q) A282 – R291	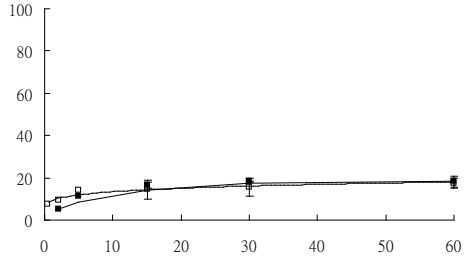	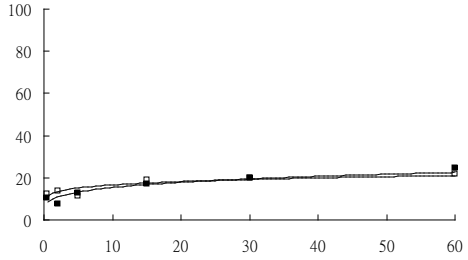	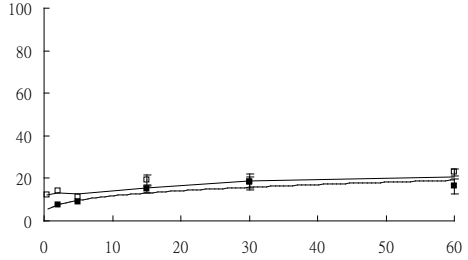
(r) H24 – L36	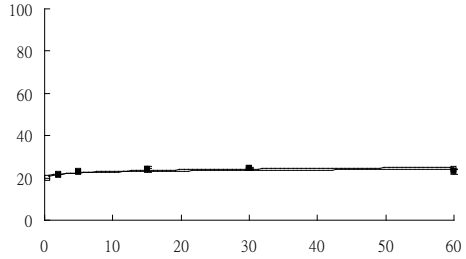	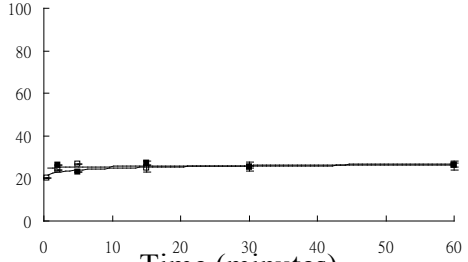	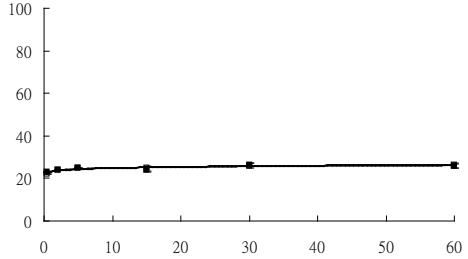

Segment	E166Cb	E166Cf	E166C
(l) I 279 – K284	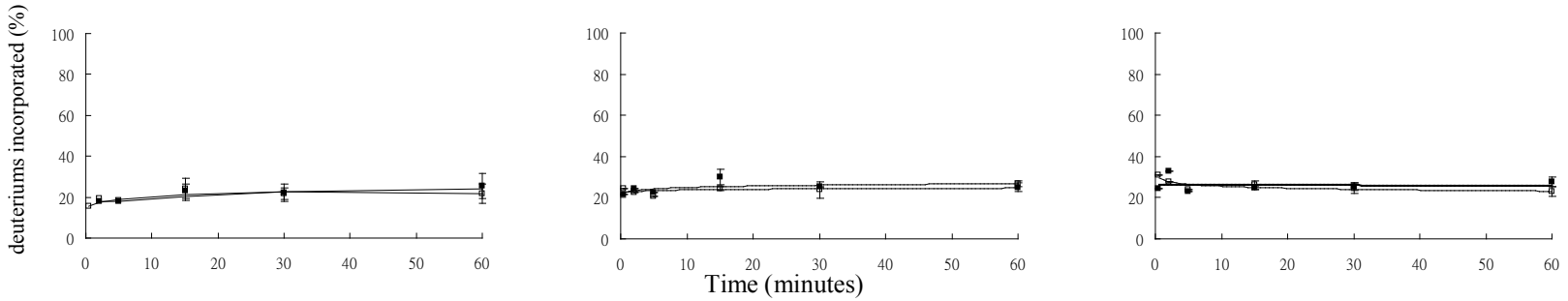		

Figure 7.2. H/D exchange-time profiles of various proteolytic segments of E166Cb, E166Cf, and E166C. The curves with solid (■) and opened square (□) correspond to the apo-state and substrate-bound state of the proteins, respectively. The error bars represent the standard deviation obtained in three independent runs.

Evidence for a 'spatial displacement' mechanism between the binding substrate and the fluorophore

To understand the mechanism by which the biosensors change their fluorescence properties upon substrate binding, we attempted to investigate the likely events that may lead to changes in local environments, i.e., solvent accessibility around the fluorophore after the binding event. The first step of our current approach is to predict the initial orientation of the fluorophore based on the effect of the fluorophore on the local H/D exchange behavior of the protein. Among 19 identified proteolytic segments, three peptide segments (A, B, and C) were found to exhibit different extents of deuterium incorporation between the apo-form of the fluorophore-labeled proteins (E166Cf and E166Cb) and E166C. According to the X-ray structures obtained for the E166C mutant and biosensors, segment A and segment B indeed are the two major constituent helices of the active binding pocket (Fig. 7.3 (b)). The center of the active binding cavity is occupied by segment A, which is positioned just after the catalytic site Ser70 and includes Lys73, a crucial residue for both acylation and deacylation.[Meroueh et al., 2005; Golemi-Kotra et al., 2004; Lietz et al., 2000] Segment B is also known to be located at one edge of the active binding pocket which bears the catalytically

important SDN loop composed of the Ser130-Asp131-Asn132 segment (Fig. 7.3 (b)).[Jacob et al., 1990]

Segment C is located quiet far away from the 166 position and the core of the active binding pocket, and is extensively shielded from position 166 by a long chain of peptide segments (Fig. 7.3). In light of this, the effect of the fluorophore on the structural/dynamics on segment C is probably indirect, and thus unlikely to provide useful information on the biosensing mechanism of the biosensors.

Based on the H/D exchange results obtained for peptide segments A and B, and the fact that the site of fluorophore attachment, the 166 position on the Ω-loop, is very close to the active site cavity, we propose that the fluorophore may be oriented directly towards and close to the core of the active binding pocket. Because of its proximity and orientation, the fluorophor could induce local structural changes / movements or 'sense' small changes in the local environment around this confined region.

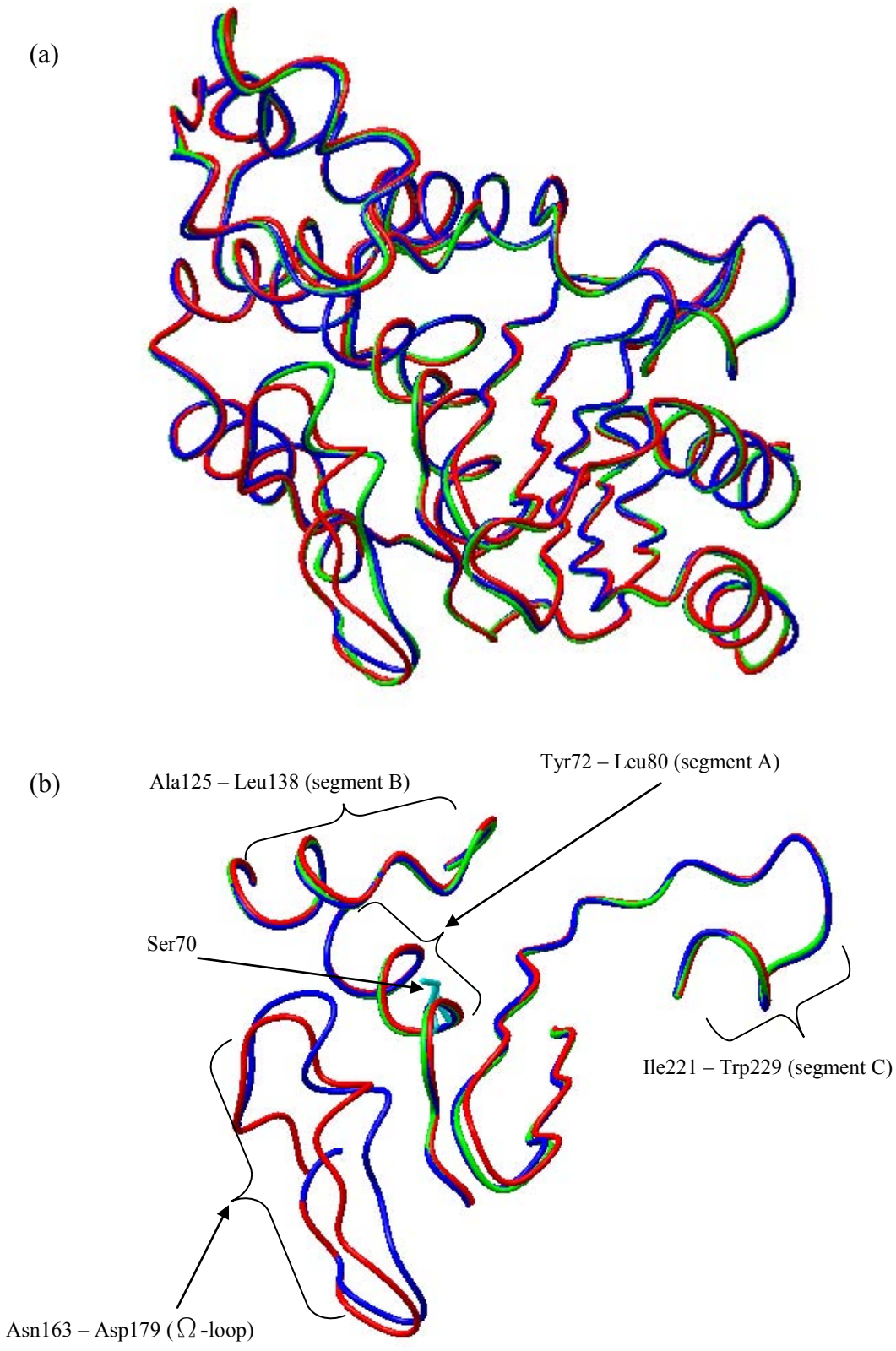

Figure 7.3 Superposition of (a) overall structures and (b) active site region of E166C (blue), E166Cf (green) and E166Cb (red) (Fluorophore molecules are not shown).

The rate and extent of H/D exchange are affected by both protein structure (conformations) and dynamics.[Maity et al., 2003; Busenlehner et al., 2005; Hoofnagle et al., 2003] Therefore, in our case, the increases in % of deuterium incorporation observed for E166Cf and E166Cb could possibly be due to either changes in conformation or dynamics, or both. However, our preliminary X-ray crystallographic data show that the conformation of the active site region is indeed very similar among E166C, E166Cf and E166Cb [Fig 7.3 (b)]. In addition, as suggested by our kinetics studies (Section 6.2.3), the binding efficiencies of the E166Cf and E166Cb are not impaired when compared with E166C, indicating that the active binding pocket of the mutants is not significantly perturbed upon incorporation of the fluorophore onto the protein. For these reasons, the changes in the extent of deuterium incorporation of the active site peptide segments observed herein (segments A and B) are likely to be related to the local dynamics (movements) of these segments instead of conformational changes of the whole protein.

We propose that the increases in extents of deuterium incorporation might be due to fluorophore-induced structural destabilization, which results in an increase in flexibility of the active site region. H/D exchange has been extensively used in

studying structural stability (flexibility) of proteins.[Powell et al., 2001; Ghaemmaghami et al., 2000] In a compactly folded protein, particularly involving helical structures like segments A and B, the amide protons are highly shielded from the solvent molecules, and thus most likely to undergo exchange with solvent deuteriums only through momentary structural fluctuations or movements of the protein molecule.[Busenlehner et al., 2005; Hoofnagle et al., 2003] These fluctuations can transiently break the intra-molecular binding interactions involved in maintaining the structural stability of the protein, resulting in the formation of the transient solvent-exposed states ("opened" state) with non-native structures, which are exchange-competent.[Maity et al., 2003; Hoofnagle et al., 2003] A reaction scheme commonly used to describe the H/D exchange reaction on protected amide protons through structural fluctuations is shown in **Scheme 1.1**. The "opened" state is in equilibrium with the native state ("closed" state), and H/D exchange is supposed to occur only under the "opened" state.[Hoofnagle et al., 2003] Under the EX2 regime, the observed rate and extent of H/D exchange at equilibrium are markedly dependent on the relative rates of formation of the "opened" state (k_{op}) and "closed" state (k_{cl}), which are in turn governed by the structural stability of the protein.[Powell et al., 2001; Ghaemmaghami et al., 2000] Typically, increases in rate and extent of H/D

exchange, like that observed for segments A and B of E166Cb and E166Cf, could be an indication of structural destabilization (increase in flexibility) due to the "opening step", which involves transient breaking of intra-molecular interactions during structural fluctuations. The exchange-competent opened state becomes relatively more stable, leading to a greater extent of H/D exchange observed for peptide segment A and B. [Powell et al., 2001; Ghaemmaghami et al., 2000; Codeanu et al., 2002]

The proposed fluorophore-induced destabilization of the active site region was postulated to proceed through two possible mechanisms. First, as described in Section 6.2.3, the fluorophore may affect the cluster of 'gluing' water molecules located between the Ω-loop and the rest of the active site.[Bös et al., 2008] If the fluorophore is oriented towards and close to the active site, it may share some common space with these water molecules and tend to expel/displace some of them away from the core of the active binding pocket. Consequently, the overall structural stability of the active site would be reduced since the stabilizing effect offered by the "structural glue" is reduced.

Comparison of the H/D exchange results between E166Cf and E166Cb shows that the increase in the extent of H/D exchange in the peptide segment A of E166Cb (~ 30 %) is more significant than that of E166Cf (~ 13 %). This observation may be due to more significant structural destabilizing effects mediated by badan than fluorescein-5-maleimide. As discussed in Section 6.2.3, badan is more hydrophobic than fluorescein-5-maleimide, and its tendency to repel water molecules is most likely greater. Hence, the water cluster for stabilizing the structural integrity of the active site pocket may be perturbed to a greater extent. For this reason, the structural stability of the active site of E166Cb is likely to be lower than that of E166Cf.

Another plausible mechanism for the fluorophore-induced structural destabilizing effects could be that the fluorophore may shield and weaken the stabilizing noncovalent interactions of the active site region. For class A β-lactamase, the structural integrity of the active site region is maintained by a network of noncovalent interactions, including some important interactions between segment A and segment B, such as hydrogen bonds between $Lys73_{seg\ A}$ - $Ser130_{seg\ B}$ and $Lys73_{seg\ A}$ - $Asn132_{seg\ B}$, and electrostatic interactions mediated by $Lys73_{seg\ A}$.[Strynadka et al., 1992; Chen et al., 1993; Atanasov et al., 2000]

We reason that if the fluorophore is oriented towards and very close to the active site, it may create shielding effects between some of these interacting structural moieties, thereby weakening/interrupting the interactions between them. Weakening of noncovalent interactions through "molecular shielding" has been reported in the literature previously. For example, the disruption of interribose hydrogen bonds resulted from the shielding of two interacting partners by an adenine moiety was observed in Lim's study on condon:anticodon interactions within ribosome.[Lim et al., 2001]

It is noted that based on the two scenarios described above, the structural stability of the Ω-loop may also be reduced since it is closely associated with the "structural glue" water cluster and the rest of the active site pocket. However, no significant difference in the H/D exchange time profiles was observed for this region between E166C, E166Cf and E166Cb. This negative result could be due to the fact that to start with, the Ω-loop in class A β-lactamase is highly flexible, and the additional destabilizing effects induced by the fluorophore may not be significantly enough to produce an observable change in H/D exchange level. Another possibility may be that the H/D exchange reaction at the Ω-loop region is already saturated (accessibility of amide protons) in the fluorophore-free state

(E166C), and therefore no further increase in the extent of exchange could be detected even if the flexibility of the loop is increased by the incorporation of the fluorophore.

As suggested in our kinetics study (Section 6.2.3), the overall binding efficiency (k_2/K_d) was not significantly impaired by the incorporation of the fluorophore located near the active site. We believe that apart from the intrinsic flexible nature of the Ω-loop as described in Section 6.2.3, the increase in flexibility of the active binding pocket suggested herein may also aid in relieving the fluorophore mediated steric blocking, and hence retaining or even enhancing the overall binding efficiency. In addition, our H/D exchange results suggest that the structural destabilizing effect induced by the badan is probably more significant than fluorescein-5-imide. This observation is consistent with the kinetic data which show E166Cb binds much more efficiently than E166Cf, most likely due to that the extra flexibility gained by the active site pocket of E166Cb, thereby alleviating further the crowded environment for better substrate binding at the active site region.

Up to this point, the experimental observations (kinetics and H/D exchange studies) are supportive of our hypothesis that in the apo-state of the biosensor,

the fluorophore is likely oriented towards and close to the active site. Here we try to answer another important question: how does the fluorophore "move" upon substrate binding, so that its local environment and hence its fluorescence properties are changed?

As shown in Fig. 7.2, no significant change in the H/D exchange time profiles could be observed for proteolytic segments of E166C upon substrate binding. Interestingly, for both E166Cf and E166Cb, the extents of H/D exchange of segments A and B, which are higher than those of E166C in the apo-state, appear to decrease and approach the levels similar to those of E166C after binding to a substrate. These observations indicate that the dynamics of the active site region of the substrate-bound E166Cf and E166Cb is similar to that of E166C. That is, the fluorophore may no longer stay close to the active site in the substrate-bound state, such that the dynamic changes induced by the fluorophore to this region are nullified by the substrate binding.

Taking all the information together, a *"spatial displacement"* mechanism was proposed to describe the changes in fluorescence properties of the biosensors upon binding to β-lactam antibiotics. First, based on the effects of the

fluorophore on the dynamics of the active site region, the fluorophore is likely oriented towards and close to the active site. In addition, since the fluorophore (badan and fluorescein-5-maleimide) is of considerable size, it may share some common space with the binding substrate in the active site. Therefore, during substrate binding, the fluorophore has to move away/displace from the active site in order to avoid the spatial crash with the incoming substrate. This spatial displacement event may cause changes in local environments, i.e. increase/decrease in solvent polarity and accessibility around the fluorophore, which may account for the change (increase) in fluorescence intensity exhibited by E166Cf and E166Cb. In the case of E166Cb, the fluorescence emission wavelength is also shifted to a lower wavelength (the blue shift) as badan is displaced to a lesser polar environment.

7.2.2 X-ray crystallographic and molecular modeling studies

X-ray crystallography

Complementary X-ray crystallographic studies were performed by Dr. Y. X. Zhao of our research group to investigate the biosensing mechanism of the biosensors. X-ray structures of apo- and substrate (cefotaxime)-bound E166Cb

are shown in Fig. 7.4 (refer to Supporting information III). In general, the crystal structures acquired for the E166C mutant and biosensors are very similar to those of other class A β-lactamases reported in the literature. In the structure of apo-E166Cb, the region around the active site, including peptide segment A, segment B, the Ω-loop and more importantly the badan molecule, are well defined. Interestingly, the badan molecule appears to be oriented rather close to the segment A and B, the two major elements constituting the active binding cavity (Fig. 7.4). This observation is consistent with our H/D exchange results that the fluorophore is oriented towards and close to the active site.

The X-ray structure of cefotaxime-bound E166Cb is very similar to that of the apo-state of the protein, and the cefotaxime molecule clearly appears to link to the catalytic Ser70 site. Unfortunately, the Ω-loop region, including the badan molecule, is not well resolved in the X-ray structure, presumably because this region is too flexible upon binding to the substrate. In spite of this, this partially resolved structure could still provide certain insights into the mechanism leading to the fluorescence change if it is overlapped with the structure of apo-E166Cb. Superposition of the structures of apo- and cefotaxime-bound E166Cb shows that apparently the badan molecule shares a common space, if not

interlocking with the cefotaxime molecule (Fig 7.4 (c)). Therefore, upon substrate binding, there is a distinct possibility that the fluorophore has to be displaced from its original position in order to avoid the spatial crash with the incoming substrate. Hence the X-ray data are consistent with the *"spatial displacement"* mechanism proposed according to our H/D exchange studies.

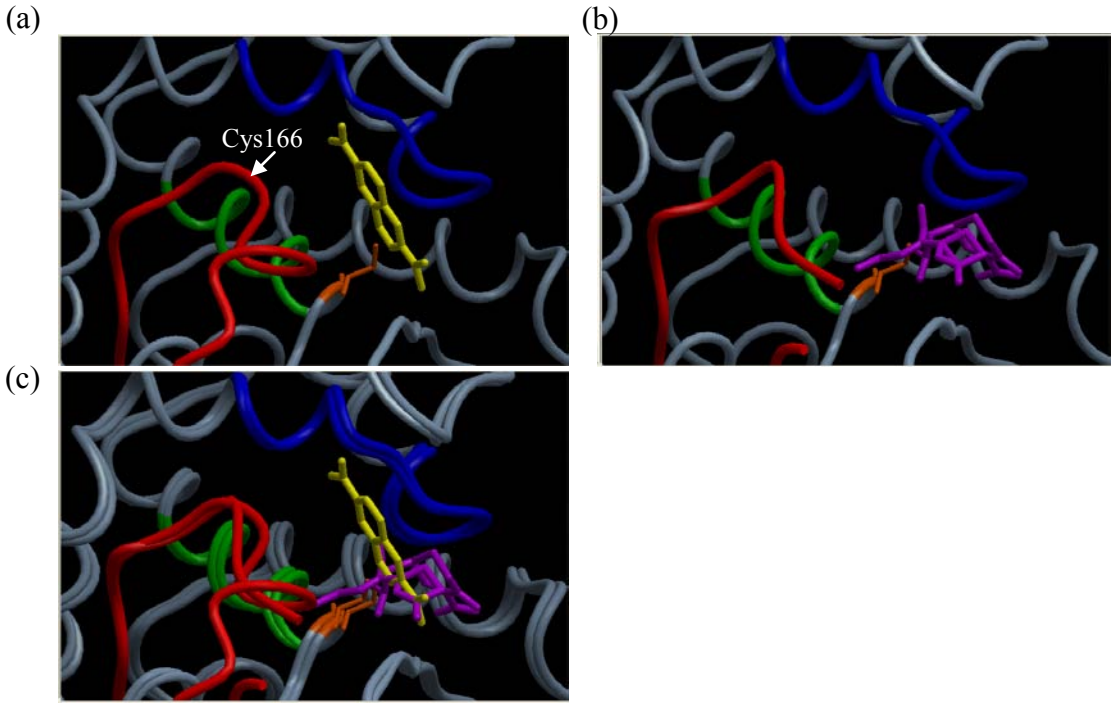

Figure 7.4 X-ray structures of (a) apo- and (b) cefotaxime-bound E166Cb. (c) Superposition of structures of apo- and cefotaxime-bound E166Cb. The catalytic site Ser70, peptide segment A, peptide segment B, and the Ω-loop of the protein are highlighted in orange, green, blue, and red, respectively. The badan is highlighted in yellow, and the cefotaxime (substrate) is highlighted in purple.

Molecular modeling

Similar to the case of cefotaxime-bound E166Cb, the Ω-loop region (with fluorescein-5-maleimide attached) was found to be significantly disordered in the X-ray structures obtained for both apo- and substrate-bound E166Cf. Thus only limited information about the mechanism by which the binding of antibiotics trigger the enhancement in fluorescence emissions could be obtained. In light of this, molecular 'docking' modeling studies were performed on the E166Cf system by Dr. D. L. Ma of our research group (refer to Supporting information II).

The protein model of E166Cf shows that both the side chain of Cys166 in the Ω-loop and the attached fluorophore are oriented towards the active site. The fluorescein-5-maleimide is buried in the active site with a solvent accessible area (SAA) of 208 $Å^2$. In order to examine whether the fluorescein-5-maleimide molecule shares a common space with the β-lactam substrate within the active site, the structure of E166Cf (with the fluorophore label staying inside the active site) was docked with an intact cefotaxime molecule (Fig. 7.5). Detailed analysis of this structure showed that both the fluorophore label and the substrate share

the same 3-D space in the active site. However, in the substrate-bound state, the fluorophore label stays out of the active site. This subtle conformational change results in a significant increase in water exposure of the fluorescein-5-maleimide in the substrate-bound state (SAA = 280 $Å^2$) as compared to that of the apo-state (SAA = 208 $Å^2$). These observations are consistent with the proposed mechanism that the spatial displacement of the fluorophore during substrate binding may result in changes in the local environments, i.e. solvent polarity and accessibility, around the fluorophore. In addition, the increase in the calculated solvent accessibility area of the fluorescein-5-maleimide upon substrate binding is consistent with the observed fluorescence enhancement exhibited by E166Cf.

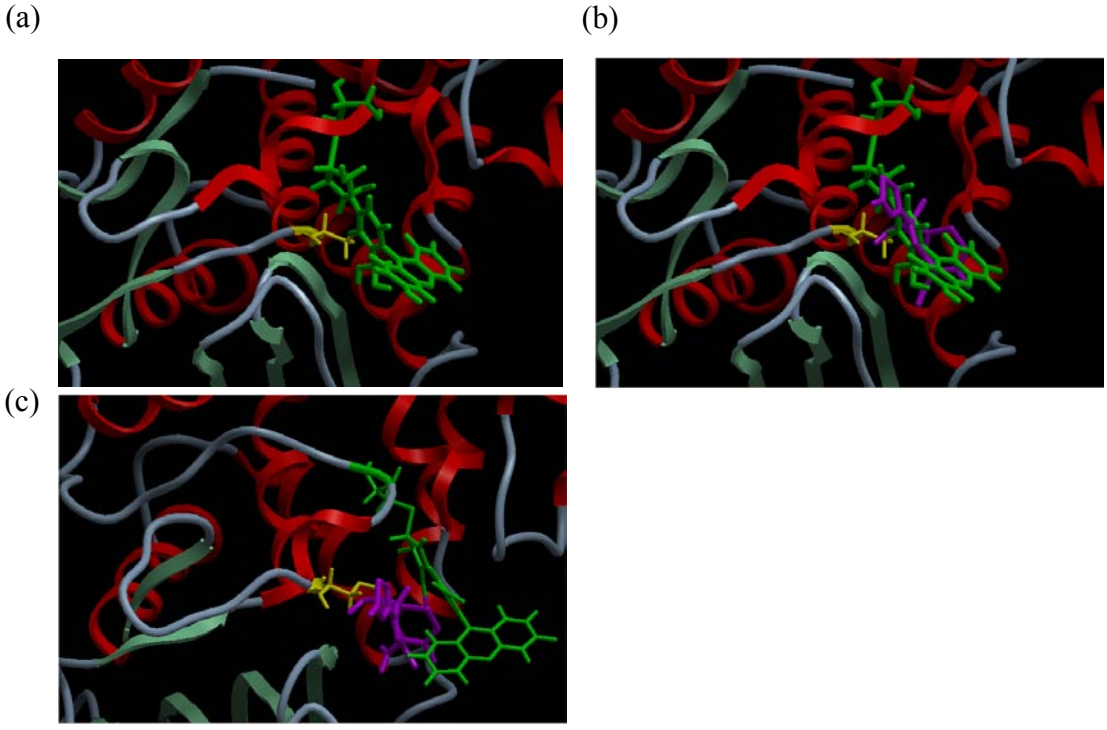

Figure 7.5 Molecular models of (a) apo-E166Cf, (b) E166Cf (with the fluorescein label staying inside the active site) docked with an intact cefotaxime molecule, and (c) cefotaxime-bound E166Cf. The active site Ser70, fluorescein-5-maleimide, and cefotaxime are represented by yellow, green, and purple, respectively.

7.3. Conclusions

In this study, we adopted mass spectrometric H/D exchange technique to study the local dynamics of the β-lactamase mutant (E166C) and biosensors (E166Cb and E166Cf), from which the mechanism of fluorescence changes exhibited by the biosensors upon substrate binding was investigated.

Two active site segments of E166Cf and E166Cb were found to exhibit higher H/D exchange levels than those of E166C. Based on this observation, we proposed that the fluorophore may be oriented towards and close to the active binding site pocket, and exert a destabilizing effect to this confined region through displacing the "structural glue" cluster of water molecules present and shielding some noncovalent interactions for maintaining the structural integrity of the pocket. Upon substrate binding, the H/D exchange levels of these two segments appeared to decrease and become resembling to that of E166C (without fluorophore attachment), suggesting that the fluorophore may have moved away from the active site, and therefore the dynamic changes initially induced to this region are withdrawn.

Consolidating all information gathered (H/D exchange, X-ray crystallography and molecular docking studies), a *"spatial displacement"* mechanism was proposed. First, the fluorophore may be oriented towards, if not partly buried in, the active site, and therefore it may indeed share some common space with the incoming binding substrate. During the process of substrate binding, the fluorophore is displaced away from the active site in order to avoid the spatial clash with the incoming substrate. As a result, the fluorophore experiences different local environments and solvent polarities before and after substrate binding, leading to the changes in fluorescence emission observed.

Chapter 8 Study of tazobactam inhibition of β-lactamases by electrospray ionization mass spectrometry (ESI-MS) under near physiological conditions

8.1 Background

Resistance to β-lactam antibiotics arising from mutation of β-lactamases has become a recognized global problem to human health.[Poole et al., 2004] β-lactamases are effective enzymes, which hydrolyze and destruct β-lactam antibiotics before they approach their target, the penicillin binding protein (PBP). [Sandanayaka et al., 2002]

To tackle the problem of antibiotic resistance mediated by β-lactamases, β-lactamase inhibitors have been discovered to retard the hydrolytic action of the enzymes, protecting the β-lactam antibiotics from hydrolysis before they reach the PBPs. Three mechanism-based β-lactamase inhibitors widely used in clinics nowadays are clavulanic acid, sulbactam and tazobactam (Fig. 1.2).[Malcolm et al., 2000] These inhibitors inactivate two major classes of β-lactamases, class A and class C, through covalent binding to the active site serine (Ser70 for class A and Ser64 for class C), resulting in the formation of a covalently bound enzyme-inhibitor complex (E-I complex) and inhibition of the enzyme activity.[Malcolm et al., 2000]

Unfortunately, owing to the evolution of bacteria, these β-lactamase inhibitors have been found to be less effective in recent years.[Bonomo et al., 1999;

Helfand et al., 2003] For instance, a single amino acid substitution at Ser130 in class A SHV β-lactamase was found to render the enzyme a lower susceptibility to inhibition by tazobactam and clavulanic acid.[Helfand et al., 2003] The phenomenon of "inhibitor resistance" highlights the urgent need for development of novel inhibitor analogs against β-lactamases.

An approach usually adopted in the design of novel mechanism-based inhibitor is to stabilize the E-I complex leading to inactivation of the protein target.[Sauve and Schramm, 2002; Borthwick et al., 2003; Padayatti et al., 2006] To accomplish this, prior knowledge on the structural identity of the E-I complex contributing to inhibition is required. The present study is focused on tazobactam (M_α = 300 Da), a triazoly-substituted penicillanic sulfone (refer to Figure 1.2). In addition to the excellent inhibition efficiency towards class A β-lactamases (IC_{50} = 0.01 – 1 uM),[Malcolm et al., 2000] tazobactam also exhibits potent inhibitory activity towards class C β-lactamases (IC_{50} = 1 – 10 uM),[Malcolm et al., 2000] a class of β-lactamase which is less effectively inhibited by clavulanic acid and sulbactam. [Malcolm et al., 2000; Bonomo et al., 2001] With this distinct advantage, tazobactam has become a desirable building block for the development of a new board spectrum β-lactamase inhibitor analogs.

The inhibition mechanism of tazobactam has been studied by various techniques, including electrospray ionization mass spectrometry (ESI-MS), X-ray crystallography and spectroscopic methods, yet the identity of the E-I complex leading to inhibition remains controversial. X-ray crystallographic and

spectroscopic data suggested that the final E-I complex is a trans-enamine-like species (Fig. (8.1 (a)) containing the entire inhibitor molecule attached to the active site of enzyme. [Padayatti et al., 2004; Kuzin et al., 2001; Bush et al., 1993] In contrast, ESI-MS studies for class A SHV-1, [Rodriguez et al., 2004] class A PC1, [Yang et al., 2000] class A TEM-1, [Yang et al., 2000] and class C CMY-2 [Bonomo et al., 2001] β-lactamases under protein denaturing conditions generally indicated that the products of the inhibition reaction were a series of enzyme–inhibitor moiety adducts, as revealed by the appearances of mass peaks at [M + 52] Da, [M + 70] Da and [M + 88] Da in the mass spectra of the E-I complexes ('M' is the measured molecular mass of apo-enzymes) (Fig. 8.1). Due to distinct discrepancies between the results obtained by ESI-MS and the other two physical techniques, we undertook a re-examination of the mass spectrometric method used in the study of inhibition mechanism of tazobactam.

The previous ESI-MS studies on tazobactam inhibition of β-lactamases were performed under typical conditions adopted for ESI-MS analysis. [Rodriguez et al., 2004; Yang et al., 2000; Bonomo et al., 2001] Briefly, the analyte solution contains the protein/protein complex in 50 % organic solvent (e.g. methanol and acetonitrile) containing ~0.5 – 2% (v/v) organic acid (e.g. formic acid and trifluoroacetic acid) (final pH ~2), for which the sensitivity and the stability of the ESI spray are optimized.[Cech et al., 2001; Tullia et al., 2005] However, these conditions, involving a high organic solvent content and very acidic pH, are highly denaturing to and significantly different from the real-life physiological conditions of most proteins. There is a distinct possibility that the "harsh" condition adopted in ESI-MS analysis may deleteriously disrupt the E-I complex

and result in the formation of reaction products that may indeed not be existing under real-physiological conditions. For this reason, we attempted to re-examine the ESI-MS analysis but under near physiological conditions, in which the enzyme/enzyme-inhibitor complexes were incubated and analysed in aqueous ammonium acetate buffer at pH 7. As expected, our results obtained under near physiological conditions are completely different from previous ESI-MS studies.

Another objective of this study is to investigate the occurrence and mechanism of dissociation of the E-I complex between tazobactam and β-lactamase, which are closely related to the inhibition efficiency of the inhibitor. Our results show that the E-I complex formed from class A PC1 β-lactamase dissociates to form an inactive dehydrated ([M - 18] Da) enzyme. Based on the experimental results obtained by the technique of protease digestion followed by tandem mass spectrometry (MS/MS), a reaction mechanism for the formation of the dehydrated enzyme was proposed.

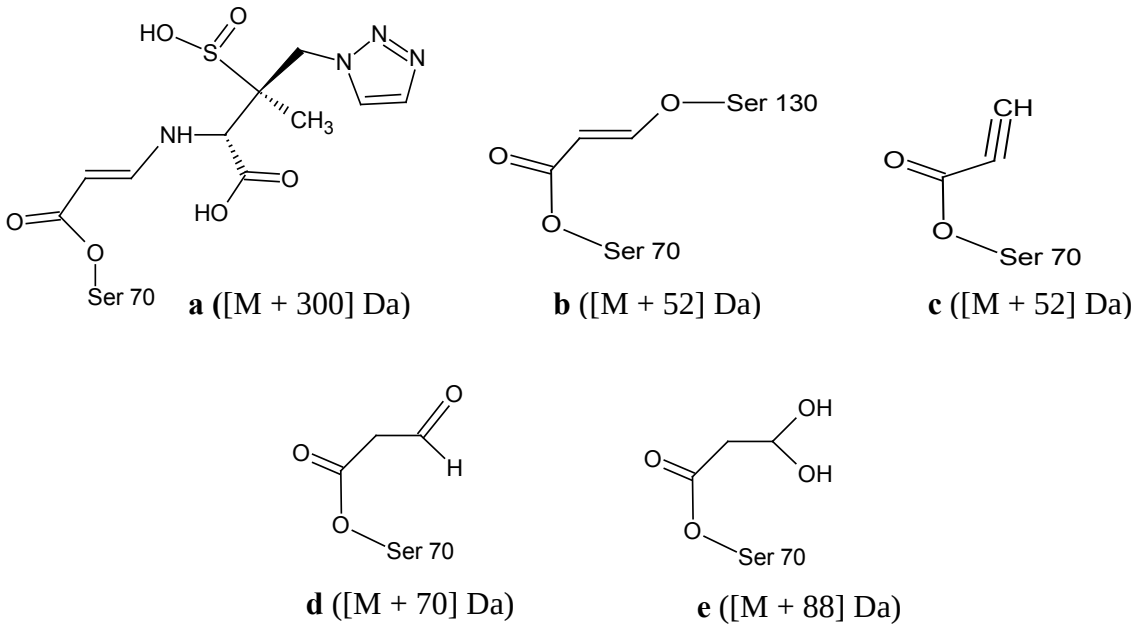

Figure 8.1 Molecular structures of β-lactamase-tazobactam inhibitor (E-I) complex: (a) trans-enamine species, (b) vinyl ether crosslink species between Ser70 and Ser130, (c) propiolylated enzyme, (d) aldehyde-like species, and (e) hydrated form of aldehyde-like species

8.2 Results and Discussion

8.2.1 ESI-MS analysis of the enzyme-inhibitor (E-I) complex under near physiological conditions

In this study, the inhibition mechanism of tazobactam (M_α = 300 Da) towards β-lactamases was re-investigated by ESI-MS but under near physiological conditions. By comparing our results with those obtained under denaturing conditions previously reported, the inhibition mechanisms previously proposed are re-evaluated. Three β-lactamases, class A PC1, TEM-1 and class C P99, were explored in the current study. PC1 and TEM-1 were used because ESI-MS data of these two class A β-lactamases are available in the literature, and therefore direct comparison of the experimental results could be made. P99 was also investigated for possible difference in inhibition behavior from its class A analogs, and it was the only class C β-lactamase available in our laboratory.

ESI-MS analysis of apo-enzymes

The identities of the three β-lactamases, PC1, TEM-1 and P99, were checked by ESI-MS. In general, the measured molecular masses (M) of three β-lactamases are in good agreement with the theoretical average molecular masses calculated based on their primary amino acid sequences (Table 8.1). Analysis of the apo-enzymes (in the absence of tazobactam) under denaturing and near physiological conditions gave similar results, except that in the case of P99, a peak at [M + 57] Da instead of M was found to be the major peak in the mass spectrum obtained under near physiological conditions (Fig. (8.2). The mass increment of 57 Da is

likely due to formation of an adduct between the protein and a small molecule present in the sample solution. The formation of adducts between protein and small molecules derived from the buffer or impurities such as Na^+ and K^+ during electrospray ionization is a commonly observed phenomenon; [Sun et al., 2006; Tolic et al., 1998] however, the identity of the adducts produced is often unknown.[Tolic et al., 1998] In our case, the mass increment of 57 Da could be attributed to the addition of a potassium cation (39 Da) and a water molecule (18 Da) to the protein.

Analysis of E-I complexes under denaturing acidic conditions

The protein samples used in this study are different from those explored in the previous reports in that a $(His)_6$-tag is conjugated to the N-terminus for convenient purification in the protein preparation procedure. To ensure the differences between the results obtained in the current and previous ESI-MS studies were solely due to the differences in conditions of analysis, but not variation of samples (effect of the $(His)_6$-tag), analysis under denaturing condition were re-examined with our protein samples.

Raw mass spectra of apo-enzymes obtained under the denaturing acidic conditions display a wide distribution of multiply charged peaks (n = 19 - 45, where n is the charge state of a particular mass peak) (Fig. (8.2 (a)). Upon incubation with tazobactam followed by addition of acidified acetonitrile, new series of multiply charged ion peaks corresponding to the E-I complexes appeared (Fig. (8.2 (b)). The average molecular masses of various E/E-I

complexes were obtained by transformation of the different series of multiply charged ion peaks.

As expected, and in agreement with previous ESI-MS reports, a series of peaks at [M + 52] Da, [M + 70] Da and [M + 88] Da were observed in the transformed mass spectra obtained for the reaction mixtures between tazobactam and the two class A β-lactamases, PC1 and TEM-1, under denaturing acidic conditions (Fig. 8.2). For P99, the ESI-MS spectrum displays only the [M + 70] Da and [M + 88] Da peaks upon incubation with tazobactam (Fig. (8.2 (h)), and is consistent with the results obtained for class C β-lactamases CMY-2 in the previous ESI-MS study.[Bonomo et al., 2001] These results indicate that the properties our $(His)_6$-tag proteins are similar to those previously reported in the literature.

The observed [M + 70] Da species was previously proposed to be an aldehyde-like molecular structure formed from dissociation of the trans-enamine species (Fig. 8.1 (d)). This aldehyde-like species is in equilibrium with its hydrated form, forming the observed [M +88] Da species (Fig. 8.1 (e)).[Rodriguez et al., 2004; Yang et al., 2000; Bonomo et al., 2001] The [M + 52] Da component was only observed in class A β-lactamase and was postulated to be of two possible structures. First, it could be a cross-link vinyl ether (Fig. (8.1 (b)), in which a moiety of the inhibitor molecule acts as a bridge to connect the active Ser70 and Ser130 sites, an important residue for the acylation inhibitor binding process.[Yang et al., 2000] Second, it could be a propiolyated enzyme (Fig. (8.1 (c)) formed from rearrangement of the cross-link vinyl ether between Ser70 and Ser130 (Fig. (8.1 (b)), and/or decomposition of the trans-enamine

species.[Yang et al., 2000] These enzyme-inhibitor complexes were previously postulated to be the possible intermediates/products leading to the inhibition of the class A β-lactamases.

Table 8.1 Calculated and measured average molecular masses of PC1, TEM-1 and P99 β-lactamases

	Calculated average molecular mass (Da)	Measured average molecular mass (Da)
PC-1	29748.2	29749.0
TEM-1	29903.2	29903.1
P99	40320.2	40322.9

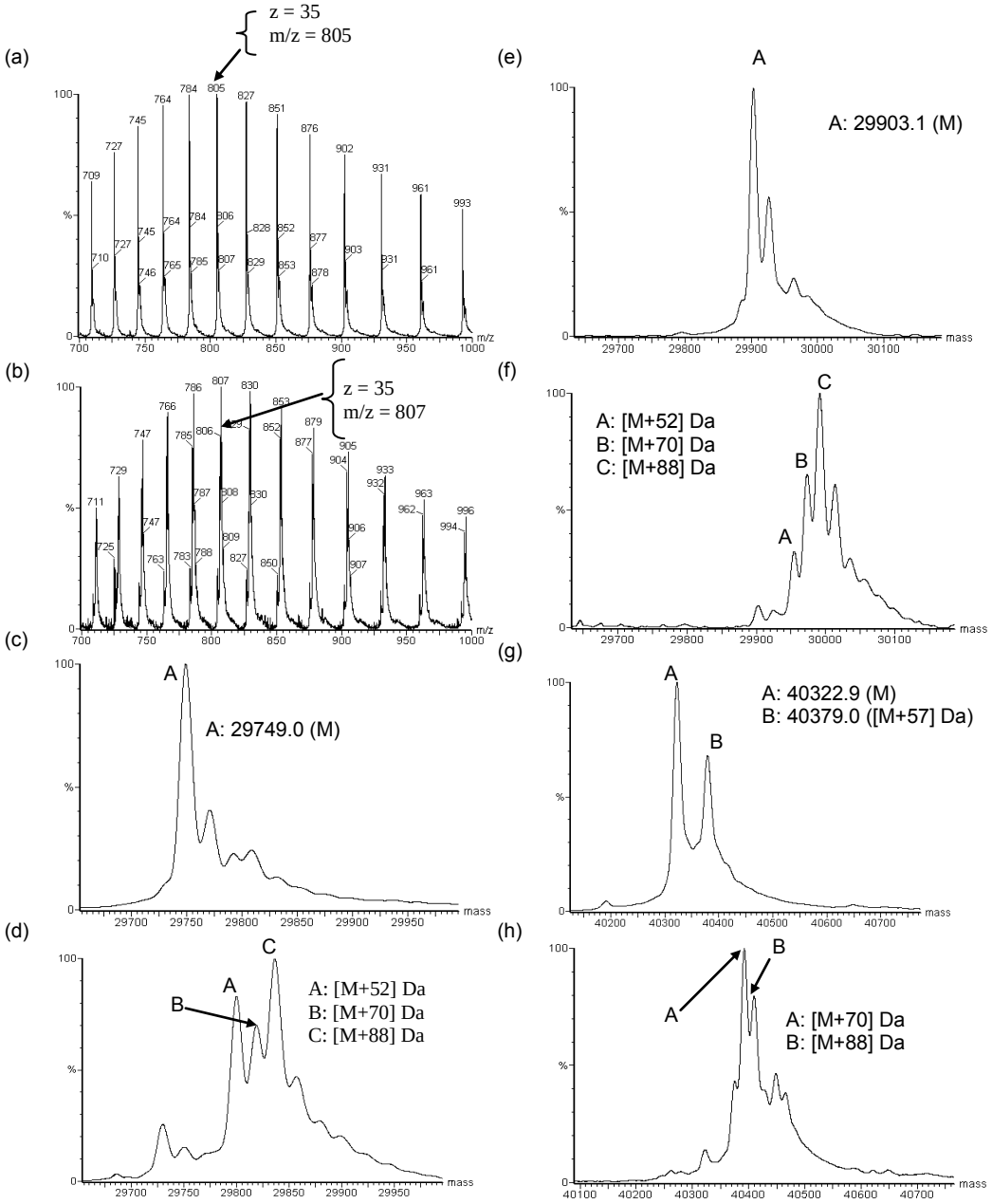

Figure 8.2 Multiply charged ESI-MS spectra of (a) apo-PC1 and (b) PC1–tazobactam E-I complex (n = charge state), and transformed mass spectra of (c) apo-PC1, (d) PC1-tazobactam E-I complex, (e) apo-TEM-1, (f) TEM-1-tazobactam E-I complex, (g) apo-P99, and (h) P99- tazobactam E-I complex obtained under denaturing acidic conditions.

Analysis of E-I complexes under near physiological conditions

Under near physiological conditions, the E-I complexes between tazobactam and various species of β-lactamases were formed in aqueous 20mM ammonium acetate buffer at pH 7. This is the most commonly used buffer system for ESI-MS studies when the protein is required to be maintained in its native state, e.g. analysis of non-covalent protein-ligand complexes.[Jorgensen et al., 1998; Zhang et al., 2003] The preferred use of the ammonium acetate buffer system is due to its compatibility with ESI ionization,[Hardouin et al. 2005] and the fact that, as revealed by ESI-MS based information in the literature, many proteins could maintain their native functions and functional oligomeric states under this buffer system.[Sanglier et al., 2002; Loo et al., 199; Benesch et la., 2007] Thus, using the ammonium acetate buffer at pH 7 can be regarded as the suitable ESI-MS compatible condition which could reasonably reflect the circumstances occurring under real-life physiological conditions. However, it should be noted that 100% aqueous buffer at neutral pH is apparently not the optimum conditions for ESI sensitivity. By our experience, the sensitivity of analysis was at least 5-fold poorer than adopting the typical ESI-MS (denaturing) conditions.

In general, the multiply charged mass spectra of E/E-I complexes obtained under near physiological conditions display narrower charge state distributions with preference for lower charged states (n = 9 - 13) when compared with those obtained under acidic denaturing conditions (n = 19 - 45) (Fig. (8.3 (a), (8.3 (b)). This observation indicates that the proteins are likely to have existed in their native (folded) states during the ESI-MS analysis.[Ashcroft et al., 2005]

In addition, there is no significant difference in the charge state distribution (CSD) between the multiply charged mass spectra of apo-enzymes and E-I complexes, indicating that no significant change in tertiary protein structure was induced upon binding to tazobactam.[Yan et al., 2004] This observation is consistent with previous structural information provided by X-ray crystallography, an authoritative technique in the study of protein structures, which showed that no remarkable change in overall structure was triggered when tazobactam was bound to class A SHV-1 β-lactamase.[Padayatti et al., 2004] Based on these findings, the structural information of E-I complexes obtained under near physiological conditions in the current study is likely to resemble closely that are found in real-life conditions.

Interestingly, the molecular masses of the E-I complexes measured under near physiological conditions are totally different from those obtained under acidic denaturing conditions. With reference to Fig. 8.3 for PC1 and TEM-1, only a single E-I peak at [M + 300] Da was observed upon tazobactam inhibition. As for P99, peaks at [M + 300 + 57] Da and [M + 300 + (57 x 2)] Da ([M + 57] Da was observed for apo-99 (Fig. (8.3 (h)). The addition of 57 x 2 mass unit was most likely due the additions of two molecules of H_2O and two potassium cations. More importantly, for all three β-lactamase species, no peaks corresponding to the previously reported enzyme – inhibitor adducts at [M + 52] Da, [M + 70] Da and [M + 88] Da could be observed under near physiological conditions.

It should be noted that the differences between our results obtained under the near physiological conditions and those in the previous reports were not due to

the use of nano-ESI injection, as we found that the results obtained by normal-ESI and nano-ESI injection are exactly the same. The reason for adopting nano-ESI instead of normal ESI in the analysis under the near physiological conditions is that the sensitivity was found to be rather poor when the aqueous sample solutions was introduced into the mass spectrometer by normal-ESI, most likely due to poor desolvation efficiency. The sensitivity was improved dramatically when using nano-ESI injection since the droplets emitted from the nanospray emitter are known to be significantly smaller, and therefore easier to be desolvated.[Morelle and Michalski, 2005]

The observation of the [M + 300] Da peak indicates that the E-I complex contains the entire inhibitor molecule, which is consistent with the formation of the trans-enamine species suggested by previous X-ray crystallographic and spectroscopic studies.[Padayatti et al., 2004; Kuzin et al., 2001] With the consistent information obtained by the three techniques, it could be concluded that the formation of the trans-enamine is likely the major pathway and product in the inhibition reaction between β-lactamase (including both class A and class C) and tazobactam.

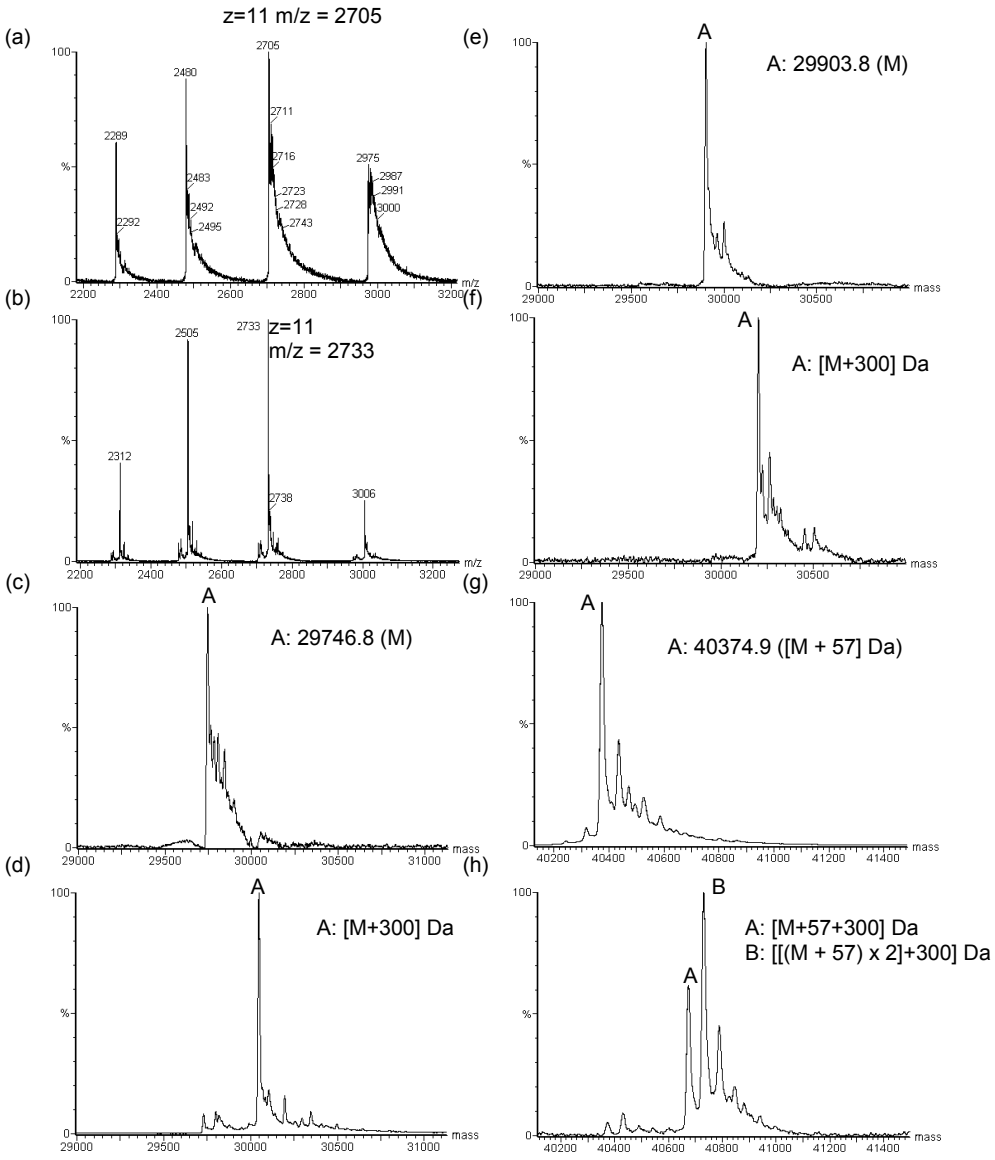

Figure 8.3 Multiply charged ESI-MS spectra of (a) apo-PC1 and (b) PC1–tazobactam E-I complex (z = charge state), and transformed mass spectra of (c) apo-PC1, (d) PC1-tazobactam E-I complex, (e) apo-TEM-1, (f) TEM-1-tazobactam E-I complex, (g) apo-P99, and (h) P99 - tazobactam E-I complex obtained under near physiological conditions.

The formations of the aldehyde-like species ([M + 70] Da and [M + 88] Da), propiolyated enzyme ([M + 52] Da), and cross-link ether species ([M + 52] Da) proposed in previous ESI-MS studies were probably due to degradation/decomposition of the trans-enamine species under acidic denaturing conditions of typical ESI-MS analysis. The trans-enamine species may be acid-

labile and thus susceptible to decomposition under the highly acidic conditions (pH ~2). Another possible reason is that the existence of the trans-enamine species might require stabilization by various intermolecular interactions mediated by the specific three dimensional structure of the protein. Under highly acidic conditions, the three dimensional structure of the protein is most likely to have disrupted. With the loss of conformational constraint offered by the native protein, the trans-enamine structure is no longer stabilized and would decompose.

As the inhibition behavior of various species of β-lactamases were found to be closely similar, it is reasonable to believe that the effects of conditions of analysis on ESI-MS results could be equally applicable to the case of SHV-1 and CMY-2 β-lactamases, which were not available in our laboratory and not included in this study. By analogy, the phenomenon observed in this study may also be applicable to the two other inhibitors, clavulanic acid and sulbactam, since early ESI-MS results and previously proposed inhibition mechanisms for these two inhibitors are very similar to that of tazobactam.[Sulton et al., 2005; Brown et al., 1996; Thomson et al., 2007]

8.2.2 Dissociation mechanism of the E-I complexes

The second aim of this study is to investigate the occurrence and mechanism of dissociation of the E-I complexes, which are important factors determining the overall inhibition efficiency of tazobactam. Our results show that the dissociation behavours of E-I complexes vary significantly among different species of β-lactamases. The E-I complex formed from class A TEM-1

β-lactamase was found to completely dissociate to regenerate the free enzyme in 12 min (Fig. (8.4 (c)). In contrast, for class C P99 β-lactamase, the E-I complex did not dissociate for as long as 6 hours of incubation. It is particularly interesting to note that the E-I complex formed from class A PC1 β-lactamase appeared to dissociate slowly to form a [M – 18] Da species (Fig 8.4 (a)), most likely the dehydrated enzyme, which was found to be more or less inactive by the nitrocefin assay (Fig. 8.4 (b)). The inability of PC1 (IC_{50} = 27 nM) and P99 (IC_{50} = 8.5 nM) β-lactamases to regenerate the active enzymes may be attributed partly to the fact that these two enzymes are more susceptible to tazobactam inhibition than TEM-1 (IC_{50} = 97 nM).[Bush et al., 1993] In addition, the formation of the inactive dehydrated protein in PC1 is consistent with kinetic data obtained by Bush et al. that PC1 is more or less turnover-deficient when reacting with tazobactam.

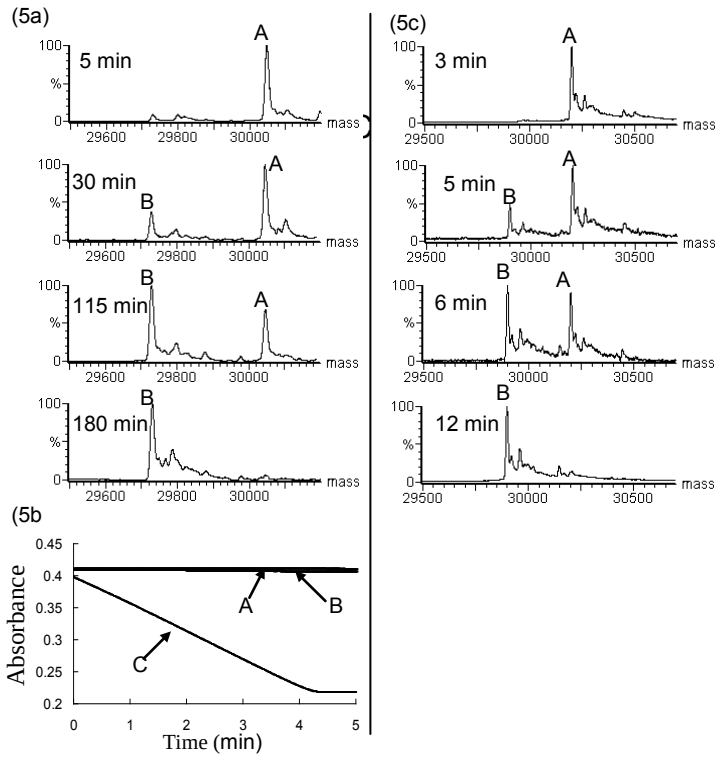

Figure 8.4 (a) Time dependent mass spectra for inhibition reaction between PC1 and tazobactam. Components A and B correspond to the E-I complex [M + 300] Da and dehydrated enzyme [M – 18] Da, respectively. (b) Nitrocefin activity assay for apo-PC1 (curve C) and dehydrated PC1 (curve B). Curve A was obtained from a control experiment in which nitrocefin was incubated in enzyme – free buffer. All time-dependent curves were obtained at 386nm. (c) Time dependent mass spectra for reaction between TEM-1 and tazobactam. Component A and B correspond to the E-I complex [M + 300] Da and apo-enzyme, respectively.

8.2.3 Mechanistic study on the formation of dehydrated PC1 β–lactamase from its E-I complex by protease digestion and tandem mass spectrometry

Although the dehydrated enzyme was first detected in Yang's study,[Yang et al., 2000] its structural identity and mechanism of formation remain poorly understood. Hence, we attempted to perform the first detailed study to determine the identity of the dehydrated protein by protease digestion followed by tandem mass spectrometry, a combination of technique widely used for locating the site of covalent modification in proteins.[Deterding et al., 2000; Shen et al., 2000]

Protease digestion

Tryptic digestion of apo-PC1 species produced 18 identifiable peptide segments, covering ~80% of the primary amino acid sequence (Table 8.2). Comparison of the peptide mass fingerprints between apo-PC1 and dehydrated PC1 shows that 17 out of 18 peptides remain unmodified in the dehydrated protein. Interestingly, the intensity of the peak corresponding to the peptide segment F66–K73 (874 m/z) which contains the active site Ser70, is much reduced and a corresponding -18 Da peak (at m/z 856) appears in the peptide mass fingerprint of the dehydrated protein (Fig. 8.5). This observation suggests that the dehydration reaction probably takes place within the peptide segment F66–K73.

As described in previous reports, Ser130 is a candidate which actively participates in the reaction between tazobactam and class A β-lactamases. [Yang et al., 2000; Kuzin et al., 2001] On the basis of this finding, we first suspected that the formation of the dehydrated enzyme was due to condensation reaction between the side chain hydroxyl groups of Ser70 and Ser130, forming an ether cross link between these two residues. However, based on the observation that the A121–K137 (m/z 1842) peptide segment containing Ser130 is predominately present in the peptide mass fingerprint of the dehydrated enzyme, this scenario is less likely to happen.

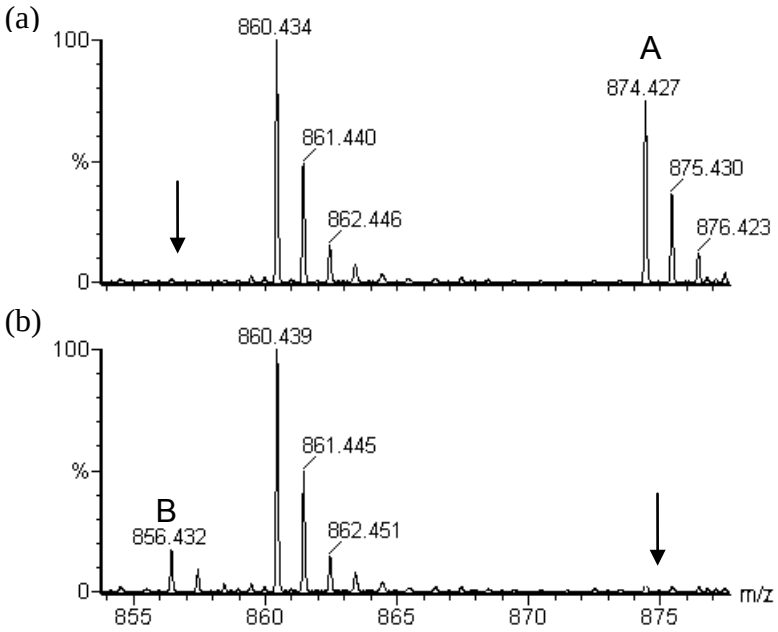

Figure 8.5 ESI-MS spectra of tryptic digests of (a) apo-PC1 and (b) dehydrated PC1. Peaks A (874.4 m/z) and B (856.4 m/z) correspond to the F66-K73 segment and its dehydrated form, respectively.

Table 8.2. List of identifiable peptide fragments produced by tryptic digestion of PC1

Peptide fragment	Calculated monoisotopic molecular mass $[M + H]^+$	Measured monoisotopic molecular mass $[M + H]^+$ (error in ppm)
L193–K198	615.392	615.382 (16.2)
S216-K222	733.409	733.406 (4.1)
L278-K284	761.44	761.438 (2.6)
F58-R65	766.384	766.384 (0)
L152-K158	802.467	802.464 (3.7)
E32–K39	860.43	860.436 (7.0)
N65–K73	***874.431***	***874.43 (1.1)***
Y112-K120	1036.604	1036.607 (2.9)
N245-K253	1052.541	1052.541(0)
K205-K215	1348.766	1348.746 (14.8)
Y165-K175	1418.684	1418.668 (11.3)
G254-K267	1544.868	1544.848 (12.9)
A74-K92	1672.927	1672.902 (14.9)
A121-K137	***1842.854***	***1842.814 (21.7)***
V95-K111	1954.064	1954.037 (13.8)
E154-K175	2627.335	2627.283 (19.8)
G254-K277	2686.405	2686.359 (17.1)
L151-K175	2868.514	2868.47 (15.3)

Tandem mass spectrometry (MS/MS)

To further narrow down the scope of investigation at the amino acid residue level, the peptide segment F66-K73 (designated as segment A) and its dehydrated segment (designated as segment B) were analyzed by tandem mass spectrometry (MS/MS), and the observed sequence-specific b_i and y_i ions were compared. [Paizs et al., 2005] MS/MS spectra of segment A and B are shown in Fig. 8.6, and the presence and absence of fragment ions are summarized in Table 8.3. MS/MS spectrum of the segment A contains a complete series of y_i ions and approximately half number of b_i ions. Under the same collision energy, y_1 - y_3 ions also appears in the MS/MS spectrum of segment B, indicating that the last three amino acids, T71-S72-K73, are likely to remain unmodified in the dehydrated enzyme. Interestingly, the y_4 to y_7 ions disappear completely and the corresponding series of -18 Da mass peaks ((y_4 - 18 Da) to (y_7 - 18 Da)) appear in the MS/MS spectrum of peptide segment B. Based on this clue, the region in which the dehydration reaction takes place is likely to be confined to the first five amino acids, F66-S70. Furthermore, based on the observation that the successive occurrences of the -18 Da fragment ions begin at the fifth amino acid at Ser70, the dehydration reaction probably involves the participation of the hydroxyl group in the side chain of the Ser70 residue. This prediction is consistent with the fact that the dehydrated enzyme is more or less inactive, probably because the catalytically active hydroxyl group in Ser70 is now removed.

Based on the experimental evidences obtained, a plausible mechanism for the formation of the dehydrated enzyme in tazobactam inhibition is proposed. We

postulate that the dehydrated enzyme may be an alkene-like species (**II** in **Scheme 8.1**) formed from dissociation of the ester linkage between the inhibitor molecule and the enzyme in the trans-enamine species **(Scheme 8.1)** . This reaction mechanism is proposed according to an established organic chemical reaction, the formation of alkene and carboxylic acid from dissociation of ester, which is particularly favorable for an ester containing a β-hydrogen.[Arnold et al., 1950; Bailey and Barclay, 1955] Since the trans-enamine speices formed from tazobactam contains the elements of an ester with a β-hydrogen (as circled structure **I** of **Scheme 8.1**), there is a distinct possibility of the occurrence of this dissociation reaction. This dissociation reaction of an ester is intrinsically a kinetically unfavorable process, and hence takes place only at significantly elevated temperatures.[Arnold et al., 1950; Bailey and Barclay, 1955] In spite of this, since the ester moiety in the trans-enamine species is buried in the active site of the enzyme, an environment full of active functional groups, some kinetically unfavorable reactions are suceptible to be catalyzed through interacting with various functional groups nearby. In the current case, we believe that the dissociation reaction may be catalyzed by the specific amino acid configuration in the active site of PC1 β-lactamase.

Although a plausible mechanism was proposed herein, it should be pointed out that more extensive studies are required to find out the detailed mechanistic and structural requirements on the formation of the dehydrated enzyme, i.e., what other amino acid residue participates in the dissociation reaction and why does this reaction occur only in PC1 β-lactamase. However, our study strikingly brings out a new idea to drug discoverers that β-lactamases could possibly exist

in an inactivated state without binding directly to an external inhibitor molecule. For this inhibition mechanism, the role of the inhibitor molecule is binding temporarily to the active site of the enzyme, followed by triggering of a dehydration reaction that would result in the formation of a dehydrated and inactivated β-lactamase. This manner of inhibition has the advantage that the enzyme could be "permanently" inhibited without involving the regeneration (turnover) of the active enzyme, which is often a factor limiting the overall inhibition efficiency of the inhibitor.

Table 8.3 Summary of the presence and absence of fragment ions produced by MSMS analysis of the F66-K73 segment and the corresponding dehydrated form of PC1 β-lactamase. (√ = present, X = absent and * = corresponding dehydrated ion present.)

Apo-PC1				Dehydrated PC1			
$\mathbf{b}_1$	X	$\mathbf{y}_1$	√	$\mathbf{b}_1$	X	$\mathbf{y}_1$	√
$\mathbf{b}_2$	√	$\mathbf{y}_2$	√	$\mathbf{b}_2$	√	$\mathbf{y}_2$	√
$\mathbf{b}_3$	√	$\mathbf{y}_3$	√	$\mathbf{b}_3$	√	$\mathbf{y}_3$	√
$\mathbf{b}_4$	√	$\mathbf{y}_4$	√	$\mathbf{b}_4$	√	$\mathbf{y}_4$	*
$\mathbf{b}_5$	X	$\mathbf{y}_5$	√	$\mathbf{b}_5$	X	$\mathbf{y}_5$	*
$\mathbf{b}_6$	X	$\mathbf{y}_6$	√	$\mathbf{b}_6$	X	$\mathbf{y}_6$	*
$\mathbf{b}_7$	X	$\mathbf{y}_7$	√	$\mathbf{b}_7$	X	$\mathbf{y}_7$	*
$\mathbf{b}_8$	X	$\mathbf{y}_8$	X	$\mathbf{b}_8$	X	$\mathbf{y}_8$	X

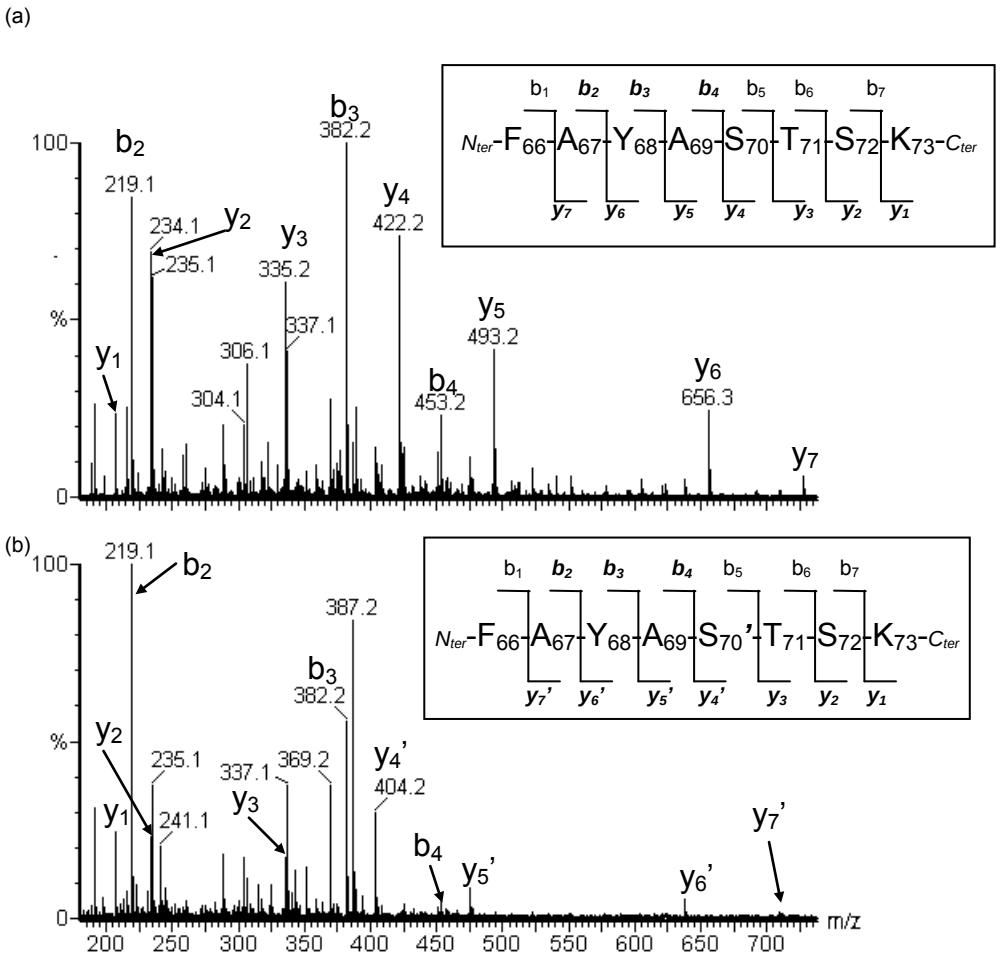

Figure 8.6 MS/MS spectra for (a) F66–K73 segment (m/z 874) and (b) the corresponding dehydrated species (m/z 856). The "dash" symbol represents the dehydrated form of individual species, i.e. S_{70}' represents the dehydrated form of Ser70, and y_4' stands for the dehydrated y_4 ion at [y_4 – 18] Da.

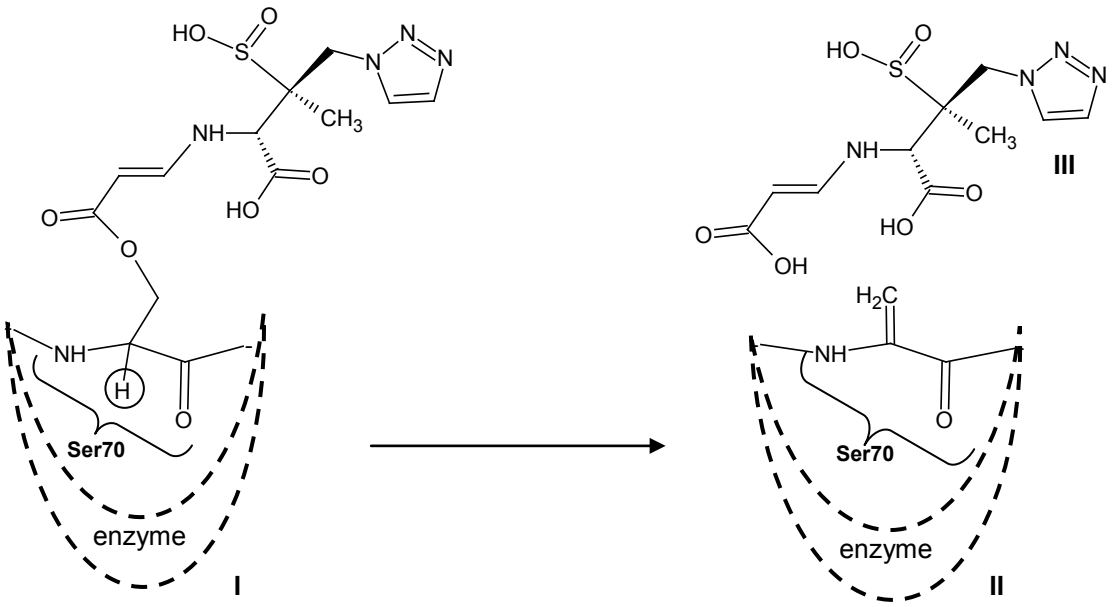

Scheme 8.1 Proposed reaction pathway for the formation of the dehydrated PC1 β-lactamase. **I**, **II** and **III** are the trans-enamine species, alkene-like species (dehydrated PC1) and hydrated form of the rearranged tazobactam molecule, respectively.

8.3 Conclusions

Taking tazobactam as an example, the present study highlights the importance of adopting near physiological conditions in ESI-MS studies of protein-inhibitor complexes. The observed peak at [M + 300] Da is consistent with the formation of a trans-enamine E-I complex between β-lactamases and tazobactam, and in agreement with previous results obtained by x-ray crystallography and spectroscopic techniques. The controversy on the identity of the E-I complexes

is resolved. In addition, our results show that the E-I complex formed from PC1 β-lactamase and tazobactam dissociates further to form an inactive, dehydrated form of the enzyme. This particular inhibition mechanism has the distinct advantage that the enzyme is 'permanently' deactivated, without the need to deal with the regeneration (turnover) of the active enzyme.

Chapter 9 S uggestions for Further Works

Design of β-lactamase biosensors with enhanced bisensing sensitivity

The "*spatial displacement*" mechanism proposed in the present H/D exchange study suggests that the fluorophore is initially oriented towards and close to the active binding site. During substrate binding, the fluorophore moves away from the active site in order to make room for the incoming substrate, thereby the local environment surrounding the fluorophore and its fluorescence properties are changed. This mechanism has provided valuable insight into the way to rationally design more sensitive and specific biosensors. For development of fluorescein-based biosensors, we reason that the biosensing sensitivity could be enhanced if the protein is engineered in such a way that the fluorophore can be initially buried deeper in the active site pocket, and therefore the increase in solvent polarity experienced by the fluorophore upon spatial displacement upon substrate binding may become more significant.

Based on this rationale, we have been attempting to construct a new fluorescein-based biosensor from the TEM-52 β-lactamase. The TEM-52 β-lactamase is produced by performing three point mutations (E104K / M182T / G238S) on the TEM-1 β-lactamase from *E.coli*. Structural analysis showed that the G238S mutation

widens the active site by 2.8 Å, and the E104K and M182T mutations are responsible for stabilizing the reorganized protein structure.[Orencia et al., 2001] We postulate that if a fluorescein-5-maleimide is placed near the active site of the TEM-52, a biosensor with enhanced biosensing sensitivity could be achieved, since the widened active site of the mutant may be more compatible with the bulky fluorescein-5-maleimide.

To construct the TEM-52 biosensor, four additional point mutations were performed on the TEM-52 β-lactamase. First, the disulphide bond near the active site was disrupted by replacing the two cysteine residues, C123 and C77, associated with the bond by alanine. The disruption of this disulphile bond may enhance the flexibility of the active site region, and relieve the steric crowding introduced by the fluorophore. In addition, the catalytically important Glu166 position was replaced by asparagine in order to impair the catalytic efficiency of the enzyme. To this disulphide bond-free and catalytic-deficient TEM-52 mutant, the Val216 position near the active site is mutated to cysteine, and onto which a fluorescein-5-maleimide is attached. The reasons for choosing this position for fluorophore attachment are that first, this position is located on a relatively flexible loop, and thus the incorporation of the fluorophore on this region will not significantly impair the binding efficiency of the

protein. Second, molecular modeling studies show that the fluorescein-5-maleimide fits well with the active site if it is oriented towards the active site from this position (data hot shown). Our preliminary results show that the increase in fluorescence intensity of this biosensor upon substrate binding is ~ 2-folds more than the E166Cf. Further studies, such as H/D exchange and X-ray crystallographic studies, will be preformed to investigate and confirm the detailed biosensing mechanism of this TEM-52 based biosensor.

For badan-based biosensors, the current study suggests that the blue shift and increase in fluorescence intensity observed upon substrate binding are due to the movement of the badan away from the active site binding pocket to an even more hydrophobic environment. On the basis of this scenario, we propose that the extent of the blue shift and fluorescence intensity enhancement may be increased by incorporating hydrophilic amino acid residues into the active site region, such that the solvent polarity initially experienced by badan will become even greater. Consequently, the change in solvent polarity (from polar to less polar) around the badan fluorophore may be more significant upon spatial displacement during substrate binding.

Discovery of new mechanism-based inhibitors for β-lactamases

Our results have confirmed that the E-I complex formed from tazobactam inhibition is most likely a trans-enamine species. By molecular modeling followed by organic synthesis, we shall attempt to design and construct new inhibitors by stabilizing the trans-enamine structure that lead to irreversible inhibition of the enzyme. In addition, further studies will be performed to understand the mechanism of formation of the inactive dehydrated protein from dissociation of the trans-enamine species. For example, X-ray crystallographic studies will be performed to identify the major amino acid residues that participate in the dehydration dissociation reaction.

Understanding the mechanism and the preferred structural factors leading to the formation of inactive dehydrated β-lactamase could initial new routes to the development of mechanism-based inhibitor.

Supporting in formation I: Mathematical studies of the e nzyme kinetics of E166Cf

The Dynamic System Method.

The enzymatic reaction scheme for E166Cf can be represented by:

$$E + S \underset{k_{-1}}{\overset{k_1}{\rightleftharpoons}} ES \xrightarrow{k_2} ES^* \xrightarrow{k_3} E + P$$

where *E* is the enzyme, *S* is an antibiotic substrate, *ES* is the non-covalent enzyme-substrate complex, *ES** is the covalently bound acyl enzyme-substrate complex and *P* is the hydrolyzed product. The set of kinetic equations describing the concentration-time profiles of various reacting species are:

$$\frac{dS}{dt} = -k_1(E)(S) + k_{-1}(ES), \quad [1]$$

$$\frac{d(ES)}{dt} = k_1(E)(S) - k_{-1}(ES) - k_2(ES), \quad [2]$$

$$\frac{d(ES^*)}{dt} = k_2(ES) - k_3(ES^*), \quad [3]$$

$$\frac{dP}{dt} = k_3(ES^*), \quad [4]$$

which is a system of first order ordinary differential equations. Using the experimental conditions and the rate parameters determined for the binding of E166Cf to cefuroxime listed in Table 3:

	Experimental data
K_d *(M)*	0.91 mM
$k_2(s^{-1})$	1.9 s^{-1}
$k_3\ (s^{-1})$	2.0 x 10^{-4} s^{-1}

and noting that $K_d = k_{-1}/k_1$, the k_1 *and* k_{-1} values can be obtained by iteration and curve-fitting the theoretical calculated [ES*]/[E_{total}] profile to the experimental curve obtained by ESI-MS shown in Figure 7(e). The curve-fitting calculations were carried out by minimizing the difference between the calculated [ES*]/[E_{total}] values to the experimental value as a function of time using the Matlab optimization toolbox. With the complete set of rate constants, k_1, k_{-1}, k_2 and k_3, and the initial concentrations of E and S known, the concentrations of *S, E, ES, ES** and *P* as a function of time can be calculated by solving the set of differential equations [1] to [4] shown above.

For fixed values of K_d, k_2 and k_3, the k_1 and k_{-1} values are found in the range of 10^3 - 10^8 $M^{-1}s^{-}1$ and 10^0 - 10^5 s^{-1}, respectively. This conforms with literature k_1 values of protein – ligand interactions reported in the range of 10^5 – 10^8 $M^{-1}s^{-1}$,[7] the physically meaningful range for concentration – time profiles of various species, including *S, E, ES, E S** and *P,* in the hydrolytic reaction. However, we found the generated concentration – time profiles are insensitive to the individual values of k_1 and k_{-1} whenever the K_d value (0.91 mM) is fixed..

Supporting information II: Molecular modeling

Molecular models of the fluorescein-labeled E166C mutant of the PenPC β-lactamase were constructed by homology modeling using the sequence builder of the CACHE software program (CACHE WorkSystem Pro 7.5.0.85), including the substrate-free E166Cf structure, the ES state of E166Cf with cefotaxime non-covalently bound to the active site, and the ES* state of E166Cf with cefotaxime covalently bound to the hydroxyl group of the side chain of Ser70. The crystal structure of the *B. licheniformis* 749/C β-lactamase (PDB code: 4BLM) was used as the template for the substrate-free enzyme structure, and the crystal structure of the acyl enzyme-substrate intermediate of the *E. coli* RTEM-1 β-lactamase complexed with cefotaxime (PDB code: 1FQG) used as the template for the ES* state. The non-covalent ES state was built by superimposing unhydrolyzed penicillin G (extracted from PDB: 1UOF) onto the ES* state. The E166C mutation and the conjugation of fluorescein-5-maleimide with the thiol group of the side chain of Cys166 in E166C were built by the CACHE program. The Ω-loop (including the manually built fluorophore) was treated with the default refinement procedure in the CACHE program to relax poor geometry. The refined models were then subjected to one round of simulated annealing using torsional molecular dynamics, followed by conjugate gradient minimization, using the CNS program. The topology and parameter files for fluoresceine-5-maleimide and cefotaxime used in the refinement were generated using the PRODRG server. The solvent accessible areas (SAA) for the fluorescein label of E166Cf in the non-covalent ES and covalent ES^* states were calculated on the basis of the final refined models using the NACCESS program.

Supporting information III: X-ray crystallography

Crystallization of E166Cb

The E166Cb protein solution was concentrated by ultra-amicon to 20 mg/ml. Crystallization of the protein was performed by "hanging drop vapour diffusion method". Crystal Screen™ (CS) and Crystal Screen 2™ (CS2) (Hampton Research) were used for screening of desired crystallization conditions. Briefly, crystal screen reagent (CS 1-50, CS2 1-48) were added to 98 different reservoirs of the VDX™ plate and to which 1µl of protein solution was added. The mixtures were allowed to incubate at 18℃, and the progresses of crystals formations were monitored by a stereo microscope (10 to 100 x magnification). To obtain protein crystal of covalently bound enzyme-substrate complex, crystal of free E166Cb was soaked into a solution of 10 mM substrate (cefotaxime) and incubated for 20 minutes.

X-ray data collection and refinement of protein structures

The protein crystals obtained were transferred into a cryoprotected mother liquor (containing 20% v/v ethylene glycol that prevents from ice formation), picked up by the cryoloop, and mounted onto the goniometer head of the Rigaku MicroMax™-007HF X-ray spectrometer (Tokyo, Japan) processed by the CrystalClear 1.3.5 SP2 (Tokyo, Japan). Refinement of the X-ray crystal structures of E166Cb was performed by the CCP4 package (Edinburgh, UK) using the X-ray structure of PenP β-lactamase as the initial model.[Knox et al., 1991]

References

Arpin, C., Labia, R., Andre, C., Frigo, C., Harrif, Z.E. and Quentin, C. "SHV-16, a β-Lactamase with a Pentapeptide Duplication in the Omega Loop". *Antimicrobial Agent and Chemotherapy*, Vol 45, pp. 2480-2485 (2001)

Arnold, R.T., Smith, G.G. and Dodson, R.M. "Mechanism of The Pyrolysis of Esters". *Journal of Organic Chemistry*, Vol 15, pp. 1256-1260 (1950)

Ashcroft, A.E. "Recent developments in electrospray ionization mass spectrometry: noncovalently bound protein complexes". *Natural Product Reports*, Vol 22, pp. 452-464 (2005)

Atanasov, B.P., Mustafi, D., and Makinen, M.W. "Protonation of the β-lactam nitrogen is the trigger event in the catalytic action of class A β-lactamases". *Proceedings of the National Academy of Sciences*, Vol 97, pp. 3160-3165 (2000)

Bailey, W.J. and Barclay, R. "Pyrolysis of Esters. V. Mechanism of l,4-Elimination". *Journal of Organic Chemistry*, Vol 21, pp. 328-331 (1955)

Banerjee, S., Peiper, U., Kapadia, G., Pannell, L.K. and Herzbery, O. " Role of the Ω-Loop in the Activity, Substrate Specificity, and Structure of Class A β-Lactamase". *Biochemistry*, Vol 37, pp. 3286-3296 (1998)

Banerjee, S., Shigematsu, N., Pannell, L.K., Ruvinov, S., Orban, J., Schwarz, F. And Herzberg, O. " Probing the Non-Proline *Cis* Peptide Bond in β-Lactamase from *Staphylococcus aureus* PC1 by the Replacement Asn136 ➔Ala". *Biochemistry*, Vol 36, pp. 10857-10866 (1997)

Benesch, J.L., Ruotolo, B.T., Simmons, D.A. and Robinson CV. "Protein Complexes in the Gas Phase: Technology for Structural Genomics and Proteomics". *Chemical Reviews*, Vol 107, pp. 3544-3567 (2007)

Bos, F. and Pleiss, J. "Conserved Water Molecules Stabilize the Ω-Loop in Class A β-Lactamases". *Antimicrobial Agent and Chemotherapy*, Vol 52, pp. 1072-1079 (2008)

Bothner, B., Chavez, R., Wei, J., Strupp, Christian., Phung, Qui., Schneemann, A. and Siuzdak, G. "Monitoring Enzyme Catalysis with Mass Spectrometry". *The Journal of Biological Chemistry*, Vol 275, pp. 13455-13459 (2000)

Borthwick, A.D., Davies, D.E., Ertl, P.F., Exall, A.M., Haley, T.M., Hart, G.J., Jackson, D.L., Parry, N.R., Patikis, A., Trivedi, N., Weingarten, G.G. and Woolven, J.M. "Design and Synthesis of Pyrrolidine-5,5¢-*trans*-Lactams (5-Oxo hexahydropyrrolo[3,2-*b*]pyrroles) as Novel Mechanism-Based Inhibitors of Human Cytomegalovirus Protease. 4. Antiviral Activity and Plasma Stability". *Journal of Medicinal Chemistry*, Vol 46, pp. 4428-4449 (2003)

Bonomo, R.A., Liu,J.Z., Chen, Y.H., Ng, L., Hujer, A.M. and Anderson, V.E." Inactivation of CMY-2 β-lactamase by tazobactam: initial mass spectroscopic characterization". *Biochimica et Biophysical Acta-Bioenergetics*, Vol 1547, pp. 196-205 (2001)

Bonomo, R.A. and Rice, L.B. "Inhibitor Resistant Class A β-Lactamases". *Frontiers in Bioscience*, Vol 4, pp. 34-41 (1999)

Brown, R.P.A., Aplin, R.T. and Schofield, C.J. "Inhibition of TEM-2 β-Lactamase from *Escherichia coli* by Clavulanic Acid: Observation of Intermediates by Electrospray Ionization Mass Spectrometry". *Biochemistry*, Vol 35, pp. 12421-12432 (1996)

Busenlehner, L.S. and Armstrong, R.N. "Insights into enzyme structure and dynamics elucidated by amide H/D exchange mass spectrometry". *Archives of Biochemistry and Biophysics*, Vol 433, pp. 34-46 (2005)

Bush, K., Macalintal, C., Rasmussen, B.A., Lee, V.J. and Yang, Y. "Kinetic Interactions of Tazobactam with β-Lactamases from All Major Structural Classes". *Antimicrobial Agent and Chemotherapy*, Vol 37, pp. 851-858 (1993)

Cech, N.B. and Enke, C.G. "Practical Implications of Some Recent Studies in Electrospray Ionization Fundamentals". *Mass spectrometry Reviews*, Vol 20, pp. 362-387 (2001)

Chen, R.F. and Scott, C.H. “Special Review, Atlas of fluorescence spectra and lifetimes of dyes attached to protein”. *Analytical letters*, Vol 18, pp. 393-421 (1985)

Chan, P.H., So, P.K., Ma, D.L. Zhao, Y., Lai, T.S., Chung, W.H., Chan, K.C., Yiu, K.F., Chan, H.W., Siu, F.M., Tsang, C.W., Leung, Y.C. and Wong, K.Y. “Fluorophore-Labeled β-Lactamase as a Biosensor for β-Lactam Antibiotics: A Study of the Biosensing Process”. *Journal of the American Chemical Society*, Vol 130, pp. 6351-6361 (2008)

Chen, Celia. C.H., Rahil, J., Pratt, R.F. and Herzberg, O. “Structure of a Phosphonate-inhibited β-lactamase: An Analog of the Tetrahedral Transition State/Intermediate of β-Lactam Hydrolysis”. *Journal of Molecular Biology*, Vol 234, pp. 165-178 (1993)

Chan, P.H., Liu, H.B., Chen, W.Y., Chan, K.C., Tsang, C.W., Leung, Y.C. and Wong, K.Y. “Rational Design of a Novel Fluorescent Biosensor for β-Lactam Antibiotics from a Class A β-Lactamase”. *Journal of the American Chemical Society*, Vol 126, pp. 4074-4075 (2004)

Chen, R.F. and Scott, C.H. “Special Review, Atlas of fluorescence spectra and lifetimes of dyes attached to protein”. *Analytical Letter*, Vol 18, pp. 393-421 (1985)

Codreanu, S.G., Ladner, J.E., Xiao, G., Stourman, N.V., Hachey, D.L., Gilliland, G.L. and Armstrong, R.N. “Local Protein Dynamics and Catalysis: Detection of Segmental Motion Associated with Rate-Limiting Product Release by a Glutathione Transferase” . *Biochemistry*, Vol 41, pp. 15161-15172 (2004)

Daniel, J.M., Friess, S.D., Rajagopalan, S., Wendt, S. and Zenobi, R. “Quantitative determination of noncovalent binding interactions using soft ionization mass spectrometry”. *International Journal of Mass Spectrometry*, Vol 216, pp. 1-27 (2002)

Deterding, L.J., Prasad, R., Mullen, G.P., Wilson, S.H. and Tomer, K.B. “Mapping of the 5’-2-Deoxyribose-5-phosphate Lyase active site in DNA polymerase beta by mass spectrometry”. *The Journal of Biological Chemistry,* Vol 275, pp 10463-10471 (2000)

De Lorimier, R.M., Smith, J.J., Dwyer, M.A., Looger, L.L., Sali, K.M., Paavola, C.D., Rizk, S.S., Sadigov, S., Conrad, D.W., Loew, L. and Hellinga, H.W. “Construction of a fluorescent biosensor family”, *Protein Science*, Vol 11, pp. 2655-2675 (2002)

Domon, B. and Aebersold, T. “Mass Spectrometry and Protein Analysis”. *Science*, Vol 312, pp. 212-217 (2006)

Fisher, J. F., Meroueh, S. O. and Mobashery, S. “Bacterial Resistance to β-Lactam Antibiotics: Compelling Opportunism, Compelling Opportunity”. *Chemical Reviews*, Vol 105, pp. 395-424 (2005)

Fonze, E., Vanhove, M., Dive, G., Sauvage, E., Frere, J.M. and Charlier P. "Crystal Structures of the *Bacillus licheniformis* BS3 Class A β-Lactamase and of the Acyl-Enzyme Adduct Formed with Cefoxitin". *Biochemistry*, Vol 41, pp. 1877-1885(2002)

Ge, X., Sirich, T.L., Beyer, M.K., Desaire, H. and Leary, J.A. "A Strategy for the Determination of Enzyme Kinetics Using Electrospray Ionization with an Ion Trap Mass Spectrometer". *Analytical Chemistry*, Vol 73, pp. 5078-5082 (2001)

Ghaemmaghami, S., Fitzgerald, M.C. and Oas, T.G. "A quantitative, high-throughput screen for protein stability". *Proceedings of the National Academy of Sciences*, Vol 97, pp. 8296-8301 (2000)

Gibson, R. M., Christensen, H. and Waley, S. G. "Site-directed mutagenesis of β-lactamase I". *Biochemical Journal*, Vol 272, pp. 613-619 (1990).

Golemi-Kotra, D., Meroueh, S.O., Kim, C., Vakulenko, S.B., Bulychev, A., Stemmler, A.J. and Mobashery, S. "The Importance of a Critical Protonation State and the Fate of the Catalytic Steps in Class A β-Lactamases and Penicillin-binding Proteins". *The Journal of Biological Chemistry*, Vol 279, pp. 34665-34673 (2004)

Guillaume, G., Vanhove, M., Lamotte-Brasseur, J., Ledent, P., Jamin, M., Joris, B. and Frere, J. M. "Site-directed Mutagenesis of Glutamate 166 in Two β-Lactamases". *The Journal of Biological Chemistry*, Vol 272, pp. 5438-5444 (1997)

Hammarstrom, P., Owenius, R., Mårtensson, L.G., Carlsson, U. and Lindgren, M. " High-Resolution Probing of Local Conformational Changes in Proteins by the Use of Multiple Labeling: Unfolding and Self-Assembly of Human Carbonic Anhydrase II Monitored by Spin, Fluorescent, and Chemical Reactivity Probes". *Biophysical Journal*, Vol 80, pp. 2867-2885 (2001)

Helfand, M.S., Bethel, C.R., Hujer, A.M., Hujer, K.M., Anderson, V.E. and Bonomo, R.A. "Understanding Resistance to β-Lactams and β-Lactamase Inhibitors in the SHV β-Lactamase". *The Journal of Biological Chemistry*, Vol 278, pp. 52724-52729 (2003)

Houston, C.T., Taylor, W.P., Widlanski, T.S. and Reilly, J.P. "Investigation of Enzyme Kinetics Using Quench-Flow Techniques with MALDI-TOF Mass Spectrometry". *Analytical Chemistry*, Vol 72, pp. 3311-3319 (2000)

Hoofnagle, A.N., Resing, K.A. and Ahn, N.G. "Protein Analysis BY Hydrogen Exchange Mass Spectrometry". *Annual R eview of Biophysics and B iomolecular Structure*, Vol 32, pp. 1-25 (2003)

Jacob, F., Joris, B., Lepage, S., Dusart, J. and Frere, J.M. "Role of the conserved amino acids of the 'SDN' loop(Ser^{130}, Asp^{131} and Asn^{132}) in a class A fI-lactamase studied by site-directed mutagenesis" . *Biochemical J ournal*, Vol 271, pp. 399-406 (1990)

Jorgensen, T.J.D., Roepstorff, P. and Heck, A.J.R. “Direct Determination of Solution Binding Constants for Noncovalent Complexes between Bacterial Cell Wall Peptide Analogues and Vancomycin Group Antibiotics by Electrospray Ionization Mass Spectrometry”. *Analytical Chemistry*, Vol 70, pp. 4427-4432 (1998)

Kebarle, P. and Tang, P.L. “From ions in solution to ions in the gas phase: The mechanism of electrospray mass spectrometry”. *Analytical Chemistry*, Vol. 65, pp. 972A-986A (1993)

Knight, W.B., Swiderek, K.M., Sakuma, T., Calaycay, J., Shively, J.E., Lee, T.R., Covey, T.R., Shushan, B., Green, B.G., Chabin, R., Shah, S., Mumford, R., Dickson, T.A. and Griffin, P.R. “Electrospray Ionization Mass Spectrometry as a Mechanistic Tool: Mass of Human Leucocyte Elastase and a β-Lactam-Derived E-I Complex”. *Biochemistry*, Vol 32, pp. 2031-2035 (1993)

Konermann, L. and Simmons, D.A. “Protein-Folding Kinetics and Mechanism Study by Pulse-Labeling and Mass Spectrometry”. *Mass Spectrometry Reviews*, Vol 22, pp. 1-26 (2003)

Kuzin, A.P., Nukaga, M., Nukaga, Y., Hujer, A., Bonomo, R.A. and Knox, J.R. “Inhibition of the SHV-1 β-Lactamase by Sulfones: Crystallographic Observation of Two Reaction Intermediates with Tazobactam”. *Biochemistry*, Vol 40, pp. 1861-1866 (2001)

Lietz, E.J., Truher, H., Kahn, D., Hokenson, M.J. and Fink, A.L. “Lysine-73 Is Involved in the Acylation and Deacylation of β-Lactamase”. *Biochemistry*, Vol 39, pp.

4971-4981 (2000)

Lim, V. and Curran, J.F. “Analysis of codon:anticodon interactions within the ribosome provides new insights into codon reading and the genetic code structure”. *The RNA Journal*, Vol 7, pp. 942-957 (2001)

Hvidt, A and Linderstrom-Lang, K. “Exchange of hydrogen atoms in insulin with deuterium atoms in aqueous solutions” *Biochemica et Biophysica* Acta, Vol 16, pp. 168-169 (1955)

Loo, J.A. “Studying noncovalent protein complexes by electrospray ionization mass spectrometry”. *Mass Spectrometry Reviews*, Vol 16, pp. 1-23 (1997)

Lu, W. P., Kincaid, E., Sun, Y. and Bauer, M. D. “Kinetics of β-Lactam Interactions with Penicillin-susceptible and β-resistant Penicillin-binding Protein 2x Proteins from *Streptococcus pneumonia*”. *The Journal of Biological Chemistry*, Vol 276, pp. 31494-31501 (2001)

Lu, W. P., Sun, Y., Bauer, M. D., Paule, S., Koenigs, P. M. and Kraft, W. G. “Penicillin-Binding Protein 2a from Methicillin-Resistant *Staphylococcus aur eus*: Kinetic Characterization of Its Interactions with ,β-Lactams Using Electrospray Mass Spectrometry”. *Biochemistry*, Vol 38, pp. 6537-6546 (1999).

Maveyraud, L., Pratt, R.F. and Samama, J.P. ” Crystal Structure of an Acylation Transition-State Analog of the TEM-1 β-Lactamase. Mechanistic Implications for

Class A β-Lactamases". *Biochemistry*, Vol 37, pp. 2622-2628 (1998)

Maity, H., Lim, W.K., Rumbley, J.N. and Englander, S.W. "Protein hydrogen exchange mechanism: Local fluctuations". *Protein Science*, Vol 12, pp. 153-160 (2003)

Mandell, J.G., Falick, A.M. and Komives, E.A. "Measurement of Amide Hydrogen Exchange by MALDI-TOF Mass Spectrometry". *Analytical Chemistry*, Vol 70, pp. 3987-3995 (1998)

Malcolm, G.P. "β-Lactamase inhibitors". *Drug Resistance Updates*, Vol 3, pp. 109-125 (2000)

Meroueh, S. O., Fisher, J. F., Schlegel, B. and Mobashery, S. "Ab Initio QM/MM Study of Class A β-Lactamase Acylation: Dual Participation of Glu166 and Lys73 in a Concerted Base Promotion of Ser70". *Journal of the American Chemical Society*, Vol 127, pp. 15397-15407 (2005)

Morelle, W. and Michalski, J. C. "The Mass Spectrometric Analysis of Glycoproteins and their Glycan Structures". *Current Analytical Chemistry*, Vol 1, pp. 29-57 (2005)

Orencia, M. C., Yoon, J. S., Ness, J. E., Stemmer, W. P. and Stevens, R. C. "Predicting the emergence of antibiotic resistance by directed evolution and structural analysis". *Nature Structural Biology*, Vol 8, pp. 238-242 (2001)

Owenius, R., Osterlund, M., Lindgren, M., Svensson, M., Olsen, O.H., Persson, E., Freskgard, P.O. and Carlsson, U. “Properties of Spin and Fluorescent Labels at a Receptor-Ligand Interface”. *Biophysical Journal*, Vol 77, pp.2237-2250 (1999)

Padayatti, P.S., Sheri, A., Totir, M.A., Helfand, M.S., Carey, M.P., Anderson, V.E., Carey, P.R., Bethel, C.R., Bonomo, R.A., Buynak, J.D. and Van den Akker, F. “Rational Design of a ,β-Lactamase Inhibitor Achieved via Stabilization of the trans-Enamine Intermediate: 1.28 Å Crystal Structure of wtSHV-1 Complex with a Penam Sulfone”. *Journal of t he A merican C hemical S ociety*, Vol 128, pp. 13235-13242 (2006)

Padayatti, P.S., Helfand, M.S., Totir, M.A., Carey, M.P., Hujer, A.M., Carey, P.R., Bonomo, R.A. and Van den Akker, F. “Tazobactam Forms a Stoichiometric *trans*-Enamine Intermediate in the E166A Variant of SHV-1 β-Lactamase: 1.63 Å Crystal Structure”. *Biochemistry*, Vol 43, pp. 843-848 (2004)

Paizs, B. and Suhai, S. “Fragmentation pathways of protonated peptides”. Mass Spectrometry Reviews, Vol. 24, pp. 508-548 (2005).

Powell, K.D. and Fitzgerald, M.C. “Measurements of Protein Stability by H/D Exchange and Matrix-Assisted Laser Desorption / Ionization Mass Spectrometry Using Picomoles of Material”. *Analytical Chemistry*, Vol 73, pp. 3300-3304 (2001)

Poole, K. “Resistance to β-Lactam antibiotics”. *Cellular and Molecular Life Science*, Vol 61, pp. 2200-2223 (2004)

Pratt, R.F. “On the Definition and Classification of Mechanism-Based Enzyme Inhibitors”. *Bioorganic & Medicinal Chemistry Letters*, Vol 2, pp. 1323-1326 (1992)

Rodriguez, D.P, Zhou, X., Simmons, R., Bethel, C.R., Hujer, A.M., Helfand, M.S., Jin, Z., Guo, B., Anderson, V.E., Ng, L.M. and Bonomo, R.A. “Tazobactam Inactivation of SHV-1 and the Inhibitor-resistant Ser130 → Gly β-Lactamase”. *The Journal of Biological Chemistry*, Vol 279, pp. 19494-19501 (2004)

Sandanayaka, V.O., Prashad, A.S. “Resistance to β-Lactam Antibiotics: Structure and Mechanism Based Design of β-Lactamase Inhibitors”. *Current Medicinal Chemistry*, Vol 9, pp. 1145-1165 (2002)

Sauve, A.A. and Schramm, V.L. “Mechanism-Based Inhibitors of CD38: A Mammalian Cyclic ADP-Ribose Synthetase”. *Biochemistry*, Vol 41, pp. 8455-8463 (2002)

Sanglier, S., Ramstrom, H., Haiech, J., Leize, E. and Dorsselaer, A.V. “Electrospray ionization mass spectrometry analysis revealed a ~310 kDa noncovalent hexamer of HPr kinase/phosphatase from *Bacillus s ubtilis*”. *International J ournal of M ass Spectrometry*, Vol 219, pp. 681-696 (2002)

Saves, Isabelle., Odile, B.S., Maveyraud, L., Samama, J.P., Prome, J.C. and Masson, J.M. “Mass Spectral Kinetic Study of Acylation and Deacylation during the

Hydrolysis of Penicillins and Cefotaxime by Beta-Lactamase TEM-1 and the G238S Mutant". *Biochemistry*, Vol 34, pp. 11660-11667 (1995)

Shen, M.L., Johnson, K.L., Mays, D.C., Lipsky, J.J. and Naylor, S. "Identification of the protein-drug adduct formed between aldehyde dehydrogenase and S-methyl-N,N-diethylthiocarbamoyl sulfoxide by on-line proteolytic digestion high performance liquid chromatography electrospray ionization mass spectrometry". *Rapid Communication in Mass Spectrometry*, Vol 14, pp. 918-923 (2000)

Strynadka, N.C.J., Adachi, H., Jensen, S.E., Johns, K., Sielecki, A., Betzel, C., Sutoh, K. and James, M.N.G. "Molecular structure of the acyl-enzyme intermediate in β-Lactam hydrolysis at 1.7 Å resolution". *Nature*, Vol 359, pp. 700-705 (1992)

Sulton, D., Rodriguez, D.P, Zhou, X., Liu, Y., Hujer, A.M., Bethel, C.R., Helfand, M.S., Thomson, J.M., Anderson, V.E., Buynak, J.D., Ng, L.M. and Bonomo, R.A. "Clavulanic Acid Inactivation of SHV-1 and the Inhibitor-resistant S130G SHV-1 β-Lactamase". *The Journal of Biological Chemistry*, Vol 280, pp. 35528-35536 (2005)

Sun, J., Kitova, E.N., Wang, Weijie. And Klassen J.S. "Method for Distinguishing specific from nonspecific protein-ligand complexes in nanoelectrospray ionization mass spectrometry". *Analytical Chemistry*, Vol 78, pp. 3101-3018 (2006)

Taibi-Tronche, P., Massova, I., Vakulenko, S.B., Lerner, S.A. and Mobashery, S. "Evidence for Structural Elasticity of Class A , β-Lactamases in the Course of

Catalytic Turnover of the Novel Cephalosporin Cefepime". *Journal of the American Chemical Society*, Vol 118, pp. 7441-7448 (1996)

Thomson, J.M., Distler, A.M. and Bonomo, R.A. "Raman Crystallographic Studies of the Intermediates Formed by Ser130Gly SHV, a β-Lactamase that Confers Resistance to Clinical Inhibitors" *Biochemistry*, Vol 46, pp. 8689-8699 (2007)

Tolic, L.P., Bruce, J.E., Lei, P., Anderson, G.A. and Smith, R.D. "In-Trap Cleanup of Proteins from Electrospray Ionization Using Soft Sustained Off-Resonance Irradiation with Fourier Transform Ion Cyclotron Resonance Mass Spectrometry". *Analytical Chemistry*, Vol 70, pp. 405-408 (1998)

Tsang, M.W. and Leung, Y.C. "Overexpression of the recombinant Enterobacter cloacae P99 AmpC β-lactamase and its mutants based on a /105 prophage system in Bacillus subtilis". *Protein Expression and Purification*, Vol 55, pp. 75-83 (2007)

Tullio, A.D., Reale, S. and De Angelis, F. "Molecular recognition by mass spectrometry". *Journal of Mass Spectrometry*, Vol 40, pp. 845-865 (2005)

Vakulenko, S.B., Taibi-Tronche, P., Toth, M., Massova, I., Lerner, S.A. and Mobashery, S. " Effects on Substrate Profile by Mutational Substitutions at Positions 164 and 179 of the Class A TEMpUC19 β-Lactamase from *Escherichia coli*". *The Journal of Biological Chemistry*, Vol 274, pp. 23052-23060 (1999)

Yamashita, M. and Fenn, J.B. "Electrospray ion source. Another variation on the Free-Jet theme". *Journal of Physical Chemistry*, Vol. 88, pp. 4451-4459 (1984)

Yang, Y., Janota, K., Tabei, K., Huang, N., Siegel, M.M., Lin, Y.I., Rasmussen, B.A. and Shlaes, D.M. “Mechanism of Inhibition of the Class A β-Lactamases PC1 and TEM-1 by Tazobactam”. *The Journal of Biological Chemistry*, Vol 275, pp. 26674-26682 (2000)

Yan, X., Watson, J., Ho, P.S. and Deinzer, M.L. “Mass Spectrometric Approaches Using Electrospray Ionization Charge States and Hydrogen-Deuterium Exchange for Determining Protein Structures and Their Conformational Changes”. *Molecular & Cellular Proteomics*, Vol 3, pp. 10-23 (2004)

Zhang, S., Pelt, C.K.V. and Wilson, D.B. “Quantitative Determination of Noncovalent Binding Interactions Using Automated Nanoelectrospray Mass Spectrometry”. *Analytical Chemistry*, Vol 75, pp. 3010-30184432 (2003)

J|A|C|S
ARTICLES

Published on Web 04/23/2008

Fluorophore-Labeled β-Lactamase as a Biosensor for β-Lactam Antibiotics: A Study of the Biosensing Process

Pak-Ho Chan,[†] Pui-Kin So,[†] Dik-Lung Ma,[†] Yanxiang Zhao,[†] Tat-Shing Lai,[†] Wai-Hong Chung,[†] Kwok-Chu Chan,[†] Ka-Fai Yiu,[‡] Hoi-Wan Chan,[‡] Fung-Ming Siu,[§] Chun-Wai Tsang,[†] Yun-Chung Leung,*[,†] and Kwok-Yin Wong*[,†]

Department of Applied Biology and Chemical Technology, Central Laboratory of the Institute of Molecular Technology for Drug Discovery and Synthesis, and Department of Applied Mathematics, The Hong Kong Polytechnic University, Hunghom, Kowloon, Hong Kong, P.R. China, and Department of Chemistry, the University of Hong Kong, Hong Kong, P.R. China

Received August 14, 2007; E-mail: K.-Y.W.: bckywong@ ; Y.-C.L.: bcleung@

Abstract: The fluorescein-labeled E166C mutant of the PenPC β-lactamase (E166Cf) represents a successful model in the construction of "switch-on" fluorescent biosensors from nonallosteric proteins (Chan P.-H. et al.; *J. Am Chem. Soc.*, **2004**, *126*, 4074). This paper focuses on the study of the biosensing mechanism by which the E166Cf biosensor changes its fluorescence upon β-lactam binding and hydrolysis. Mass spectrometric and stopped-flow fluorescence studies of E166Cf with cefuroxime, penicillin G, and 6-aminopenicillanic acid reveal that the formation of enzyme−substrate complex enhances the fluorescence of E166Cf, and the subsequent regeneration of the free enzyme restores the weak fluorescence of E166Cf. Molecular modeling studies of E166Cf with penicillin G show that the fluorescein label is likely to share a common space with the β-lactam and thiazolidine rings of the antibiotic in the active site. This spatial clash appears to cause the fluorescein label to move from the active site to the external aqueous environment upon substrate binding and hence experience higher water exposure. Steady-state fluorescence measurements indicate that the fluorescence of E166Cf can be enhanced by 6-aminopenicillanic acid, which consists of the β-lactam and thiazolidine rings only. Thermal denaturation experiments of the wild-type enzyme, E166C, and E166Cf reveal that the E166C mutation is likely to increase the flexibility of the Ω-loop. This "modified" structural property might compensate for the possible steric effect of the fluorescein label on substrate binding.

1. Introduction

β-Lactam antibiotics such as penicillins and cephalosporins have been routinely used in the treatment of bacterial infections over the past several decades. These antibacterial agents can inactivate penicillin-binding proteins (PBP), which are responsible for synthesizing bacterial cell walls through the formation of stable covalent acyl complexes.[1−4] As a consequence of this 'irreversible' substrate binding, the cell-wall-synthesizing activity of PBP is strongly inhibited, thus leading to cell death.[1−4]

The overuse of these drugs, however, has led to the increasing emergence of antibiotic-resistant bacteria, which are able to produce β-lactamase enzymes to destroy β-lactam antibiotics.[1−4] In this enzyme family, serine β-lactamases from classes A, C, and D can efficiently catalyze β-lactam hydrolysis according to a three-step model, which involves the acylation of the enzymes with β-lactam antibiotics (Scheme 1).[1,2] The subsequent deacylation of the covalent acyl enzyme−substrate complexes leads to the generation of carboxylic acids as products.[1,2]

Scheme 1. Catalytic Pathway of Serine β-Lactamases: where E is the Enzyme β-Lactamase, S is an Antibiotic Substrate, ES is a Non-Covalent Enzyme−Substrate Complex, ES* is a Covalent Acyl Enzyme−Substrate Complex, and P is the Product.

$$E + S \underset{k_{-1}}{\overset{k_1}{\rightleftharpoons}} ES \xrightarrow[\text{Acylation}]{k_2} ES^* \xrightarrow[\text{Deacylation}]{k_3} E + P$$

One of the effective ways to reduce the emergence of antibiotic-resistant bacteria is to prevent the improper use of β-lactam antibiotics. In this regard, the abuse of β-lactam antibiotics in the food industry (e.g., dairy products) is recognized as a major route of spreading antibiotic resistance in bacteria. To combat this problem, we have recently constructed a "switch-on" fluorescent biosensor (E166Cf) for β-lactam antibiotics from the class A PenPC β-lactamase.[5] Unlike allosteric ligand-binding proteins which usually undergo

[†] Department of Applied Biology and Chemical Technology, Central Laboratory of the Institute of Molecular Technology for Drug Discovery and Synthesis, The Hong Kong Polytechnic University.
[‡] Department of Applied Mathematics, The Hong Kong Polytechnic University.
[§] Department of Chemistry, The University of Hong Kong.

(1) Matagne, A.; Dubus, A.; Galleni, M.; Frere, J. M. *Nat. Prod. Rep.* **1999**, *16*, 1−19.
(2) Matagne, A.; Lamotte-Brasseur, J.; Frere, J. M. *Biochem. J.* **1998**, *330*, 581−598.
(3) Fisher, J. F.; Meroueh, S. O.; Mobashery, S. *Chem. Rev.* **2005**, *105*, 395−424.
(4) Wilke, M. S.; Lovering, A. L.; Strynadka, N. C. *Curr. Opin. Microbiol.* **2005**, *8*, 525−533.
(5) Chan, P. H.; Liu, H. B.; Chen, Y. W.; Chan, K. C.; Tsang, C. W.; Leung, Y. C.; Wong, K. Y. *J. Am. Chem. Soc.* **2004**, *126*, 4074−4075.

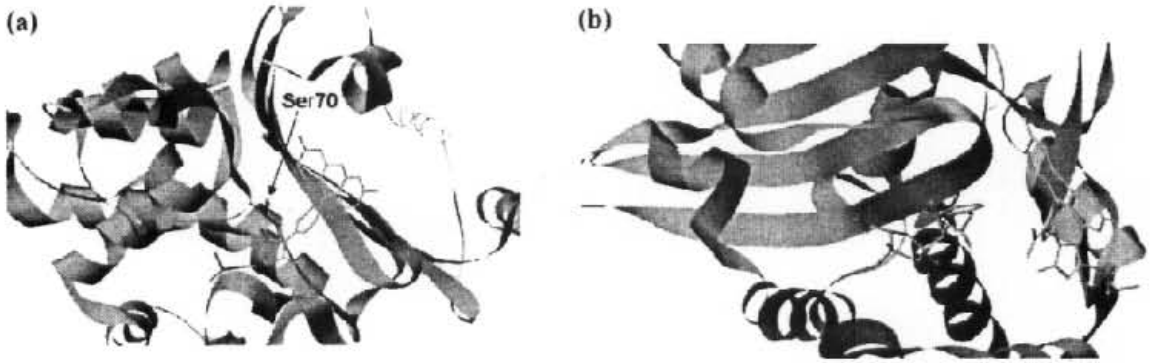

Figure 1. Molecular models of E166Cf with and without penicillin G. (a) Stereoview of the active site of E166Cf without binding to an antibiotic substrate.[5] The fluorescein label (green) is buried inside the active site in the substrate-free E state. (b) Stereoview of the active site of E166Cf in the covalent ES* state.[5] Note that the fluorescein label (green) stays out of the active site to avoid the spatial clash with the penicillin G molecule (red) in this state. The Ser70 and Cys166 residues are shown in blue and magenta, respectively.

large conformational changes upon ligand binding.[6–16] this bacterial enzyme is nonallosteric, and therefore, detecting the substrate binding in the enzyme's active site requires the placement of a fluorophore close to this local environment. The catalytically important residue Glu166 in the flexible Ω-loop (close to the active site)[17–20] of the wild-type enzyme was first replaced with a cysteine, which was subsequently labeled with the environment-sensitive fluorophore fluorescein-5-maleimide.[5] The removal of the catalytic residue significantly reduces the hydrolytic activity of E166Cf, thus allowing E166Cf to serve as a "ligand-binding" protein (with very low k_{cat}).[5] The E166Cf mutant fluoresces more strongly upon binding to penicillins (e.g., penicillin G and ampicillin) and cephalosporins (e.g., cefuroxime and cefoxitin). For the penicillin antibiotics, the E166C mutant can still hydrolyze these substrates, albeit slowly, and gives declining fluorescence signals.[5] In contrast, the E166Cf mutant gives stronger fluorescence with the cephalosporin antibiotics over a sustained period of time due to their strong resistance to the hydrolytic activity of the enzyme. Molecular modeling studies of E166Cf have shown that the fluorescein label moves out of the active site upon binding to an antibiotic (Figure 1).[5] This subtle motion causes the fluorescein label to gain higher water exposure and hence give stronger fluorescence.[5] Surprisingly, the attached fluorophore does not significantly impair the E166Cf−antibiotic binding, presumably due to the flexible nature of the Ω-loop.[17–20]

The E166Cf mutant represents a successful case in the construction of fluorescent biosensors from nonallosteric proteins. Understanding the biosensing mechanism of E166Cf is of particular importance because this can provide an insight into the way of constructing "switch-on" fluorescent biosensors for biologically significant substrates/ligands from nonallosteric proteins in general. This biosensor development will advance the analytical science in a variety of important fields, ranging from clinical diagnosis to environmental monitoring.

In this study, we further investigated the biosensing mechanism of the E166Cf mutant, using a variety of biophysical techniques including electrospray ionization mass spectrometry (ESI-MS), stopped-flow fluorescence spectroscopy, and circular dichroism (CD) spectropolarimetry. Parallel mass spectrometric and stopped-flow fluorescence measurements show that the formation of enzyme−substrate complex causes E166Cf to enhance its fluorescence. The subsequent hydrolysis of the bound substrate causes E166Cf to restore its weak fluorescence signal. In addition, molecular modeling studies reveal that the fluorescein label is likely to share a common space within the active site with the bicyclic structure of β-lactam antibiotics. This spatial clash appears to cause the fluorescein label to depart from the active site upon substrate binding and gain higher exposure to the external aqueous environment. This observation is further supported by the findings of the proteolytic studies of E166Cf. In addition, thermal unfolding experiments monitored by CD spectropolarimetry reveal that the Ω-loop of E166Cf, where the fluorescein label resides, gains higher flexibility compared to that of the wild-type enzyme.

2. Experimental Section

2.1. Chemicals. Penicillin G, cefuroxime, 6-aminopenicillanic acid (6-APA), chloramphenicol, potassium dihydrogenphosphate, guanidine hydrochloride (GdnHCl), sodium chloride, TrisHCl, ammonium bicarbonate, ammonium acetate, trypsin from bovine pancreas, and myoglobin from horse heart were obtained from Sigma Co. Fluorescein was purchased from Fluka. Fluorescein-5-maleimide was obtained from Molecular Probes, Inc. The structures of the antibiotics and the fluorophore used in this study are shown in Figure 2.

(6) Tolosa, L.; Gryczynski, I.; Eichhorn, L. R.; Dattelbaum, J. D.; Castellano, F. N.; Rao, G.; Lakowicz, J. R. *Anal. Biochem.* **1999**, *267*, 114–120.
(7) Ye, K.; Schultz, J. S. *Anal. Chem.* **2003**, *75*, 3451–3459.
(8) Salins, L. L.; Ware, R. A.; Ensor, C. M.; Daunert, S. *Anal. Biochem.* **2001**, *294*, 19–26.
(9) Gilardi, G.; Zhou, L. Q.; Hibbert, L.; Cass, A. E. *Anal. Chem.* **1994**, *66*, 3840–3847.
(10) Benson, D. E.; Conrad, D. W.; de Lorimier, R. M.; Trammell, S. A.; Hellinga, H. W. *Science* **2001**, *293*, 1641–1644.
(11) Sandros, M. G.; Gao, D.; Benson, D. E. *J. Am. Chem. Soc.* **2005**, *127*, 12198–12199.
(12) Salins, L. L.; Goldsmith, E. S.; Ensor, C. M.; Daunert, S. *Anal. Bioanal. Chem.* **2002**, *372*, 174–180.
(13) Brune, M.; Hunter, J. L.; Corrie, J. E.; Webb, M. R. *Biochemistry* **1994**, *33*, 8262–8271.
(14) Brune, M.; Hunter, J. L.; Howell, S. A.; Martin, S. R.; Hazlett, T. L.; Corrie, J. E.; Webb, M. R. *Biochemistry* **1998**, *37*, 10370–10380.
(15) Lager, I.; Fehr, M.; Frommer, W. B.; Lalonde, S. *FEBS Lett.* **2003**, *553*, 85–89.
(16) Shrestha, S.; Salins, L. L.; Mark Ensor, C.; Daunert, S. *Biotechnol. Bioeng.* **2002**, *78*, 517–26.
(17) Castillo, R.; Silla, E.; Tunon, I. *J. Am. Chem. Soc.* **2002**, *124*, 1809–1816.
(18) Herzberg, O. *J. Mol. Biol.* **1991**, *217*, 701–719.
(19) Knox, J. R.; Moews, P. C. *J. Mol. Biol.* **1991**, *220*, 435–55.
(20) Jelsch, C.; Mourey, L.; Masson, J. M.; Samama, J. P. *Proteins* **1993**, *16*, 364–383.

Penicillins

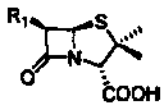

R_1	
NH_2	6-Aminopenicillanic acid (6-APA)
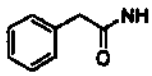	Penicillin G

Cephalosporin

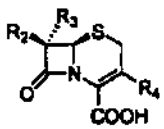

R_2	R_3	R_4	
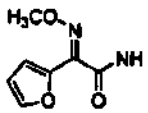	H	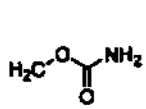	Cefuroxime

Fluorescein-5-maleimide

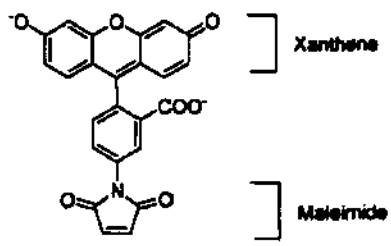

Figure 2. Structures of the β-lactam antibiotics and fluorescein-5-maleimide used in this study.

2.2. Protein Preparation and Characterization. The wild-type PenPC β-lactamase was expressed and purified as described.[5] The E166C mutant of the PenPC β-lactamase was expressed by fermentation and purified with Celite 545 (see Supporting Information). The fluorophore labeling of E166C was performed according to the method described in our previous studies.[5] The mass values of the wild-type and mutant enzymes (E166C and E166Cf) were analyzed by ESI-MS.[5] The kinetic parameters of the wild-type and mutant enzymes were determined by the spectrophotometric method[5] in which the hydrolysis of penicillin G, 6-APA and cefuroxime were monitored at 232, 240 and 260 nm, respectively. Steady-state fluorescence measurements of the E166Cf mutant with penicillin G, 6-APA and cefuroxime were performed as described.[5] The experimental details for molecular modeling and mathematical simulation are described in Supporting Information.

2.3. Enzyme Kinetics Studies by Mass Spectrometry. 2.3.1. Sample Preparation. The E166C and E166Cf samples were further purified prior to mass spectrometric measurements as follows. The protein samples in phosphate buffer (pH 7.2) were loaded onto a CM column (HiTrap CM Sepharose FF, 1 mL, GE Healthcare), which was pre-equilibrated with 50 mM sodium phosphate buffer (pH 7.2). The proteins were eluted by a linear gradient of NaCl (0–0.5 M). The desired fractions were collected, concentrated, and buffer-exchanged with 20 mM ammonium acetate (pH 7.0) for at least five cycles by means of Amicon Ultra-15 (NMWL = 10,000) centrifugal filter devices (Millipore).

2.4. Detection of Covalent Acyl Enzyme–Substrate Complexes. Covalent acyl enzyme–substrate complexes formed by β-lactamases and PBP can be detected by ESI-MS[21–24] and fluorescence spectroscopy.[25,26] In this study, we studied the catalytic processes of the mutant enzymes with cefuroxime and 6-APA by the mass spectrometric method.[21–24] The enzyme–substrate binding reaction was initiated by mixing 60 μL of 1 μM E166Cf (in 20 mM ammonium acetate buffer, pH 7.0) with 60 μL of 10 μM antibiotic (cefuroxime and 6-APA, in 20 mM ammonium acetate buffer, pH 7.0). The reaction was allowed to take place at room temperature. At desired time intervals, the reaction was quenched by adding 120 μL of 8% formic acid in CH_3CN to the enzyme solution (to unfold the protein), giving a reaction mixture in buffer/CH_3CN (1:1 v/v) containing 4% formic acid (pH ≈ 2). For short reaction times, the reaction was initiated and quenched by a quench-flow system (Biologic SFM-400/Q, Claix, France). All quenched samples were stored on ice prior to mass spectrometric analysis. The resulting ESI spectrum was found to show two major peaks (A and B) attributed to the free enzyme E and the enzyme–substrate complex ES*, respectively (refer to Figure S1 and Figure 4). The relative amount of ES* can be expressed as the ratio of the amount of ES* to the total amount of the enzyme, $[ES^*]/[E_{total}]$, where [ES*] is the peak area of peak B and $[E_{total}]$ (= [E] + [ES*]) is the sum of peak areas of peak A and B in the transformed ESI mass spectrum. Similar experiments were also performed with the unlabeled E166C mutant. For comparison, parallel stopped-flow fluorescence measurements were also performed with E166Cf (0.5 μM) with 5 μM cefuroxime, 6-APA and penicillin G in 20 mM ammonium acetate (pH 7.0), using a stopped-flow instrument equipped with a fluorescence readout device (Applied Photophysics SX.18MV-R, Leatherhead, UK). The sample was excited at 494 nm and the fluorescence signal monitored at 515 nm. Both excitation and emission slit widths were 5 nm.

2.5. Determination of Kinetic Parameters. The methodology described by Lu et al. for studying PBP, which shows mechanistic and kinetic properties similar to those of class A β-lactamases in the binding of β-lactam antibiotics,[23,24] was adopted in this study. According to Scheme 1, K_d ($= k_{-1}/k_1$) is the equilibrium dissociation constant for the formation of the reversible noncovalent ES complex, k_2 is the rate constant for the formation of the covalent acyl ES* complex, and k_3 is the rate constant for the hydrolysis of ES* to the free enzyme (deacylation). Taking into consideration that (i) the k_3 values for the Glu166-substituted mutants of the class A TEM-1 and *S. albus G* β-lactamases with β-lactam antibiotics are much lower than those of the wild-type enzymes (~5–9 orders of magnitude lower),[27] (ii) the acylation step remains to be active in the Glu166-substituted β-lactamase mutants with β-lactam antibiotics, as reflected by their relatively high acylation efficiency (k_2/K_d),[27] and (iii) the predicted k_2 value for the E166D mutant of the PenPC β-lactamase is ~2 s^{-1},[28] which is much larger than the

(21) Aplin, R. T.; Baldwin, J. E.; Schofield, C. J.; Waley, S. G. *FEBS Lett.* **1990**, *277*, 212–214.
(22) Saves, I.; Burlet-Schiltz, O.; Maveyraud, L.; Samama, J. P.; Prome, J. C.; Masson, J. M. *Biochemistry* **1995**, *34*, 11660–11667.
(23) Lu, W. P.; Kincaid, E.; Sun, Y.; Bauer, M. D. *J. Biol. Chem.* **2001**, *276*, 31494–31501.
(24) Lu, W. P.; Sun, Y.; Bauer, M. D.; Paule, S.; Koenigs, P. M.; Kraft, W. G. *Biochemistry* **1999**, *38*, 6537–6546.
(25) Frere, J. M.; Ghuysen, J. M.; Iwatsubo, M. *Eur. J. Biochem.* **1975**, *57*, 343–351.
(26) Frere, J. M.; Ghuysen, J. M.; Perkins, H. R. *Eur. J. Biochem.* **1975**, *57*, 353–359.
(27) Guillaume, G.; Vanhove, M.; Lamotte-Brasseur, J.; Ledent, P.; Jamin, M.; Joris, B.; Frere, J. M. *J. Biol. Chem.* **1997**, *272*, 5438–5444.

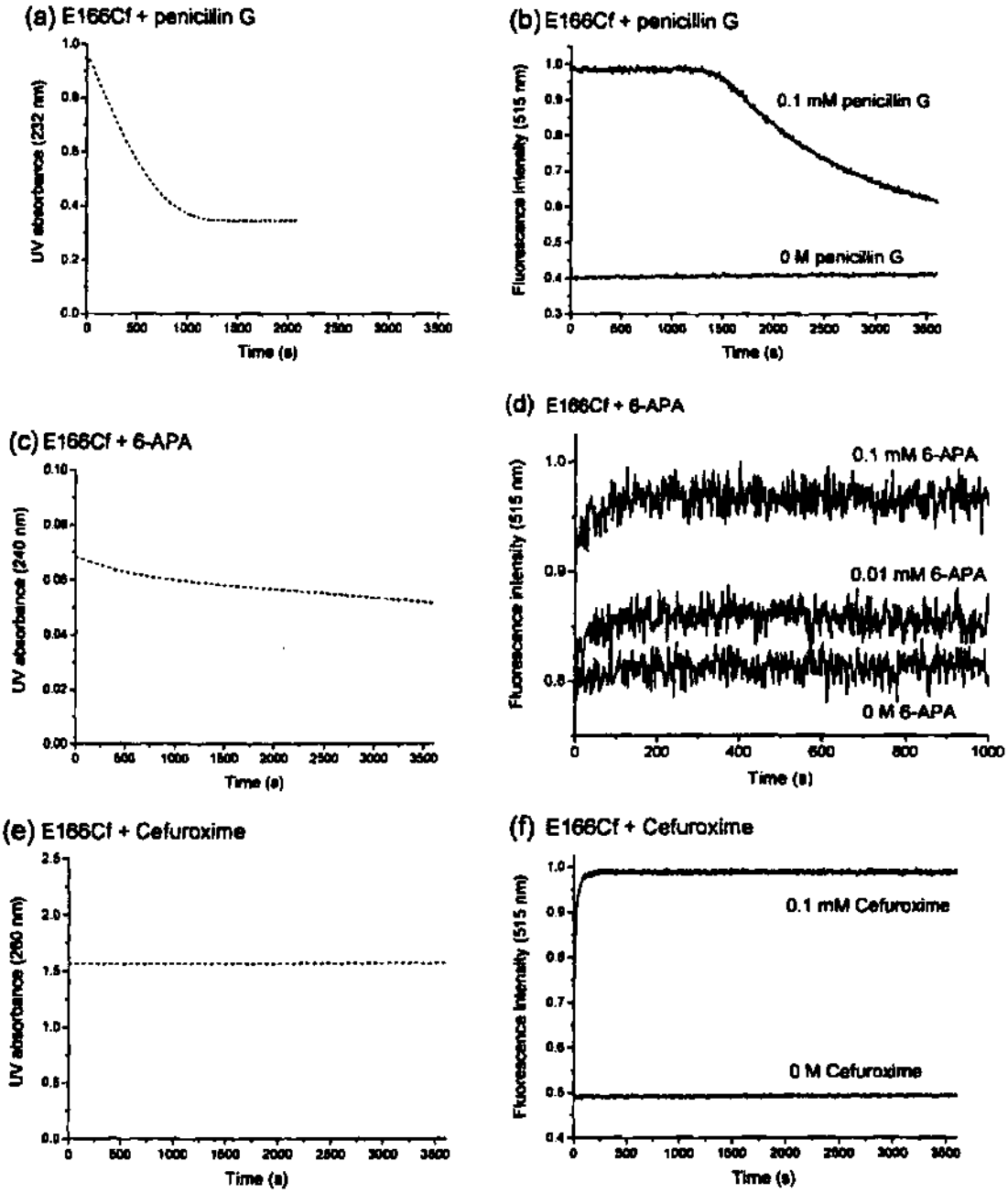

Figure 3. Time course of the hydrolysis of penicillin G, 6-APA, and cefuroxime by E166Cf monitored by UV absorption and fluorescence measurements. The reaction was initiated by mixing E166Cf with each of the antibiotics in 50 mM potassium phosphate (pH 7.0) in both experiments. The UV absorbances of penicillin G, 6-APA, and cefuroxime (0.1 mM) in the presence of E166Cf (0.12 μM) are shown in (a), (c), and (e), respectively. The decreases in absorbance at 232, 240, and 260 nm arise from the cleavage of the β-lactam amide bond of penicillin G, 6-APA, and cefuroxime, respectively. The experimental data for penicillin G are from ref 5. The fluorescence signals of E166Cf (0.12 μM) with and without penicillin G, 6-APA and cefuroxime are shown in (b), (d), and (f), respectively. Excitation wavelength: 494 nm; excitation and emission slit widths: 5 nm.

k_3 value of the TEM-1 E166N mutant ($\sim 10^{-6}$ s^{-1}),[27] it is reasonable to assume that the deacylation step is significantly slower than the acylation step. That is, the contribution of deacylation to the formation of ES* is negligible. Thus, the formation of ES* for E166Cf (or E166C) can be regarded as a pseudo-single-turnover process, as in the case of PBP.[23,24] In addition, the deacylation rate k_3 for the TEM-1 E166N mutant[27] is in the same order of magnitude as those of several PBPs,[23,24] further indicating the similarity in the kinetic properties of Glu166-substituted class A β-lactamase and PBP. Thus, the kinetic equation for the formation of ES* is given by eq 1:

$$[ES^*]/[E_{total}] = 1 - \exp - (k_2 t) \quad (1)$$

(28) Gibson, R. M.; Christensen, H.; Waley, S. G. *Biochem. J.* **1990**, *272*, 613–619.

k_s, the apparent first-order rate constant for the formation of ES*, was obtained by computer-fitting the experimental value of $[ES^*]/[E_{total}]$ versus time (t) to equation [1].

For the mechanism shown in Scheme 1, k_s is related to K_d and k_2 according to equation [2]:

$$k_s = k_2 \frac{[S_0]}{K_d + [S_0]} \quad (2)$$

where $[S_0]$ is the initial substrate concentration and k_2 and K_d were obtained by computer fitting the experimental data of k_s versus $[S_0]$ to equation [2].

The first-order deacylation rate constant k_3 was obtained by monitoring the degradation of ES* as a function of time.

$$[ES^*]/[E_{total}] = 1 - \exp - (k_3 t) \quad (3)$$

The $k_3$values were obtained by fitting the experimental data of $[ES^*]/[E_{total}]$ versus time to eq 3. All curve fittings were performed with Origin 6.1.

2.6. Determination of K_d and k_2. The kinetics studies of E166Cf with cefuroxime and 6-APA were performed using a quench-flow device (Biologic SFM-400/Q, Claix, France). The hydrolytic reaction was initiated by mixing 72.5 μL of 1 μM E166Cf (or E166C) in 20 mM ammonium acetate buffer (pH = 7.0) with 72.5 μL of desired concentrations of antibiotic (cefuroxime and 6-APA) in 20 mM ammonium acetate buffer (pH = 7.0), and then quenched at various time intervals by addition of 145 μL of 8% (v/v) formic acid. The final pH of the quenched solution was ~2. The reaction times were computer-controlled by varying the flow rate of the reactants. The quenched reaction mixtures were injected into the ESI source of the Q-TOF 2 mass spectrometer (Waters-Micromass, Manchester, UK). The mass spectrometer was scanned over a m/z range of 700−1600, and the raw spectra were deconvoluted by the MassLynx 3.5 Transform Program (Waters, Manchester, UK). The ratio of the concentration of the covalent enzyme−substrate complex to the total enzyme concentration ($[ES^*]/[E_{total}]$) at different time intervals was determined by measuring the peak areas of the [E] and [ES*] peaks in the mass spectrum, where $[E_{total}] = [E] + [ES^*]$. The experimental profile of $[ES^*]/[E_{total}]$ versus time was fitted into eq 1, from which the first order apparent rate constant k_s was obtained. The k_s values at several different substrate concentrations, $[S_0]$, were then determined. The K_d and k_2 values were obtained by fitting the data of k_s versus $[S_0]$ into eq 2.

Similar to the kinetics study by Lu et al. on PBP, the present mass spectrometric study on the kinetics of the β-lactamase mutants was also based on the "rapid-equilibrium assumption" (i.e., $k_2 \ll k_{-1}$), such that K_d could be regarded as an equilibrium dissociation constant for the noncovalent ES complex. In our case, with the relatively large K_d (~1 mM) and small k_2 (~2 s^{-1}) values, and the fact that the reported k_1 values for protein−ligand interactions in the literature are in the range of 10^5−10^8 M^{-1} s^{-1},[24] the estimated k_{-1} value is 10^2−10^4-fold larger than the k_2 value. This argues that the kinetic properties of our E166C mutant are in agreement with the "rapid-equilibrium" assumption,[23,24] which is equally applicable to the case of the E166Cf biosensor.

2.7. Determination of k_3. A 500 μL portion of 1 μM E166Cf (or E166C) was allowed to react with 500 μL of 1 μM antibiotic (cefuroxime and 6-APA) long enough until most of the mutant enzyme was converted to the covalent acyl enzyme−substrate complex, and the deacylation rate constant k_3 was determined by monitoring the dissociation of ES* with time by ESI-MS. At different sampling points, a 70 μL portion of the reaction mixture was taken out and quenched with formic acid (final concentration: 4% (v/v)). The ratios of the concentration of the covalent enzyme−substrate complex to the total enzyme concentration, $[ES^*]/[E_{total}]$, at different time intervals were determined as described, and the experimental data were fitted into eq 3, from which the k_3 value was determined.

The kinetic data for E166C and E166Cf so obtained are presented in Figures S1−S7 (Supporting Information) and Figure 4.

2.8. Proteolytic Studies. 2.8.1. Fluorescence Measurements. E166Cf (0.2 mg/mL) was mixed with trypsin (0.01 mg/mL) in 50 mM potassium phosphate buffer (pH 7.0) in a quartz cuvette of 1 cm path length. The fluorescence spectra of this sample were then recorded at various time intervals using a Perkin-Elmer LS50B spectrofluorimeter. The excitation wavelength was 460 nm, and the excitation and emission slit widths were 2.5 nm.

2.8.2. Mass Spectrometric Measurements. Proteolysis of E166Cf (or E166C, ~0.3 mg/mL) was performed by incubation with trypsin (~0.01 mg/mL) in 20 mM ammonium acetate (pH 7.0) at 37 °C overnight. The digested sample was mixed with the MALDI matrix composed of 10 mg/mL CHCA in acetonitrile/ethanol/0.1% trifluoroacetic acid (49.5: 49.5: 1 (v/v)). A 1.5 μL portion of the sample/matrix mixture was spotted onto a 96-well stainless steel target plate, air-dried, and then analyzed by a Waters MicroMX MALDI-TOF mass spectrometer (Waters, Manchester, UK) controlled by MassLynx 4.1 (Waters, Manchester, UK). Peptide ions were generated by a 337 nm pulse laser and accelerated by a voltage of 1.9 kV with a pulse delay of 500 ns. The resulting mass spectra were obtained by accumulation of at least 50 single scans. The peptide fragments of trypsin were identified by accurate mass measurements as follows. A m/z range of 700−3000 Da was calibrated externally with a polyethylene glycol (PEG) mixture (PEG600/PEG1000/PEG2000/NaI = 1:1:3:1 (w/w)). The accurate mass values of the peptide fragments of trypsin were then determined, using a phosphorylase B tryptic digest standard as the internal standard for internal lock mass calibration to achieve a mass accuracy of <20 ppm. The mass peaks of the individual protein fragments were assigned, using the Findpept Program at http://us.expasy.org/tools/findpept.html.

2.8.3. Circular Dichroism Measurements. Digested E166Cf was prepared as described above (section 2.8.2.). The far-UV CD spectrum of this sample was recorded on a JASCO-J810 CD spectropolarimeter at a scan rate of 50 nm/min and a bandwidth of 2 nm, using a quartz cuvette of 1 mm path length. For comparison, similar CD measurements were also performed with E166Cf (~0.3 mg/mL) without subjection to trypsin digestion.

2.9. Thermal Unfolding Studies. The thermal unfolding studies of the wild-type PenPC β-lactamase, E166C, and E166Cf in 50 mM potassium phosphate buffer (pH 7.0) were performed on a JASCO J-810 CD spectropolarimeter. The far-UV CD signal at 222 nm was recorded every 1 °C from 20 to 80 °C for the wild-type enzyme and from 20 to 70 °C for E166C and E166Cf, using a quartz cuvette of 1 mm path length. The heating rate and the slit width were 30 °C/h and 2 nm (respectively), and the response time was 2 s. The enzymes unfolded reversibly upon thermal denaturation. The CD signals of the enzymes were subtracted from those contributed by the buffer.

The thermal unfolding curves of the enzymes were then fitted to the following equation to determine the midpoints of transitions based on a two-state model for the transition between the native and unfolded states of a protein:[27]

$$y_{obs} = \frac{\{y_N + pT\} + \{y_U + qT\}\exp\{b\}}{1 + \exp\{b\}}$$

where $b = [\Delta H_m(1 - T/T_m)]/RT$, y_{obs} is the measured variable parameter at a given temperature, y_N and y_U are the variable parameters for the native and denatured states (respectively), T_m is the midpoint of the heat-induced transition, ΔH_m is the enthalpy change for unfolding at T_m, p and q are the slopes of the pre- and post-unfolding baselines (respectively), R is the gas constant, and T is the absolute temperature.

3. Results

3.1. Steady-State Fluorescence and Spectrophotometric Studies. The origin of the fluorescence changes of E166Cf in the presence of penicillin G, 6-APA, and cefuroxime was investigated by both UV absorption and fluorescence measurements.

Cefuroxime is resistant to the hydrolytic action of E166Cf, whereas penicillin G is not.[5] These antibiotics are good candidates for studying the fluorescence behavior of E166Cf. For 6-APA, this antibiotic is structurally similar to penicillin G except that it has no R_1 chain (Figure 2). Thus, the effect of the bicyclic structure of the β-lactam and thiazolidine rings on the fluorescence response of E166Cf can be examined.

Figure 3a shows the real-time UV absorbance of E166Cf (0.12 μM) with penicillin G (0.1 mM) in 50 mM phosphate buffer (pH 7.0).[5] The UV absorption signal at 232 nm, which arises from the UV absorption by the β-lactam amide bond of penicillin G,[29] decreases rapidly within 20 min as a result of the hydrolytic action of E166Cf toward the β-lactam ring. After 20 min of β-lactam hydrolysis, the UV absorption signal becomes steady. Interestingly, under similar conditions, E166Cf exhibits a sustained fluorescence plateau for about 20 min in the presence of the same concentration of penicillin G (Figure 3b).[5] This fluorescence change, however, was not observed when the unlabeled E166C mutant was incubated with free fluorescein under similar conditions (Figure S8), indicating that the fluorescence change observed with E166Cf is likely to arise from the local environmental change around the fluorescein label induced by antibiotic binding. Taking these observations together, the fluorescence enhancement of E166Cf is likely to be triggered by the binding of penicillin G to the active site. It is interesting to note that the fluorescence of E166Cf declines slowly after the hydrolysis of penicillin G (t > 20 min). This observation is presumably due to the slow return of the fluorescein label to the vacant active site after β-lactam hydrolysis because of its bulky nature.

Unlike penicillin G, 6-APA shows only a slight decrease in UV absorbance over the time course, indicating that the hydrolysis of 6-APA by E166Cf is very slow (Figure 3c). In addition, fluorescence measurements showed that the fluorescence of E166Cf with 6-APA increases as a function of time (Figure 3d). This increasing fluorescence profile is similar to the fluorescence/time profiles corresponding to the initial phase of hydrolysis of penicillin and cephalosporin antibiotics.[5] Unlike the case of penicillin G,[5] the fluorescence enhancement for 6-APA is much less significant, and no detectable fluorescence decline appears over the time course. These observations are presumably due to the weaker binding and activity of E166Cf toward 6-APA compared to that toward penicillin G.

For cefuroxime, this antibiotic shows no significant decrease in UV absorbance, indicating its high resistance to the hydrolytic action of E166Cf (Figure 3e). Moreover, E166Cf shows a sustained fluorescence plateau over the time course, similar to the case of 6-APA (Figure 3f). These results, together with those obtained with penicillin G, highlight the significant role of β-lactam binding in enhancing the fluorescence of E166Cf.

3.2. Mass Spectrometric and Stopped-Flow Fluorescence Studies. In order to further investigate the effects of antibiotic binding and hydrolysis on the fluorescence of E166Cf, the hydrolytic processes of cefuroxime, 6-APA, and penicillin G by E166Cf at different time intervals were analyzed by ESI-MS. This technique can distinguish ES* from E according to their different mass values and determine the population of ES* over the time course. Briefly, E166Cf was mixed with each of the antibiotics, and the hydrolytic process was quenched by acid-unfolding of the labeled enzyme at different time intervals. The population of the covalent acyl enzyme−substrate complex ES* at each time interval was then determined (see Experimental Section).

As shown in Figure 4e, the population of the ES* state for cefuroxime increases slowly as a function of time (up to 15 min), indicating that this antibiotic is resistant to the acylating action of E166Cf. For 6-APA, the population of ES* also increases over the time course (Figure 4f). In both cases, no significant decline in the ES* population was observed over the time course, indicating that cefuroxime and 6-APA are resistant to the deacylating action of E166Cf. In the case of penicillin G, the population of ES* increases rapidly in the first 60 s and then declines gradually (Figure 4g). The decrease in the ES* population indicates that penicillin G is less resistant to the deacylating action of E166Cf compared to cefuroxime and 6-APA.

Similar mass spectrometric experiments were also performed with the unlabeled E166C mutant, and the kinetic parameters for E166C and E166Cf were then analyzed (see Experimental Section). As similar to the case of E166Cf, the ES* state of E166C with cefuroxime accumulates over the time course, indicating that this antibiotic is also resistant to the acylating action of E166C (Figure S3). Detailed analysis of the mass spectral data for E166C and E166Cf showed that the k_{cat} values of both mutant enzymes with cefuroxime are similar, implying that the fluorescein label does not significantly impair the enzymatic activity (Table 1). The k_{cat} values for E166C and E166Cf with cefuroxime are lower than that of the wild-type enzyme (~100-fold lower, Table 1), an observation consistent with the fact that Glu166 is important for β-lactam hydrolysis in class A β-lactamases.[28,30] Moreover, the K_d value of E166C is similar to that of E166Cf, indicating that the fluorescein label does not significantly impair the substrate binding ability of the mutant enzyme.

For 6-APA, the ES* populations of E166Cf and E166C also increase over the time course (Figures S5 and S6). The k_{cat} value of E166Cf is similar to that of E166C but much lower than that of the wild-type enzyme, as similar to the case of cefuroxime (Table 1). Moreover, the k_{cat} value for 6-APA is similar to that for cefuroxime but significantly lower than that for penicillin G (~4 orders of magnitude lower), indicating that 6-APA and cefuroxime are more resistant to the hydrolytic action of E166Cf compared to penicillin G. This observation is consistent with the findings of the spectrophotometric experiments that the decrease in UV absorbance of penicillin G with E166Cf is much more significant than those of cefuroxime and 6-APA (Figure 3).

We then performed stopped-flow fluorescence measurements on E166Cf with each of the antibiotics under similar conditions. As shown in Figure 4e, the fluorescence signal of E166Cf increases as a function of time upon addition of cefuroxime. Interestingly, this time-dependent fluorescence profile matches closely with the mass spectral [ES*]/time profile (Figure 4e), implying that the fluorescence enhancement is likely to arise from substrate binding. Similar observations were also obtained with 6-APA (Figure 4f). For penicillin G, the fluorescence of E166Cf increases rapidly in the early stage of the time course and then declines slowly (Figure 4g). This fluorescence profile also matches closely with the mass spectral [ES*]-time profile. All these observations indicate that the fluorescence enhance-

(29) Waley, S. G. *Biochem. J.* **1974**, *139*, 789–790.

(30) Leung, Y. C.; Robinson, C. V.; Aplin, R. T.; Waley, S. G. *Biochem. J.* **1994**, *299*, 671–678.

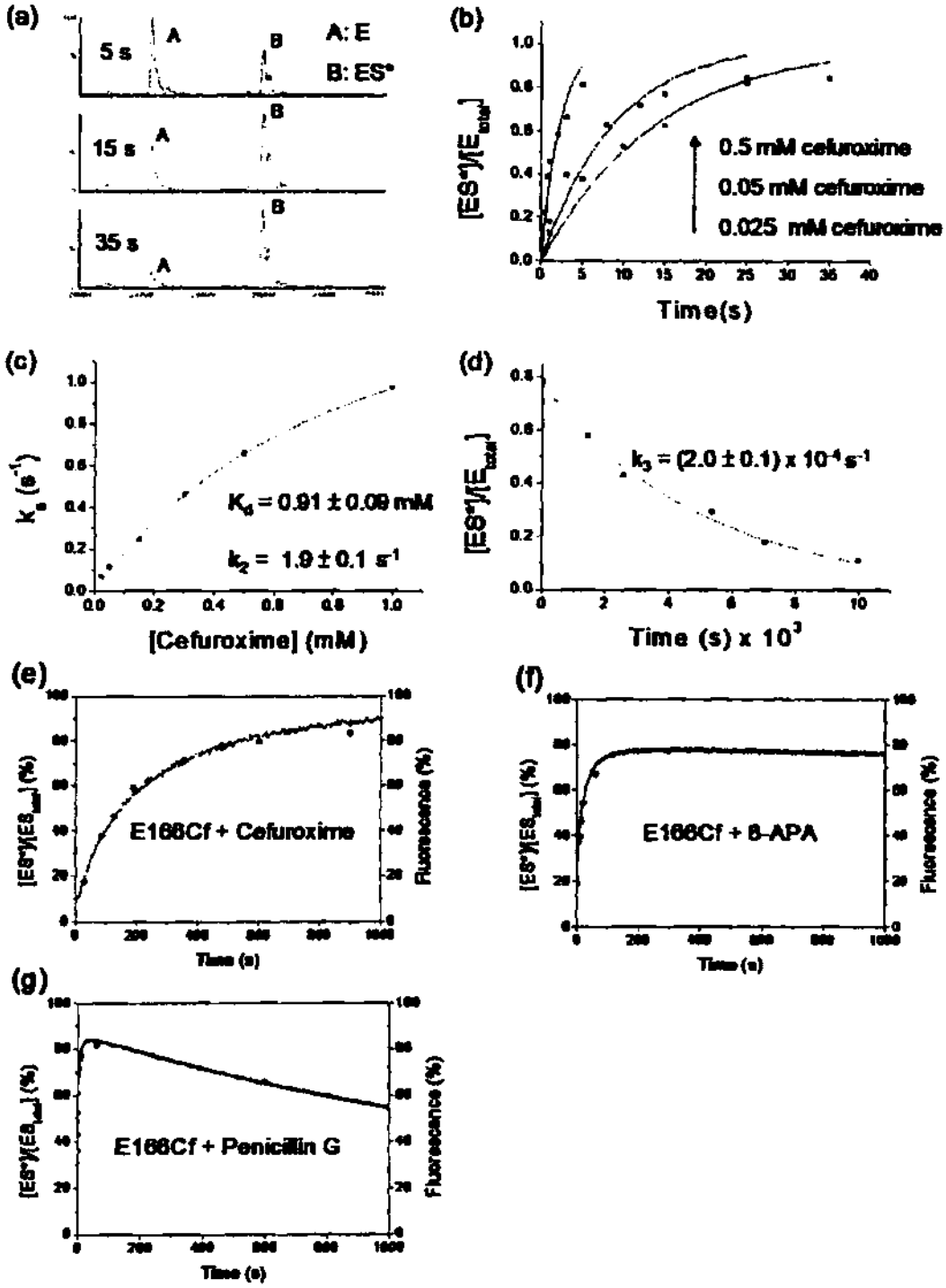

Figure 4. Mass spectrometric and stopped-flow fluorescence studies of E166Cf binding with cefuroxime, 6-APA, and penicillin G. (a) Transformed mass spectra acquired after incubating E166Cf with 0.1 mM cefuroxime at different time intervals. (b) Time course for the acylation of E166Cf with different concentrations of cefuroxime. The solid lines represent the fit of experimental data to eq 1, from which the k_s values were obtained. (c) Plot of the k_s values as a function of cefuroxime concentrations. The solid line represents the fit of experimental data to eq 2, from which the K_d and k_2 values were found to be 0.91 ± 0.09 mM and 1.9 ± 0.1 s^{-1}, respectively. (d) Time course for the deacylation of the E166Cf–cefuroxime complex. The solid line represents the fit of experimental data to eq 3, from which the k_3 value was determined. (e–g) Time course for the binding of E166Cf (0.5 μM) with 5 μM cefuroxime, 6-APA, and penicillin G (respectively) monitored by ESI-MS and stopped-flow fluorescence spectroscopy. The solid lines represent the fluorescence signals, and the red circles represent the $[ES^*]/[E_{total}]$ values of the E166Cf–antibiotic complexes determined by ESI-MS. Buffer: 20 mM ammonium acetate (pH 7.0).

Table 1. Kinetic Parameters of the Wild-Type PenPC β-Lactamase, E166C and E166Cf for the Hydrolysis of Cefuroxime, Penicillin G, and 6-APA Determined by ESI-MS and UV−Visible Spectrophotometry[a]

	K_m (μM)	K_d (mM)	k_2 (s^{-1})	k_2/K_d (k_{cat}/K_m) (M^{-1} s^{-1})	k_3 (s^{-1})	k_{cat} (s^{-1})[d]
wild-type + cefuroxime[b]	85 ± 4	–	–	(0.2 ± 0.1) × 10^3	–	0.02 ± 0.01
E166C + cefuroxime[c]	–	2.9 ± 0.3	2.5 ± 0.2	(0.9 ± 0.1) × 10^3	(7.0 ± 0.3) × 10^{-5}	(7.2 ± 0.9) × 10^{-5}
E166Cf + cefuroxime[c]	–	0.91 ± 0.09	1.9 ± 0.1	(2.0 ± 0.2) × 10^3	(2.0 ± 0.1) × 10^{-4}	(2.0 ± 0.2) × 10^{-4}
wild-type + penicillin G.[e]	48 ± 3	–	–	(5.4 ± 0.1) × 10^7	–	2612 ± 320
E166C + penicillin G.[e]	72 ± 3	–	–	(2.9 ± 0.2) × 10^4	–	2.07 ± 0.02
E166Cf + penicillin G.[e]	213 ± 11	–	–	(2.5 ± 0.2) × 10^4	–	5.28 ± 0.09
wild-type + 6-APA[b]	1374 ± 42	–	–	(5.5 ± 0.2) × 10^5	–	760 ± 10
E166C + 6-APA[c]	–	0.23 ± 0.02	16.7 ± 0.7	(7.3 ± 0.7) × 10^4	(2.4 ± 0.4) × 10^{-3}	(2.4 ± 0.4) × 10^{-3}
E166Cf + 6-APA[c]	–	0.7 ± 0.1	0.28 ± 0.02	(4.0 ± 0.6) × 10^2	(8.0 ± 1.0) × 10^{-4}	(8.0 ± 1.0) × 10^{-4}

[a] ESI-MS was used to study the enzyme kinetics in which the catalytic process could not be monitored by the spectrophotometric method (e.g., E166C/cefuroxime, E166C/6-APA, E166Cf/cefuroxime, and E166Cf/6-APA). For the wild-type enzyme, the kinetics was so fast that the MS method could not determine the catalytic parameters for the antibiotics. This is also the case for the reaction of the wild-type and mutant enzymes with penicillin G. [b] Monitored by UV−visible spectrophotometry. [c] Monitored by ESI-MS. [d] $k_{cat} = k_2k_3/k_2 + k_3$. [e] Reference 5; – not determined.

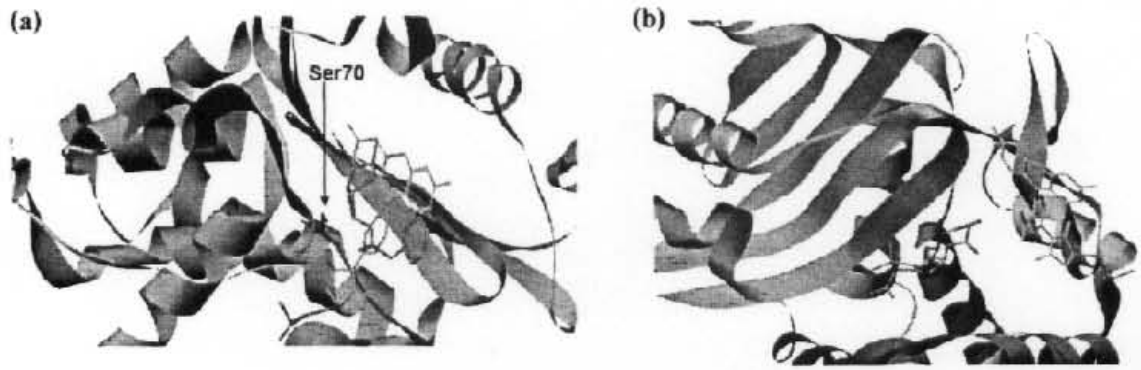

Figure 5. Molecular models of E166Cf with penicillin G. (a) Stereoview of the active site of E166Cf (with the fluorescein label staying inside the active site) docked with an intact penicillin G molecule. Note that the xanthene ring and the benzoic group of the fluorescein label (green) clash spatially with the thiazolidine ring and the exocyclic R_1 amide group of the penicillin G molecule (red), respectively. (b) Stereoview of the active site of E166Cf in the noncovalent ES state. The fluorescein label (green) stays out of the active site to avoid the spatial clash with the penicillin G molecule (red) in this state. The Ser70 and Cys166 residues are shown in blue and magenta, respectively.

ment of E166Cf arises from the formation of enzyme−substrate complex, whereas the subsequent regeneration of the free enzyme restores the weak fluorescence of E166Cf.

3.3. Molecular Modeling. In order to investigate the mechanism by which E166Cf enhances its fluorescence upon binding to β-lactam antibiotics, molecular modeling was performed with this mutant enzyme in the presence and absence of penicillin G. This antibiotic was chosen because it can bind to E166Cf and the crystal structures of various class A β-lactamases complexed with this drug have been extensively studied.[31-33] Figure 1a shows the stereoview of the active site of E166Cf in the free enzyme state.[5] The protein model shows that both the side chain of Cys166 in the Ω-loop and the attached fluorescein label are oriented toward the active site. The fluorescein label is buried in the active site with a solvent accessible area (SAA) of 191 Å^2. In order to examine whether the fluorescein label shares a common space with the β-lactam substrate within the active site, the structure of E166Cf (with the fluorescein label staying inside the active site) was docked with an intact penicillin G molecule (Figure 5a). Detailed analysis of this structure showed that both the fluorescein label and the substrate share the same space within the active site; the xanthene ring and the benzoic group (above the maleimide linker) of the fluorescein label clash spatially with the thiazolidine ring and the exocyclic R_1 amide group of the antibiotic, respectively (see Figures 2 and 5a). In the ES state, the fluorescein label stays out of the active site (Figure 5b). This subtle conformational change results in a significant increase in water exposure for the fluorescein label in the ES state (SAA = 350 Å^2) compared to that of the E state (SAA = 191 Å^2). Similar observations were also obtained with the covalent ES* state in which the hydroxyl group of the side chain of Ser70 is acylated with the β-lactam carbonyl group of the substrate;[1-3] the fluorescein label resides in the external aqueous environment with a SAA of 350 Å^2 after the covalent binding of the substrate to the active site (Figure 1b).[5]

The steric effect of the bicyclic structure of β-lactam antibiotics on the positioning of the fluorescein label is further supported by the fluorescence experiments on 6-APA (consisting of the β-lactam and thiazolidine rings only (i.e., no R_1 chain, Figure 2)); the fluorescence signal of E166Cf with 6-APA increases over the time course (Figure 3(d)). This observation also appears in the fluorescence-time profiles corresponding to the initial phase of hydrolysis of penicillin and cephalosporin antibiotics.[5]

3.4. Proteolytic Studies. The water exposure change induced by antibiotic binding can be probed by investigating the fluorescence response of the fluorescein label (whose emission

(31) Strynadka, N. C.; Adachi, H.; Jensen, S. E.; Johns, K.; Sielecki, A.; Betzel, C.; Sutoh, K.; James, M. N. *Nature* **1992**, *359*, 700–705.
(32) Shimamura, T.; Ibuka, A.; Fushinobu, S.; Wakagi, T.; Ishiguro, M.; Ishii, Y.; Matsuzawa, H. *J. Biol. Chem.* **2002**, *277*, 46601–46608.
(33) Chen, C. C.; Herzberg, O. *Biochemistry* **2001**, *40*, 2351–2358.
(34) Klonis, N.; Sawyer, W. H. *Photochem. Photobiol.* **2000**, *72*, 179–185.

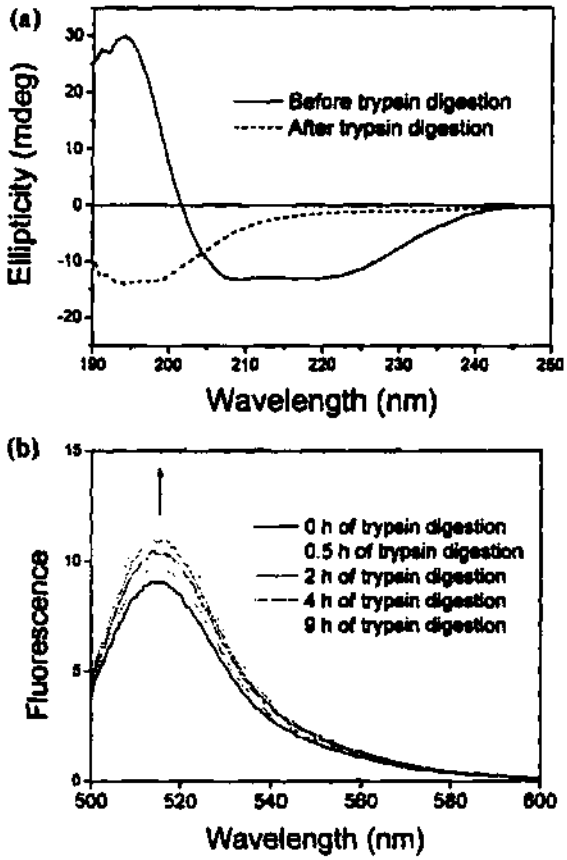

Figure 6. Proteolytic studies of E166Cf analyzed by CD spectropolarimetry and fluorescence spectroscopy. (a) Far-UV CD spectra of E166Cf (~0.3 mg/mL) before (solid line) and after (dash line) trypsin digestion in 20 mM ammonium acetate (pH 7.0). The CD signals were recorded at a scan rate of 50 nm/min and a bandwidth of 2 nm, using a quartz cell of 1 mm path length. The concentration of trypsin was 0.01 mg/mL. (b) Fluorescence spectra of E166Cf in the presence of trypsin recorded at different time intervals. The concentrations of E166Cf and trypsin were 0.2 mg/mL and 0.01 mg/mL, respectively. Excitation wavelength: 460 nm; excitation and emission slit widths: 2.5 nm.

is solvent-sensitive)[34,35] before and after proteolytic digestion, since this fluorophore is expected to be buried in the active site of native E166Cf but largely exposed to the aqueous environment when attached to a peptide fragment resulting from proteolytic digestion. This method was used instead of chemical denaturation because chemical denaturants (e.g., guanidine hydrochloride) can quench the fluorescence of fluorescein (data not shown).

The ability of the proteolytic enzyme trypsin to digest E166Cf was first investigated by CD spectropolarimetry. Figure 6a shows the far-UV CD spectra of E166Cf before and after trypsin digestion. In the absence of trypsin, E166Cf shows negative peaks at 210 and 222 nm, which are characteristic of the α-helix. After trypsin digestion, these peaks vanish, and a new negative peak in the wavelength range of 190−200 nm appears, indicating that the native structure of E166Cf is lost. The proteolytic digestion of E166Cf by trypsin was then analyzed by matrix-assisted laser desorption/ionization time-of-flight mass spectrometry (MALDI-TOF-MS). MALDI-TOF-MS is, in general, more preferable than ESI-MS in the analysis of proteolytic peptide fragments because time-consuming HPLC separation is not required prior to mass spectrometric measurements. Nine detectable peptide fragments of E166Cf resulting from trypsin digestion were observed (Table S1). A similar profile of peptide fragments was also obtained with the unlabeled E166C mutant under similar experimental conditions (Table S1). The F165-R178 fragment, corresponding to part of the Ω-loop, was obtained after proteolytic digestion of E166C and E166Cf. The mass difference between the F165-R178 fragment derived from E166C and that from E166Cf is 445.1 Da, which is consistent with the molecular mass of the fluorescein label plus a water molecule (427 + 18 = 445 Da), as also observed in the previous ESI-MS measurements of E166C and E166Cf. In this context, we noted that formation of protein−water adduct complexes under MALDI-TOF-MS conditions is also a commonly observed phenomenon.[36] The MALDI mass spectral data reveal that the fluorescein label is attached to the partial fragment of the Ω-loop, most likely at the Cys166 position, as revealed by the SDS-PAGE assay performed in our previous study.[5] Taking the mass spectral and CD data together, the fluorescein-labeled Ω-loop is likely to exist as an unfolded peptide fragment in solution after native E166Cf is digested with trypsin.

The fluorescence response of the fluorescein label of E166Cf in the presence of trypsin was then studied. As shown in Figure 6b, the fluorescence signal of E166Cf increases upon trypsin digestion, a proteolytic process that can release the fluorescein label from the confined active site of E166Cf to the external aqueous environment. This observation indicates that the fluorescein label is likely to gain lower water exposure in the active site with respect to the external aqueous environment.

3.5. Mathematical Simulation. In order to estimate the relative contributions of the ES and ES* states to the enhanced fluorescence of E166Cf, mathematical simulations of the concentration/time profiles of different species in the hydrolysis of cefuroxime were performed, using the kinetic parameters determined in the mass spectrometric studies. As shown in Figure S9, the concentration of ES* increases with concomitant decreases in the concentrations of E and ES over the time course. The concentration-time profiles of ES and ES* indicate that the concentration of ES* is, in general, larger than that of ES over the time course; the ratio of [ES*]/[ES] increases from 2 to 1700 over the time interval of 1−300 s.

3.6. Thermal Denaturation. It has been shown that the replacement of Glu166 in the class A TEM-1 E166N mutant destabilizes the protein structure, rendering the Ω-loop more flexible.[27] To investigate whether this phenomenon is also associated with E166Cf, the stabilities of the wild-type enzyme, E166C and E166Cf against thermal denaturation were studied by far-UV CD spectropolarimetry. The midpoints of thermal denaturation (T_m) for the wild-type enzyme, E166C and E166Cf were found to be 56(±1), 50(±1), and 49(±1) °C, respectively. These results indicate that the E166C mutation causes a destabilizing effect on the protein structure and increases the flexibility of the Ω-loop.

4. Discussion

Cysteine is a reactive amino acid that is often strategically incorporated into the structures of proteins for fluorophore

(35) Klonis, N.; Sawyer, W. H. *J. Fluoresc.* **1996**, *6*, 147–157.

(36) De Hoffman, E.; Stroobant, V. *Mass Spectrometry: Principles and Applications*, 2nd ed.; Wiley: New York, 2002.

labeling in the studies of protein−protein[37−40] and protein−ligand[6,8,9,12−14,16] interactions. The class A PenPC β-lactamase contains no cysteine[41,42] and therefore introducing this residue into the structure of this enzyme allows site-specific fluorophore labeling. In this study, the catalytically important Glu166 residue of this wild-type enzyme[28,30] was replaced with a cysteine and subsequently labeled with the environment-sensitive fluorophore fluorescein-5-maleimide. Recent studies have shown that Glu166 is likely to play critical roles in both the acylation[27,43−46] and deacylation[27,30,31,47,48] steps in β-lactam hydrolysis; in the former step, Glu166 is likely to deprotonate the hydroxyl group of Ser70 via the bridging water molecule for β-lactam acylation,[27,43−46] whereas in the latter step Glu166 appears to act as the general base for hydrolyzing the covalent acyl enzyme−substrate complex.[27,30,31,47,48] Replacement of this catalytically important residue should, therefore, significantly reduce the activity of the enzyme, thus allowing the fluorophore-labeled E166Cf mutant to serve as a ligand-binding protein (with very low k_{cat}) for biosensing purposes. Moreover, Glu166 is located in the flexible Ω-loop (close to the active site) with its side chain pointing toward the active site.[17−20] These structural properties allow the fluorophore attached to this residual position to probe local environmental changes within the active site and can reduce the possible steric effect of the fluorophore on the enzyme−substrate binding.

The comparative fluorescence studies of E166Cf and E166C showed that the fluorescein label can sense the local environmental change in the active site induced by antibiotic binding (Figure S8). Moreover, the mass spectrometric and stopped-flow fluorescence experiments revealed that the fluorescence enhancement of E166Cf is very likely to arise from the formation of enzyme−substrate complex (Figure 4e−g). This observation is common to both penicillins (e.g., penicillin G and 6-APA) and cephalosporins (e.g., cefuroxime). With β-lactamase-sensitive antibiotics such as penicillin G, the ES* state of E166Cf is reactive and returns to the E state readily with the generation of acid product, thus leading to the reduction in the ES* population during the course of β-lactam hydrolysis. This phenomenon appears to lead to the restoration of the weak fluorescence of E166Cf, as revealed by the observation that both the mass spectrometric and fluorescence signals decline consistently in the later stage of β-lactam hydrolysis (Figure 4g). In the case of 6-APA and cefuroxime, E166Cf does not show this phenomenon, an observation consistent with the fact that these antibiotics are resistant to the hydrolytic action of the mutant enzyme (low k_{cat}).

The mechanism by which the binding of antibiotics triggers the fluorescence of E166Cf was unraveled by the molecular modeling studies of the E, ES, and ES* states. An important finding is that the fluorescein label is likely to share a common space with the bicyclic structure of β-lactam antibiotics within the active site (Figure 5a). This observation implies that the fluorescein label has to depart from the active site in order to make room for an incoming antibiotic. Indeed, the protein models of the ES and ES* states reveal that the fluorescein label stays out of the active site in order to avoid the spatial clash with the bound substrate (Figures 1b and 5b). This steric effect is further supported by the finding of the fluorescence study of E166Cf with 6-APA; the binding of 6-APA, which consists of the bicyclic structure only, can also enhance the fluorescence of E166Cf, as similar to the case of penicillin G and cefuroxime (Figure 3d). Taken together, the fluorescein label in the E state appears to occupy, at least in part, the space within the active site where the bicyclic structure of β-lactam antibiotic resides, and this spatial clash is likely to be the major factor inducing the departure of the fluorescein label from the active site upon antibiotic binding.

The substrate-induced movement of the fluorescein label from the active site to the external aqueous environment appears to increase its water exposure, as revealed by the larger solvent-accessible areas of the ES and ES* states compared to that of the E state (Figures 1 and 5). This observation is consistent with the findings of the proteolytic studies of E166Cf analyzed by fluorescence spectroscopy, CD spectropolarimetry, and MALDI-MS; the fluorescein label, which fluoresces more strongly in a more polar environment,[34,35] shows stronger fluorescence upon digesting native E166Cf into unfolded peptide fragments by trypsin (Figure 6 and Table S1).

The facts that E166Cf gives stronger fluorescence in the ES* state and the fluorescein label gains a similar increase in solvent accessibility in the ES and ES* states imply that, in addition to the covalent ES* state, the noncovalent ES state is also likely to enhance the fluorescence of E166Cf. When E166Cf binds to a β-lactam antibiotic to form the ES complex, the fluorescein label will move away from the active site to avoid the spatial clash with the bound substrate (Figures 1a and 5b). This noncovalent state will then undergo acylation and proceed to the ES* state, where the fluorescein label remains out of the active site (Figure 1b). As a result of gaining higher water exposure, the ES and ES* states give stronger fluorescence with respect to the E state. Upon returning to the E state, the fluorescein label on the Ω-loop enters the vacant active site again. This motion might be hindered due to the bulky nature of the fluorescein label, thus leading to the slow return of the fluorophore. In the E state, the fluorescein label experiences lower water exposure in the active site, thereby restoring its weak fluorescence.

Despite the bulky nature of the fluorescein label, the ability of E166Cf to bind to β-lactam antibiotics is not significantly impaired, as revealed by the similar K_d values of E166C and E166Cf with 6-APA and cefuroxime (Table 1). This surprising observation is presumably due to the flexible nature of the Ω-loop.[17−20] In this regard, it is interesting to note that replacement of Glu166 in the Ω-loop of the class A TEM-1 β-lactamase with an asparagine can increase the mobility of the Ω-loop and hence destabilize the protein structure.[27]

(37) Hamman, B. D.; Oleinikov, A. V.; Jokhadze, G. G.; Traut, R. R.; Jameson, D. M. *Biochemistry* **1996**, *35*, 16672−16679.
(38) Hamman, B. D.; Oleinikov, A. V.; Jokhadze, G. G.; Traut, R. R.; Jameson, D. M. *Biochemistry* **1996**, *35*, 16680−16686.
(39) Miller, R. A.; Presley, A. D.; Francis, M. B. *J. Am. Chem. Soc.* **2007**, *129*, 3104−3109.
(40) Carter, D. M.; Miousse, I. R.; Gagnon, J. N.; Martinez, E.; Clements, A.; Lee, J.; Hancock, M. A.; Gagnon, H.; Pawelek, P. D.; Coulton, J. W. *J. Biol. Chem.* **2006**, *281*, 35413−35424.
(41) Ambler, R. P.; Coulson, A. F.; Frere, J. M.; Ghuysen, J. M.; Joris, B.; Forsman, M.; Levesque, R. C.; Tiraby, G.; Waley, S. G. *Biochem. J.* **1991**, *276*, 269−270.
(42) Madgwick, P. J.; Waley, S. G. *Biochem. J.* **1987**, *248*, 657−662.
(43) Minasov, G.; Wang, X.; Shoichet, B. K. *J. Am. Chem. Soc.* **2002**, *124*, 5333−5340.
(44) Hermann, J. C.; Ridder, L.; Mulholland, A. J.; Holtje, H. D. *J. Am. Chem. Soc.* **2003**, *125*, 9590−9591.
(45) Nukaga, M.; Mayama, K.; Hujer, A. M.; Bonomo, R. A.; Knox, J. R. *J. Mol. Biol.* **2003**, *328*, 289−301.
(46) Lamotte-Brasseur, J.; Dive, G.; Dideberg, O.; Charlier, P.; Frere, J. M.; Ghuysen, J. M. *Biochem. J.* **1991**, *279*, 213−221.
(47) Escobar, W. A.; Tan, A. K.; Fink, A. L. *Biochemistry* **1991**, *30*, 10783−10787.
(48) Adachi, H.; Ohta, T.; Matsuzawa, H. *J. Biol. Chem.* **1991**, *266*, 3186−3191.

Previous structural studies of the class A RTEM-1 and TEM-1 β-lactamases have shown that the side-chain carboxylic group of Glu166 forms hydrogen bonds with the side-chain nitrogen atoms of Lys73 and Asn170,[21,43,49] which are highly conserved residues in many class A β-lactamases, including the PenPC β-lactamase used in the present study.[41,42] Moreover, in the E166N mutant of the TEM-1 β-lactamase, the replacement of Glu166 in the Ω-loop is likely to weaken the hydrogen-bonding interactions, thus increasing the flexibility of the Ω-loop and destabilizing the structure of the enzyme; the T_m values of the wild-type form and E166N mutant of TEM-1 were found to be 51.1(±0.2) and 43(±1.4) °C, respectively.[27] These perturbing structural effects might also occur in the E166C mutant of the PenPC β-lactamase because the thermal stabilities of the Glu166-substituted mutants of the PenPC and TEM-1[27] β-lactamases are both reduced (compared to their respective wild-type structure) as a result of the replacement of Glu166. In the case of E166Cf, the E166C mutation and the fluorophore conjugation appear to cause a similar destabilizing effect on the protein structure, as revealed by the similar decrease in thermal stability of E166Cf compared to that of the wild-type enzyme. This structural perturbation is likely to increase the flexibility of the Ω-loop and hence compensate for the possible steric effect of the bulky fluorescein label on the enzyme–substrate binding. Analogous to this case, some β-lactamase variants in the class A TEM family have been found to be able to improve the binding interactions with bulky cephalosporins by relaxing the conformation of their Ω-loop through the replacement of the Ω-loop residue (e.g., Arg164) responsible for forming salt bridges with the rest of the protein structure.[50–52] With the increased flexibility of the Ω-loop, E166Cf appears to be able to largely restore its substrate-binding ability even though its active site is considerably shielded by the fluorophore in the free enzyme state.

5. Conclusions

In this study, we have studied the biosensing mechanism of the nonallosteric E166Cf mutant toward β-lactam antibiotics. The catalytic Glu166 residue was replaced with a cysteine, which was subsequently labeled with environment-sensitive fluorescein. This residue is located in the flexible Ω-loop with its side chain pointing toward the active site.[17–20] The replacement of Glu166 further increases the flexibility of the Ω-loop. With these advantageous structural properties, the attached fluorescein label can stay close to the active site to sense antibiotic binding without significantly impairing the substrate binding ability of the mutant enzyme. In the E state, the fluorescein label is likely to occupy, at least in part, the active-site space where the bicyclic structure of β-lactam antibiotics resides. This spatial clash appears to cause the fluorescein label to depart from the active site when an antibiotic enters this local region. As a result of this subtle motion, the fluorescein label in the ES and ES* states experiences higher water exposure and hence gives stronger fluorescence with respect to the E state. After hydrolyzing the bound substrate, the fluorescein label returns to the vacant active site and restores its weak fluorescence.

Acknowledgment. This work was supported by the Research Grants Council (PolyU 5014/04P, 5017/06P, and 5380/04M), the Area of Excellence Fund of the University Grants Committee (AoE/P-10/01), and the Research Committee of the Hong Kong Polytechnic University. We thank Mr. S.-C. Choi and Mr. K.-H. Law for technical assistance in protein expression.

Supporting Information Available: Experimental details for fermentation, molecular modeling of E166Cf, and mass spectral data for E166C and E166Cf. This material is available free of charge via the Internet at http://pubs.acs.org.

JA076111G

(49) Maveyraud, L.; Pratt, R. F.; Samama, J. P. *Biochemistry* **1998**, *37*, 2622–2628.
(50) Raquet, X.; Lamotte-Brasseur, J.; Fonze, E.; Goussard, S.; Courvalin, P.; Frere, J. M. *J. Mol. Biol.* **1994**, *244*, 625–639.
(51) Vakulenko, S. B.; Taibi-Tronche, P.; Toth, M.; Massova, I.; Lerner, S. A.; Mobashery, S. *J. Biol. Chem.* **1999**, *274*, 23052–23060.
(52) Wang, X.; Minasov, G.; Shoichet, B. K. *J. Mol. Biol.* **2002**, *320*, 85–95.